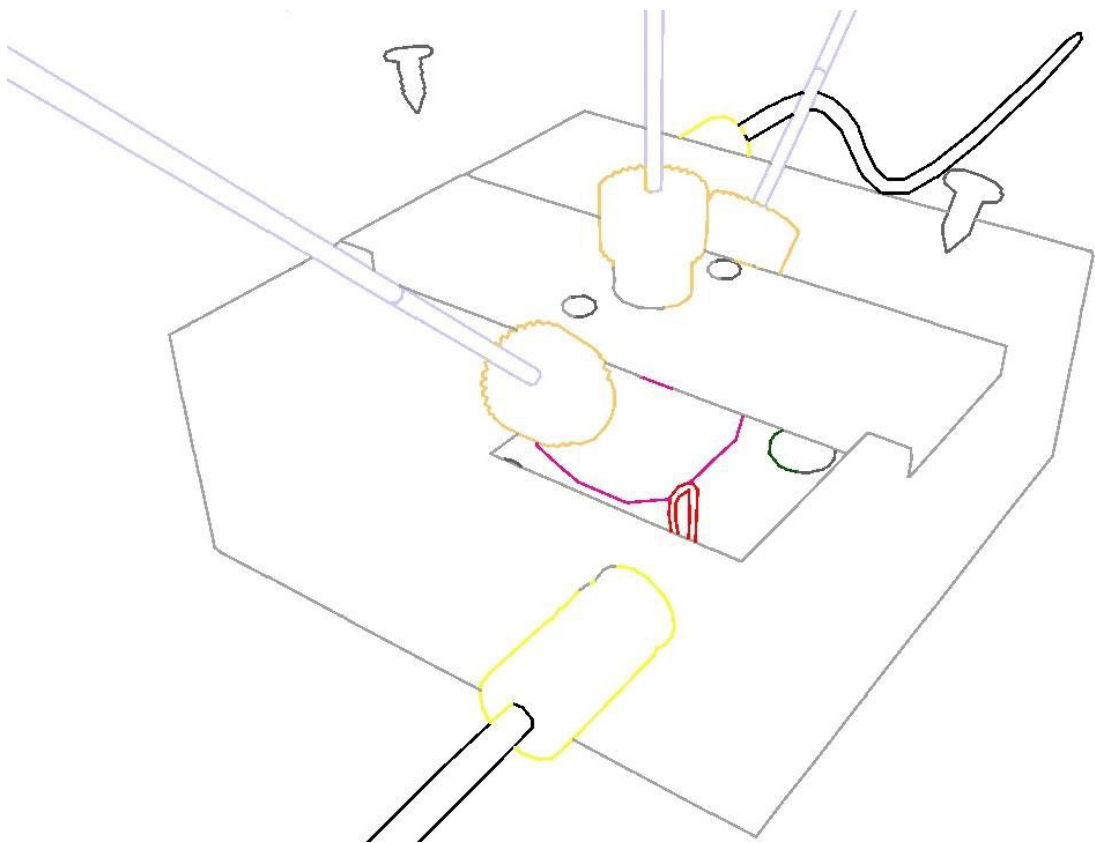


POLYDIMETHYLSILOXANE-COATED INTERDIGITATED ELECTRODES FOR CAPACITIVE DETECTION OF ORGANIC POLLUTANTS IN WATER

- A SYSTEMATIC GUIDE -



JUDITH STAGINUS

POLYDIMETHYLSILOXANE-COATED INTERDIGITATED ELECTRODES FOR CAPACITIVE DETECTION OF ORGANIC POLLUTANTS IN WATER

- A SYSTEMATIC GUIDE -

Proefschrift

Ter verkrijging van de graad van doctor
aan de Technische Universiteit Delft,
gezag van de Rector Magnificus prof. ir. K. C. A. M. Luyben,
voorzitter van het College voor Promoties,
in het openbaar te verdedigen
op 4 november 2015 om 10:00 uur

door

Judith STAGINUS

Master in Industrial Sciences: Chemical Engineering,
Groep T – Leuven Hogeschool, Leuven, België
Master in Environmental Science and Technology,
Katholieke Universiteit Leuven, Leuven, België
geboren te Düsseldorf, Duitsland

Dit proefschrift is goedgekeurd door de promotor:

Prof. dr. E. J. R. Sudhölter

Copromotor:

Dr. ir. L. C. P. M. de Smet

Samenstelling promotiecommissie:

Rector Magnificus	voorzitter		
Prof. dr. E. J. R. Sudhölter	Technische promotor	Universiteit	Delft,
Dr. ir. L. C. P. M. de Smet	Technische copromotor	Universiteit	Delft,

Onafhankelijke leden:

Prof. dr. B. Dam	Technische Universiteit Delft
Prof. dr. C. J. M. van Rijn	Universiteit Wageningen
Prof. dr. J. G. E. Gardeniers	Universiteit Twente
Dr. ir. M. J. J. Mayer	EasyMeasure B.V., Amersfoort

Overige afhankelijke leden van de promotiecommissie:

Dr. H. Miedema	Wetsus, Leeuwarden
Em. prof. dr. ir. G. C. M. Meijer	Technische Universiteit Delft

Reservelid:

Prof. dr. S. J. Picken	Technische Universiteit Delft
------------------------	-------------------------------



This work was performed in the cooperation framework of Wetsus, European Centre of Excellence for Sustainable Water Technology (www.wetusus.nl). Wetsus is funded by the Dutch Ministry of Economic Affairs and Ministry of Infrastructure and Environment.

Cover Design: Isabelle M. Aerts

Printed by Ipskamp Drukkers B.V., Enschede in the Netherlands

ISBN: 978-94-6186-565-6

Copyright © 2015 by Judith Staginus

All rights reserved. No part of this publication may be reproduced, stored in a retrieval system or transmitted in any form or by any means: electronic, mechanical, photocopying, recording or otherwise, without prior written permission of the author.

A free electronic version of this thesis can be downloaded from:
<http://www.library.tudelft.nl/dissertations>

Für Omi und Opi.

CONTENTS

1 Introduction: Surface-Engineered Sensors.....	1
1.1 Sensorization.....	2
1.2 Water – The Global Issue	2
1.3 Sensors.....	3
1.3.1 Chemical Sensors	3
1.3.2 Surface-Engineered Sensors	4
1.3.3 Interdigitated Electrode Sensors.....	6
1.3.4 Towards Smart Sensor Systems	8
1.4 Thesis Motivation and Goal.....	9
1.5 Organization of this Thesis	10
1.6 References.....	13
2 Theoretical Background: Principles of Capacitive Measurements	19
2.1 The Capacitor.....	20
2.2 The Capacitance.....	22
2.3 Electronic Representation	23
2.4 Capacitance Measurements.....	24
2.5 Parasitic Effects and Noise	25
2.5.1 Shielding and Guarding.....	26
2.5.2 Two-Port Measurement Technique	27
2.5.3 Three-Signal Measurement Technique.....	28
2.5.4 Sensor Packaging	28
2.4 Concluding Remarks.....	29
2.5 References.....	30
3 Detection Principles of Polymer-Coated Interdigitated Electrodes	33
3.1 IDE Platforms	34
3.1.1 IDE Capacitance.....	34
3.1.2 Design Parameters.....	35
3.2 Polymeric Sensing Layers	37

3.2.1 Polydimethylsiloxane.....	38
3.2.2 Preparation of Thin Polymeric Sensing Layers	39
3.3 Principles of Pollution Detection.....	40
3.3.1 Pollutant Partitioning	40
3.3.2 Detection Mechanisms.....	41
3.4 Complexity in Water Sensing Techniques	43
3.4.1 Water-Enhanced Electrical Coupling.....	44
3.4.2 The Role of Swelling	48
3.4.3 Polymer Layer Requirements.....	49
3.4.4 The Physico-Chemical Complexity	50
3.5 Concluding Remarks	51
3.6 References	52
4 Measurement Setup and Technique.....	57
4.1 Interdigitated Electrode Platform	58
4.2 Polydimethylsiloxane Layer	60
4.3 Printed Circuit Board.....	62
4.4 Electric Connectors	63
4.5 Flow Cell System	65
4.6 Universal Transducer Interface	67
4.7 LabVIEW-Program	70
4.8 Temperature Dependency.....	70
4.9 Concluding Remarks	72
4.10 References	73
5 Water-Enhanced Guarding of Polymer-Coated IDE Platforms.....	75
5.1 Introduction	76
5.2 Materials and Methods	77
5.2.1 Chemicals	77
5.2.2 IDE Platform.....	78
5.2.3 PDMS Layer	78
5.2.4 Universal Transducer Interface.....	78

5.2.5 Drop Experiment.....	78
5.2.6 Continuous Flow Experiment.....	79
5.3 Experimental Investigation.....	79
5.3.1 Droplet Detector.....	80
5.3.2 Flow Detector.....	84
5.4 Concluding Remarks.....	87
5.5 References.....	89
6 Capacitive Response of PDMS-Coated IDEs to Volatile Organic Compounds and Their Aqueous Solutions.....	93
6.1 Introduction.....	94
6.2 Materials and Methods.....	94
6.2.1 Chemicals.....	94
6.2.2 IDE Platform.....	95
6.2.3 PDMS Layer.....	95
6.2.4 Universal Transducer Interface.....	95
6.2.5 Drop Experiment.....	95
6.2.6 Continuous Flow Experiment.....	95
6.3 Experimental Investigation.....	96
6.3.1 Drop Experiment.....	96
6.3.2 Continuous Flow Experiment.....	100
6.4 Concluding Remarks.....	107
6.5 References.....	108
7 Outlook.....	111
7.1 Challenges and Future Prospects.....	112
7.1.1 Polymer Design.....	112
7.1.2 Polymer/Transducer Interface Design.....	116
7.1.3 Electrode Design.....	119
7.1.4 Lead Design.....	121
7.1.5 Setup Design.....	122
7.2 Concluding Remarks.....	124

7.3 References	125
Appendix A Supplementary Information Chapter 4.....	129
A.1 Phase Shift versus Frequency	130
Appendix B Supplementary Information Chapter 5	133
B.1 Dimensions and Material Properties	134
B.2 Solution Conductivity	135
B.3 Detection Performance of Guarded and Unguarded IDE Chips	136
Appendix C Supplementary Information Chapter 6.....	139
C.1 Contact Angle Measurements	140
Summary	143
Samenvatting.....	147
Recognition.....	153
Acknowledgment	157
About the Author.....	163

INTRODUCTION: SURFACE-ENGINEERED SENSORS

There is an eager effort spent on the research and development of surface-engineered sensors for biomedical and environmental monitoring purposes. These sensors consist of physical transducer platforms that are (bio-)chemically modified with bioorganic receptors and inorganic and organic monolayers or films to undergo a specific or partially selective interaction with a compound of interest. By integrating the sensing element together with the electronic readout device onto a single chip, smart sensor systems with an enhanced device performance are developed. In particular, chemical sensors based on interdigitated electrode platforms covered with polymeric sensing layers are of great interest for the detection of pollutants in air. The goal of this thesis is to study these sensor types when they are directly exposed to water for the capacitive detection of organic water pollutants.

1.1 Sensorization

Sensorization is considered to be the next revolutionary trend, following the period of information and mechanization. It implies the use of a large number of sensors to provide us with any information about a system that we could otherwise not perceive with only our human senses. Such a system may be our own human body, an engine, an industrial process, or an entire atmosphere. The heart of a sensor system is the sensing element, which is basically a transducer platform that transforms the measured signal from its energy domain (*e.g.*, mechanical, thermal, chemical, magnetic, or radiant) into, *e.g.*, the electrical domain.¹ The electrical domain is of special interest as it allows easy signal modification and further processing. The information provided by the sensor allows us to monitor and control the system under investigation, such as to keep the system in balance, to optimize the process involved, to prevent it from damage or degradation, or to keep its surrounding away from harm. Needless to say, sensorization describes a vibrant, diverse, and interdisciplinary field of science nowadays. The urgent need for the development of reliable, sensitive, and selective chemical and biomedical sensors that are robust enough for online and on-field applications while being affordable, communicating wirelessly, and having a low power consumption at the same time requires a close cooperation of experts of many disciplines. This also demands to open one's mind to new research approaches and ideas.

1.2 Water - The Global Issue

The growing awareness of environmental pollution puts a great demand on the research and engineering society to develop sophisticated smart sensor systems that can monitor the quality of the different environmental compartments soil, water, and air. A well-known example of a major global problem are the dwindling resources of clean fresh water for sanitary and drinking purposes but also for agricultural and industrial uses.² The quality of water is an important today's issue as the presence of diverse pollutants poses risks to the health and safety of humans, flora, and fauna. Water pollution is frequently related to anthropogenic sources, such as industry, households, and agricultural activities, and brings along the need for costly site remediation and water treatment techniques.³ The pollution composition can be very diverse, including the presence of heavy metal ions, surfactants, pharmaceuticals, pesticides, fertilizers, and various other organic and inorganic compounds.

Many contaminants may occur as different chemical species, depending on the environmental conditions of water, such as the pH and the redox potential, which determine the tendency of a chemical compound for (de)protonation and electron acquisition, respectively. This is a crucial piece of information as the chemical speciation of a component, *e.g.*, of a heavy metal ion, also determines its intrinsic toxicity and whether it bio-accumulates and persists in the environment.⁴ Contaminants can be present at high concentrations as frequently encountered at spilling points or be strongly diluted as in natural water streams and reservoirs. Toxic compounds can occur at trace levels, shadowed by the presence of many other and highly concentrated contaminants. Finally, water conditions can favor the growth of certain microorganisms, such as bacteria and viruses, and hence support the spread of diseases. Indeed, the local water quality is usually closely linked to the health of the locals, a fact that is most obvious for developing countries where appropriate water treatment techniques and sanitation facilities are lacking. This all makes environmental monitoring a very complex and challenging research and engineering task.

1.3 Sensors

1.3.1 Chemical Sensors

Chemical sensors that are capable of analyzing any system of unknown atomic or (bio)molecular composition could support environmental monitoring systems as needed, for instance, in the case of a gasoline spill. Most technologies for the detection and concentration determination of the constituents of fuel in water make use of the principle that the primarily volatile organic compounds (VOCs) distribute themselves between the water phase and the gas/vapor phase, *i.e.*, the so-called headspace. They apply analytical techniques like gas chromatography (GC) in combination with mass spectrometry (MS)⁵⁻⁹ and flame ionization detection¹⁰ to analyze gas samples from the headspace. Although recent advances have made it possible to develop field-portable instrumentation based on such techniques,¹¹ environmental monitoring of fuel constituents in water is commonly performed with standard water sampling techniques and off-site analysis equipment in the lab as also in compliance with governmental procedure protocols¹² to obtain satisfactory qualitative and quantitative information (Figure 1.1).

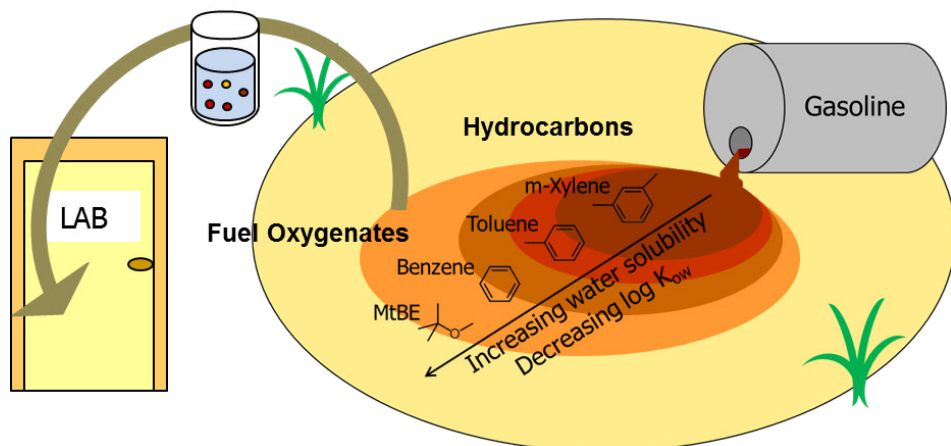


Figure 1.1. Schematic representation of a contamination plume of gasoline compounds as demonstrated by some of its constituents, which in this case are the aromatics m-xylene, toluene, and benzene as well as the fuel oxygenate methyl tert-butyl ether (MtBE). The left-handed side of the figure illustrates that samples are (typically) analyzed off-site in a laboratory.

Chemical sensors are classified according to the operating principle of the transducer element, which are typically optical, electrical, electrochemical, mass sensitive, magnetic, and thermometric devices that transform the chemical information into an analytical useful signal.¹³ For example, optical sensors measure changes in an optical property, such as in the absorbance or in the refractive index of the system upon interaction with a target compound.¹³ This group of sensors stands for high accuracy, sensitivity, and selectivity, however, optical sensors usually come in complex and expensive instrument setups that bring along high maintenance costs.¹⁴

Electrochemical sensors including electrical sensors form the largest group of chemical sensors. They detect changes in impedance, which they can relate to changes in the chemical or biochemical composition of a system or surrounding.¹⁵ Compared with optical sensors, electrical sensors are low-cost, easy to fabricate and to maintain but have struggled in the past to compete in terms of their sensitivity and selectivity.¹⁴

1.3.2 Surface-Engineered Sensors

Chemical sensors typically consist of a physical transducer element that is surface-engineered with a chemically (partially) selective layer to achieve an affinity and hence specific or non-specific interaction with the compound of interest.^{16, 17} Well-known

examples of sensor transducer platforms for (bio)chemical sensing applications are nanowire-based field effect transistors (NW-FETs) and interdigitated electrodes (IDEs). The detection technique depends on the nature of the event to be detected and can, *e.g.*, be amperometric, potentiometric, or conductometric if an electrochemical reactions is involved,¹⁸ or, *e.g.*, be resistive or capacitive for chemical or physical sorption processes occurring.¹⁹ The surface-engineered sensor platforms aim to mimic naturally occurring interaction processes. Therefore, this disciplinary field is very much inspired by environmental and biological systems.¹⁶ Specific interactions are achieved via a ‘lock-and-key’ design: an immobilized, specific receptor is used to bind selectively the analyte of interest.²⁰ However, this approach requires the synthesis (or isolation and purification) of a separate, highly selective sensing element for each analyte to be detected.²⁰ Alternatively, it is also possible to apply an array of different sensing surfaces, such as of different metal oxide or polymer layers, with every surface element responding (partially) selectively to different chemical compounds.^{16, 18, 20-25}

Sensing surfaces can also be structurally engineered as by growing nanostructures, such as nanoparticles, nanotubes, and nanowires, on top of the transducer platforms that, for example, increase the electrode area.^{25, 26} The surface-area-to-volume ratio is an important design parameter. This is because the increase of the surface-area-to-volume ratio is expected to enhance the interaction-response mechanisms and hence sensitivity of the sensor devices similar to natural systems, such as living cells.²⁷ It plays among others a significant role in nanowire-based sensors where electronic coupling between the close-by chemical environment and the surface modified nanowire occurs (Figure **1.2a**).²⁸ The deposition of vertical nanowires is another innovative strategy to increase the surface area of interdigitated electrodes (Figure **1.2b**).²⁶

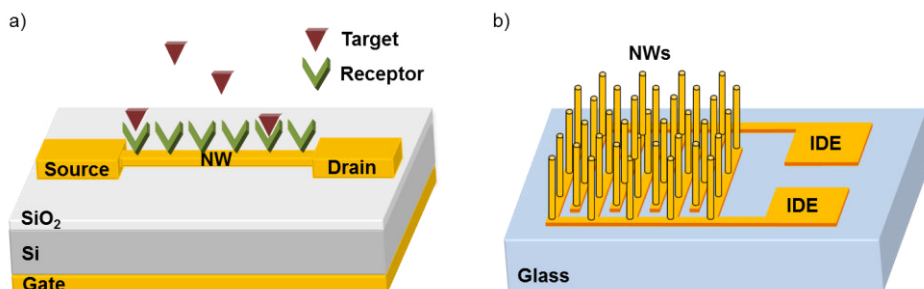


Figure 1.2. Schematic representation of two selected sensor platforms that make use of nanowires (not to scale): a) a receptor-covered nanowire-based field effect transistor (NW-FET) sensor platform with specific interactions of a target compound with the immobilized receptors, and b) a structurally engineered surface of an interdigitated electrode (IDE) sensor platform with vertically assembled nanowires (NWs).

1.3.3 Interdigitated Electrode Sensors

Several sensor transducer platforms have been explored and found to be suited for the detection of VOCs. Examples include the use of (combinations of) resistors, cantilevers and silicon disks, thermoelectric calorimeters, and surface acoustic wave devices.²⁹⁻³⁴ In particular, interdigitated electrodes for capacitive but also resistive, impedimetric, and electrochemical measurements have proven to be an interesting technology in this field.³⁵⁻³⁹ This design is an arrangement of two interlocked comb electrodes⁴⁰ and is therefore sometimes referred to as simply comb or finger electrodes. IDE platforms are favorable due to their robust and simple structure, providing long-term stability.³⁸ In addition, IDEs can be fabricated cost-effectively and reproducibly as micro- and nanostructures with photolithographic and electron-beam deposition techniques.³⁹ It is further a popular transducer platform for chemical sensing applications as the planar electrode structure offers a large interaction area to the environment.⁴¹ The interdigitated electrodes are deposited onto an insulating, inert substrate, such as a quartz or glass wafer, or a semi-conducting material, such as silicon with an insulating native oxide layer in between.⁴²⁻⁴⁴ Besides metals, also polysilicon is an attractive electrode material as its deposition on native SiO₂ allows to easily functionalize both the electrodes and the space between them in a silanization process.³⁸ Moreover, by covering the electrodes with affinity layers, *e.g.*, oxide layers⁴⁵ or polymer layers^{16, 41} (Figure 1.3), the selectivity of the sensing elements can be tuned. Also, it is possible to

fabricate entire multi-arrays of IDEs coated with different polymer layers via lithographic techniques⁴⁶⁻⁴⁸ or inkjet printing.⁴⁹

Gas mixtures have been successfully analyzed with polymer-based IDE multi-arrays, utilizing pattern recognition techniques for response interpretation.⁵⁰ A prototype of a gas sensor system based on a multi-array of IDEs coated with different oxide layers for the selective detection of the fuel additive methyl tert-butyl ether has been reported.⁵¹ Furthermore, the transducer elements, electronic circuitry, and interfacing units can be fully integrated in single chip devices⁵² and advanced integrated sensor systems have been developed.⁵³⁻⁵⁵

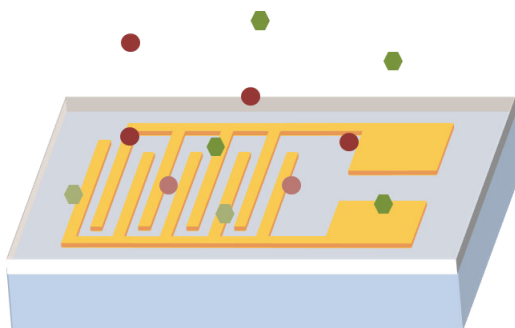


Figure 1.3. Schematic representation (not to scale) of polymer-coated interdigitated electrode platform and a non-specific interaction with two unknown compounds as depicted by the purple circles and green hexagons, which are adsorbed onto the polymer surface and absorbed into the polymer bulk material.

Capacitive-type chemical sensors based on polymeric sensing layers transduce the change in physical properties of the sensing element, *i.e.*, the dielectric constant of the sensing layer, into a change of electrical capacitance and then measure and convert the capacitive signal into an electrical output signal.⁵⁶ They make use of polymer swelling and dielectric changes by either placing the thin polymer film in between a (porous) top and bottom electrode^{48, 57} or by depositing the thin polymer film on a planar electrode structure such as the IDEs.^{48, 58} Sensors that rely on changes in the dielectric properties of a sensing material upon analyte exposure are also referred to as chemocapacitors or dielectrometers.⁵⁹ As polymeric sensing layers are partially selective, not only a single but several compounds of similar properties have an affinity for the polymer layer. That is, chemically similar compounds are likely to interact with the same sensor element,

resulting in an overlap signal for the individual sensor element and in a multivariate response of the sensor array. The analytes can then be identified and quantified by means of multi-component analysis tools and pattern recognition algorithms,⁶⁰⁻⁶² a technique which is also applied in electronic nose technology (Figure 1.4).⁶³

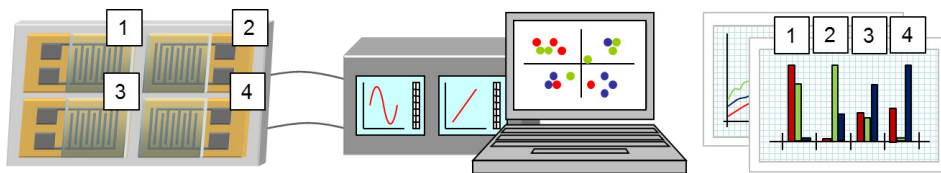


Figure 1.4. Schematic representation of a multi-array of four polymer-coated interdigitated electrode platforms and of the electronic readout device, and the graphical representation of the multivariate response obtained via pattern recognition algorithm and multi-component analysis tools.

1.3.4 Towards Smart Sensor Systems

The overall sensitivity and selectivity of a sensor system depends on many aspects, such as the performance of the individual system devices, the degree of device integration, the specification of the electronic readout, and the algorithm applied for signal processing. By smart-design of the (bio-)chemical sensing element, the degree of interaction of the target compound with the sensing material can be influenced and the degree of transformation of the chemical information into an electrical signal can be tuned. Whether this signal can be read-out electronically, that is being detected, depends then on the resolution of the electronic readout device and the capability to suppress interferences and noise. The problem of measuring low capacitor values by low-cost means has been overcome by smart sensor systems. A smart sensor combines the sensor element, the analog interface circuit, and the analog-to-digital converter as well as the bus interface into one housing.¹ The integration of these functions on one chip is then referred to as an *integrated smart sensor system*.¹ In fact, chip integration is considered a necessity as capacitive micro-sensors have small capacitance values and even much smaller capacitance variation as compared with parasitic capacitances of interconnections between chips.⁶⁴ Furthermore, full chip integration permits control and monitoring of the integrated sensor functions and enables on-chip signal amplification and conditioning that further contributes to the improvement of the overall sensor

performance.⁵⁴ Finally, proper packaging, advanced measurement techniques, higher functions such as self-testing and auto-calibration, and guarding and shielding techniques are further factors that determine the systems and response stability, sensitivity, and reliability.^{56, 65} Therefore, the development of a successful sensor system requires a full-system-based approach in order to provide compatibility between the system components and to exploit their functionalities.

1.4 Thesis Motivation and Goal

Polymer-coated interdigitated electrodes as chemically modified transducer platforms for chemical capacitive sensors have already been studied for the detection of organic pollutants in the air phase.^{58, 66-68} Sensor systems based on multi-arrays of metal oxide-coated IDEs have shown potential in the resistive detection of the volatile organic compound methyl tert-butyl ether as water pollutant in a headspace.⁵¹ Headspace applications are primarily suitable for volatile compounds that readily distribute into the air phase. The current research project represents an in-depth study of the fundamental issues of this sensor type for the capacitive detection of organic pollutants when being directly exposed to the polluted water phase. With this work we seek to contribute to the knowledge of capacitive sensor systems that are capable of pollution detection *directly* in water. This configuration is illustrated in Figure 1.5c, whereas Figures 1.5a and 1.5b depict an indirect way of analyzing volatile compounds present in water.

To achieve such a direct analysis, we studied the capacitive response of polymer-coated interdigitated electrode platforms as read out by a low-cost universal transducer interface operating at a single frequency. Using a self-designed flow cell system, changes in the real-time system capacitance of polydimethylsiloxane-coated interdigitated electrode platforms have been measured upon adsorption/absorption and desorption of the VOCs in the water phase. In addition, the differences in physical and electrical properties as compared to the gaseous phase application of IDEs have been addressed and discussed.

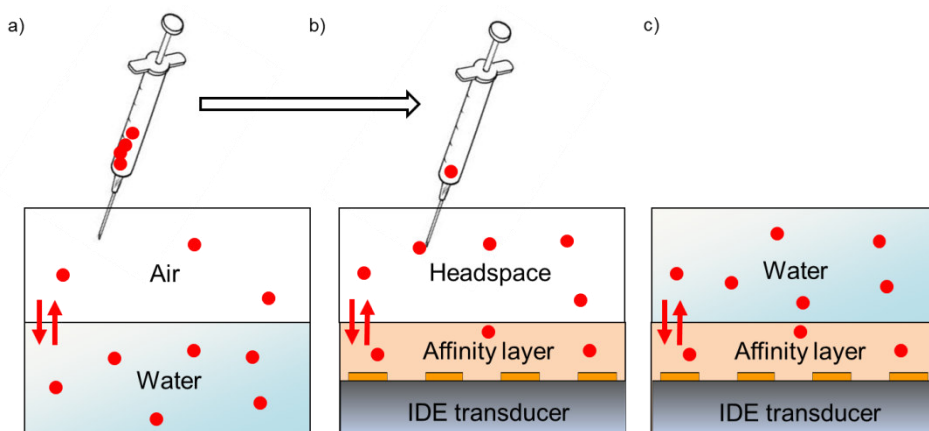


Figure 1.5. Schematic overview of a) sampling from the gas space above the aqueous sample for b) further analysis from the gas phase, the so-called headspace, by an IDE transducer with an affinity layer, and c) the system under study: the direct analysis in the aqueous phase by means of an IDE transducer covered with an affinity layer.

1.5 Organization of this Thesis

This work is the result of an intense collaboration with technicians, engineers, and researchers of different disciplines. For this reason, a prerequisite of its content is to make it accessible to people of different professional backgrounds. To this end, the thesis is built up as a systematic guide that covers the theoretical basics, demonstrates the proof-of-principle, points out (future) system requirements, addresses future research and engineering tasks, and shares all relevant expertise as gathered throughout the study and research phases.

Chapter 1: Introduction to surface-engineered sensors with a clear focus on the IDE platforms and the current investigation of their application as gas sensors, followed by the presentation of a proposed application directly in water, the thesis motivation, and the thesis outline.

Chapter 2: This chapter represents a theoretical background section, providing fundamental knowledge on the principles of capacitors and capacitive measurements, including basics on the two-port and three-signal measurement

techniques as well as on shielding and guarding techniques for a reliable sensing performance.

Chapter 3: The properties of polymer-coated IDE platforms are reviewed and the most important design parameters are introduced. Then, the detection mechanisms of these platforms that contribute to the overall capacitive response and the challenges of applying these sensor platforms in aqueous environments are discussed.

Chapter 4: A detailed description of the measurement setup is given. This includes information on the designed interdigitated electrode platforms, the individual components of the flow cell setup, and the measurement principles of the universal transducer interface that is used throughout this work.

Chapter 5: Water increases parasitic electrical coupling to other system parts and the surrounding, which in turn introduces an undesired device sensitivity to the water composition. It is shown how water-enhanced electrical coupling of the IDE sensing field to guarding electrodes is an effective way to reduce response sensitivity to such parasitic events.

Chapter 6: The capacitive response of PDMS-coated interdigitated electrode platforms directly exposed to aqueous solutions containing different pollutants (chloroform, 1-hexanol, methyl tert-butyl ether, toluene, m-xylene, and n-hexane) for stable ambient and water conditions is experimentally investigated and discussed.

Chapter 7: This chapter recaps the main fundamental issues and various challenges that have been encountered throughout the study, research, and development phase. It points out system requirements and future work prospects that promote the development of reliable detection and measuring systems based on polymer-coated IDE technology.

The thesis is finalized with a summary in both English and Dutch, an information part on the received recognition, and the acknowledgement and the short biography of the author.

1.6 References

- 1 J. H. Huijsing, Smart sensor systems: Why? Where? How?, in *Smart Sensor Systems*, ed. by G. C. M. Meijer (Chichester, U.K.: John Wiley & Sons, Ltd., 2008), pp. 1-22.
- 2 E. Cominelli, M. Galbiati, C. Tonelli, and C. Bowler, Water: the invisible problem. Access to fresh water is considered to be a universal and free human right, but dwindling resources and a burgeoning population are increasing its economic value, *EMBO Report*, 10 (2009), 671-676.
- 3 C. Vandecasteele, Block, C., Milieuproblemen en -technologie; lucht, water en bodem, rol van de industrie (Leuven, Belgium: Lanoo-campus, 2006).
- 4 A. Kungolos, P. Samaras, V. Tsiridis, M. Petala, and G. Sakellaropoulos, Bioavailability and toxicity of heavy metals in the presence of natural organic matter, *Journal of Environmental Science and Health, Part A*, 41 (2006), 1509-1517.
- 5 C. Achten, and W. Puttmann, Determination of methyl tert-butyl ether in surface water by use of solid-phase microextraction, *Environmental Science & Technology*, 34 (2000), 1359-1364.
- 6 F. Fang, C. S. Hong, S. G. Chu, W. P. Kou, and A. Bucciferro, Reevaluation of headspace solid-phase microextraction and gas chromatography-mass spectrometry for the determination of methyl tert-butyl ether in water samples, *Journal of Chromatography A*, 1021 (2003), 157-164.
- 7 F. Piazza, A. Barbieri, F. S. Violante, and A. Roda, A rapid and sensitive method for methyl tert-butyl ether analysis in water samples by use of solid phase microextraction and gas chromatography-mass spectrometry, *Chemosphere*, 44 (2001), 539-544.
- 8 J. Klinger, C. Stieler, F. Sacher, and H. J. Branch, MTBE (methyl tertiary-butyl ether) in groundwaters: Monitoring results from Germany, *Journal of Environmental Monitoring*, 4 (2002), 276-279.
- 9 S. Nakamura, and S. Daishima, Simultaneous determination of 22 volatile organic compounds, methyl-tert-butyl ether, 1,4-dioxane, 2-methylisoborneol and geosmin in water by headspace solid phase microextraction-gas chromatography-mass spectrometry, *Analytica Chimica Acta*, 548 (2005), 79-85.
- 10 G. W. Schade, G. B. Dreyfus, and A. H. Goldstein, Atmospheric methyl tertiary butyl ether (MTBE) at a rural mountain site in California, *Journal of Environmental Quality*, 31 (2002), 1088-1094.
- 11 J. D. Fair, W. F. Bailey, R. A. Felty, A. E. Gifford, B. Shultes, and L. H. Volles, Quantitation by portable gas chromatography: Mass spectrometry of VOCs associated with vapor intrusion, *International Journal of Analytical Chemistry*, 2010 (2010), 1-6.
- 12 Y. Madrid, and Z. P. Zayas, Water sampling: Traditional methods and new approaches in water sampling strategy, *TrAC Trends in Analytical Chemistry*, 26 (2007), 293-299.
- 13 A. Hulanicki, Glab, S., Ingman, F., Chemical sensors: Definitions and classification, *Pure & Applied Chemistry*, 63 (1991), 1247-1250.
- 14 T. Ishihara, and S. Matsubara, Capacitive type gas sensors, *Journal of Electroceramics*, 2 (1998), 215-228.

- 15 J. Janata, Electrochemical sensors and their impedances: A tutorial, *Critical Reviews in Analytical Chemistry*, 32 (2002), 109-120.
- 16 B. Adhikari, and S. Majumdar, Polymers in sensor applications, *Progress in Polymer Science*, 29 (2004), 699-766.
- 17 J. Janata, and A. Bezegh, Chemical sensors, *Analytical Chemistry*, 60 (1988), 62R-74R.
- 18 D. Grieshaber, R. MacKenzie, J. Vörös, and E. Reimhult, Electrochemical biosensors: Sensor principles and architectures, *Sensors*, 8 (2008), 1400-1458.
- 19 H. Farahani, R. Wagiran, and M. Hamidon, Humidity sensors principle, mechanism, and fabrication technologies: A comprehensive review, *Sensors*, 14 (2014), 7881-7939.
- 20 K. J. Albert, N. S. Lewis, C. L. Schauer, G. A. Sotzing, S. E. Stitzel, T. P. Vaid, and D. R. Walt, Cross-reactive chemical sensor arrays, *Chemical Reviews*, 100 (2000), 2595-2626.
- 21 J. W. Grate, Nelson, D. A., Kaganove, S. N., Polymers for chemical sensors using hydrosilylation chemistry (Richland, Washington, U.S.A.: Pacific Northwest National Laboratory, 2001).
- 22 B. R. Goldsmith, J. J. Mitala, J. Josue, A. Castro, M. B. Lerner, T. H. Bayburt, S. M. Khamis, R. A. Jones, J. G. Brand, S. G. Sligar, C. W. Luetje, A. Gelperin, P. A. Rhodes, B. M. Discher, and A. T. C. Johnson, Biomimetic chemical sensors using nanoelectronic readout of olfactory receptor proteins, *ACS Nano*, 5 (2011), 5408-5416.
- 23 Y.-F. Sun, S.-B. Liu, F.-L. Meng, J.-Y. Liu, Z. Jin, L.-T. Kong, and J.-H. Liu, Metal oxide nanostructures and their gas sensing properties: A review, *Sensors*, 12 (2012), 2610-2631.
- 24 M. M. Arafat, B. Dinan, S. A. Akbar, and A. S. M. A. Haseeb, Gas sensors based on one dimensional nanostructured metal-oxides: A review, *Sensors*, 12 (2012), 7207-7258.
- 25 G. Jimenez-Cadena, J. Riu, and F. X. Rius, Gas sensors based on nanostructured materials, *Analyst*, 132 (2007), 1083-1099.
- 26 V. A. Antohe, Radu, A., Yunus, S., Attout, A., Bertrand, P., Matefi-Tempfli, M., Piraux, L., Matefi-Tempfli, S., A versatile method to grow localized arrays of nanowires for highly sensitive capacitive devices, *Journal of Optoelectronics and Advanced Materials*, 10 (2008), 2936-2941.
- 27 P. Malik, V. Katyal, V. Malik, A. Asatkar, G. Inwati, and T. K. Mukherjee, Nanobiosensors: Concepts and variations, *ISRN Nanomaterials*, 2013, Article ID 327435 (2013).
- 28 X. Chen, C. K. Y. Wong, C. A. Yuan, and G. Zhang, Nanowire-based gas sensors, *Sensors and Actuators B-Chemical*, 177 (2013), 178-195.
- 29 O. Brand, B. Mizaikoff, Membrane-based sensor measures pollutants present in aqueous and gaseous environments, *Membrane Technology*, 1 (2008), 9-10.
- 30 C. K. Ho, A. Robinson, D. R. Miller, and M. J. Davis, Overview of sensors and needs for environmental monitoring, *Sensors*, 5 (2005), 4-37.
- 31 C. K. Ho, E. R. Lindgren, K. S. Rawlinson, L. K. McGrath, and J. L. Wright, Development of a surface acoustic wave sensor for in-situ monitoring of volatile organic compounds, *Sensors*, 3 (2003), 236-247.

- 32 C. K. Ho, and R. C. Hughes, In-situ chemiresistor sensor package for real-time
detection of volatile organic compounds in soil and groundwater, *Sensors*, 2
(2002), 23-34.
- 33 C. K. Ho, McGrath, L. K., Davis, C. E., Thomas, M. L., Wright, J. L., Kooser,
A. S., Hughes, R. C., SAND-Report, SAND2003-3410, (2003).
- 34 C. Jin, P. Kurzawski, A. Hierlemann, and E. T. Zellers, Evaluation of
multitransducer arrays for the determination of organic vapor mixtures,
Analytical Chemistry, 80 (2008), 227-236.
- 35 R. V. Harrison, Chemical sensors: properties, performance and applications
(New York, U.S.A.: Nova Science Pub., Inc., 2010).
- 36 A. Hierlemann, Integrated chemical microsensor systems in CMOS-
technology, *Solid-State Sensors, Actuators and Microsystems, Digest of
Technical Papers, TRANSDUCERS '05*, 2 (2005), 1134-1137.
- 37 M. Graf, D. Barretino, H. P. Baltes, and A. Hierlemann, eds., CMOS hotplate
chemical microsensors. ed. by D. Liepmann H. Fujita, *Microtechnology and
MEMS* (Heidelberg, Germany: Springer Verlag, 2007).
- 38 R. de la Rica, C. Fernandez-Sanchez, and A. Baldi, Polysilicon interdigitated
electrodes as impedimetric sensors, *Electrochemistry Communications*, 8
(2006), 1239-1244.
- 39 M. Paeschke, U. Wollenberger, C. Kohler, T. Lisek, U. Schnakenberg, and R.
Hintsche, Properties of interdigital electrode arrays with different geometries,
Analytica Chimica Acta, 305 (1995), 126-136.
- 40 T. Hofmann, K. Schröder, J. Zacheja, and J. Binder, Fluid characterization
using sensor elements based on interdigitated electrodes, *Sensors and
Actuators B-Chemical*, 37 (1996), 37-42.
- 41 G. Harsanyi, Polymer films in sensor applications: a review of present uses and
future possibilities, *Sensor Review*, 20 (2000), 98-105.
- 42 T. Islam, U. Mittal, A. T. Nimal, and M. U. Sharma, A nanoporous thin-film
miniature interdigitated capacitive impedance sensor for measuring humidity,
International Journal of Smart and Nano Materials, 5 (2014), 169-179.
- 43 K.-S. Chou, and C.-H. Lee, Fabrication of silver interdigitated electrode by a
stamp method, *Advances in Materials Science and Engineering*, 2014 (2014),
5.
- 44 X. Tang, D. Flandre, J.-P. Raskin, Y. Nizet, L. Moreno-Hagelsieb, R. Pampin,
and L. A. Francis, A new interdigitated array microelectrode-oxide-silicon
sensor with label-free, high sensitivity and specificity for fast bacteria
detection, *Sensors and Actuators B-Chemical*, 156 (2011), 578-587.
- 45 G. Eranna, B. C. Joshi, D. P. Runthala, and R. P. Gupta, Oxide materials for
development of integrated gas sensors - A comprehensive review, *Critical
Reviews in Solid State and Materials Sciences*, 29 (2004), 111-188.
- 46 M. Kitsara, K. Beltsios, D. Goustouridis, S. Chatzandroulis, and L. Raptis,
Sequential polymer lithography for chemical sensor arrays, *European Polymer
Journal*, 43 (2007), 4602-4612.
- 47 M. Kitsara, D. Goustouridis, S. Chatzandroulis, K. Beltsios, and L. Raptis, A
lithographic polymer process sequence for chemical sensing arrays,
Microelectronic Engineering, 83 (2006), 1192-1196.

- 48 M. Kitsara, D. Goustouridis, S. Chatzandroulis, M. Chatzichristidi, I. Raptis, T. Ganetsos, R. Igreja, and C. J. Dias, Single chip interdigitated electrode capacitive chemical sensor arrays, *Sensors and Actuators B-Chemical*, 127 (2007), 186-192.
- 49 B. J. de Gans, P. C. Duineveld, and U. S. Schubert, Inkjet printing of polymers: State of the art and future developments, *Advanced Materials*, 16 (2004), 203-213.
- 50 S. Dimopoulos, M. Kitsara, D. Goustouridis, S. Chatzandroulis, and I. Raptis, A chemocapacitive sensor array system for gas sensing applications, *Sensor Letters*, 9 (2011), 577-583.
- 51 B. Costello, P. S. Sivanand, N. M. Ratcliffe, and D. M. Reynolds, The rapid detection of methyl tert-butyl ether (MtBE) in water using a prototype gas sensor system, *Water Science and Technology*, 52 (2005), 117-123.
- 52 C. Hagleitner, Multi-sensor interfaces. ed. by J. H. Huijsing, M. Steyaert and A. VanRoermund, *Analog Circuit Design: Sensor and Actuator Interface Electronics, Integrated High-Voltage Electronics and Power Management, Low-Power and High-Resolution ADC's* (Dordrecht: Springer, 2004), pp. 43-64.
- 53 P. Oikonomou, G. P. Patsis, A. Botsialas, K. Manoli, D. Goustouridis, N. A. Pantazis, A. Kavadias, E. Valamontes, T. Ganetsos, M. Sanopoulou, and I. Raptis, Performance simulation, realization and evaluation of capacitive sensor arrays for the real time detection of volatile organic compounds, *Microelectronic Engineering*, 88 (2011), 2359-2363.
- 54 C. Hagleitner, A. Hierlemann, D. Lange, A. Kummer, N. Kerness, O. Brand, and H. Baltes, Smart single-chip gas sensor microsystem, *Nature*, 414 (2001), 293-296.
- 55 P. Kurzawski, C. Hagleitner, and A. Hierlemann, Detection and discrimination capabilities of a multitransducer single-chip gas sensor system, *Analytical Chemistry*, 78 (2006), 6910-6920.
- 56 X. Li, and G. C. M. Meijer, Capacitive sensors, in *Smart Sensor Systems*, ed. by G. C. M. Meijer (Chichester, U.K. : John Wiley & Sons, Ltd., 2008), pp. 225-248.
- 57 S. V. Patel, T. E. Mlsna, B. Fruhberger, E. Klaassen, S. Cemalovic, and D. R. Baselt, Chemicapacitive microsensors for volatile organic compound detection, *Sensors and Actuators B-Chemical*, 96 (2003), 541-553.
- 58 R. Igreja, and C. J. Dias, Analytical evaluation of the interdigital electrodes capacitance for a multi-layered structure, *Sensors and Actuators A-Physical*, 112 (2004), 291-301.
- 59 A. M. Kummer, A. Hierlemann, and H. Baltes, Tuning sensitivity and selectivity of complementary metal oxide semiconductor-based capacitive chemical microsensors, *Analytical Chemistry*, 76 (2004), 2470-2477.
- 60 J. W. Gardener, Barlett, B. N., *Techniques and mechanism in gas sensing* (Bristol, England: IOP-Publishing, 1991).
- 61 A. Hierlemann, M. Schweizer-Berberich, U. Weimar, G. Kraus, A. Pfau, and W. Göpel, Pattern recognition and multicomponent analysis, *Sensors Update*, 2 (1996), 119-180.

- 62 G. C. Osbourn, J. W. Bartholomew, A. J. Ricco, and G. C. Frye, Visual-empirical region-of-influence pattern recognition applied to chemical microsensor array selection and chemical analysis, *Accounts of Chemical Research*, 31 (1998), 297-305.
- 63 T. Zhou, L. Wang, and T. Jionghua, Pattern recognition of the universal electronic nose, in *Intelligent Information Technology Application, 2008. IITA '08. International Symposium on*, (2008), pp. 249-253.
- 64 G. Amendola, G.-N. Lu, and L. Babadjian, Signal-Processing Electronics for a Capacitive Micro-Sensor, *Analog Integrated Circuits and Signal Processing*, 29 (2001), 105-113.
- 65 G. C. M. Meijer, Interface Electronics and Measurement Techniques for Smart Sensor Systems, in *Smart Sensor Systems*, ed. by G. C. M. Meijer (Chichester, U.K.: John Wiley & Sons, Ltd., 2008), pp. 23-54.
- 66 R. Igreja, and C. J. Dias, Organic vapour discrimination using sorption sensitive chemocapacitor arrays, *Advanced Materials Forum Iii, Pts 1 and 2*, 514-516 (2006), 1064-1067.
- 67 R. Igreja, and C. J. Dias, Dielectric response of interdigital chemocapacitors: The role of the sensitive layer thickness, *Sensors and Actuators B-Chemical*, 115 (2006), 69-78.
- 68 R. Igreja, and C. J. Dias, Capacitance response of polysiloxane films with interdigital electrodes to volatile organic compounds, *Advanced Materials Forum Ii*, 455-456 (2004), 420-424.

THEORETICAL BACKGROUND: PRINCIPLES OF CAPACITIVE MEASUREMENTS

The fundamentals of capacitors, capacitance, and capacitive measurement techniques are discussed in this chapter. Capacitors are used as temporary storage components or as sensing devices and in common applications such as filters. Capacitive measurements can accurately be performed with instrumentation based on harmonic Inductance-Capacitance (LC) oscillators. However, this technology is not very suited to be applied in integrated circuits of low-cost transducer interfaces. Instead of this, usually block-shaped excitation signals are used, which are generated with so-called relaxation oscillators. The performance of capacitive measurement systems can significantly be enhanced by applying the so-called two-port and three-signal measurement methods that allow the reduction of parasitic capacitances, off-sets, and gains. Furthermore, shielding and guarding techniques are used to remedy the problem of external interferences and parasitic electric-field bending so that ultimate detection performances can be achieved.

2.1 The Capacitor

If a voltage is applied to an electrical circuit, the induced electric current experiences an opposition, which is called impedance. Impedance can be a combination of electrical resistance, capacitance, and inductance. The resistor dissipates energy and the capacitor and the inductor store energy in an electrical and magnetic field, respectively. Capacitors are extensively used as temporary energy storage devices in the electrical circuits of electronics to perform a variety of tasks, such as memory storage.¹ In addition, capacitors can be used as transducer platforms for, *e.g.*, position and speed measurements, material characterization, and other sensing purposes.² Capacitors commonly consist of two electrodes separated by an insulating material, the dielectric, which can be configured in different ways, including parallel plates, rolled (foiled) films, and interdigitated electrodes (IDEs) as shown in Figure 2.1.

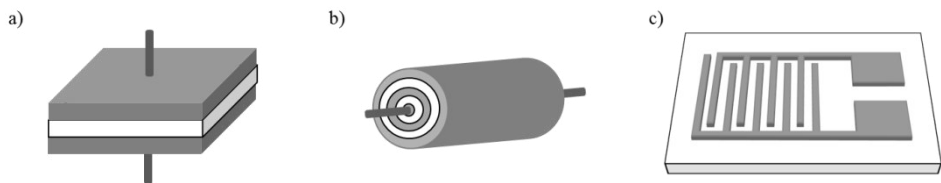


Figure 2.1. Schematic representation of a) a parallel-plate capacitor, b) a (simplified) foiled capacitor, and c) an interdigitated electrode (IDE) capacitor. The grey areas represent the electrodes and the white areas represent the dielectric materials (a, b) and the support substrate for the IDEs (c).

The concept of capacitance can easily be explained by considering a parallel-plate capacitor that is charged by a voltaic cell (V). A parallel-plate capacitor is composed of two conducting plates (the electrodes) of a certain area (A), which are separated by an insulating material (the dielectric) that is of a certain thickness, defining the distance or spacing (d) between the plate electrodes. In the simplest example, the plates can be separated by vacuum or air. In commercial capacitors the dielectric is, *e.g.*, a polymer, a ceramic, or an oxide. The choice of dielectric material typically depends on the capacitor size and the application and operation conditions. For a start, we consider a capacitor with a vacuum being present between the electrodes. When one electrode of the capacitor is connected to the positive pole of a direct voltage source while the other electrode is connected to ground potential, then an electric current can flow as depicted

in Figure 2.2. The voltage is sometimes referred to as the driving force for the electric current, which is the flow of electric charges. In solid materials, such as metals, these are only the electrons capable of creating the charge flow. Yet, by convention the direction of the current flow is assigned from the positive towards the negative (or ground) pole and hence in the opposite direction of the electron flow. The electric current i_1 towards the plate electrode connected to the positive pole may then be viewed as a flow of positive charges (holes). The positive charges on the plate electrode attract electrostatically negative charges on the opposing plate electrode, to which—as according to convention—the electric current i_2 is assigned. The charges are hence electrostatically held or stored on the plate electrodes. For an ideal parallel-plate capacitor, the electric field established between the electrodes is homogeneous over the total plate area, and the electric field line length is equal to the distance between the electrode plates. However, at the edges of the plate electrodes a stray field can form, which is represented as bended field lines in Figure 2.2b.

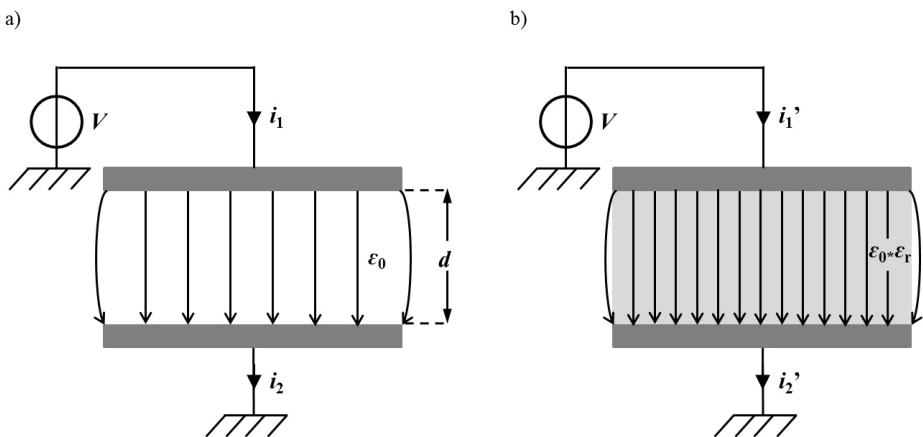


Figure 2.2. Schematic representation of a parallel-plate capacitor connected to the positive pole of a direct voltage source (V); the negative pole is connected to the earth or ground potential and the resulting currents (i_1) and (i_2) for a) a vacuum ($\epsilon_r = 1$) and b) an inserted dielectric ($\epsilon_r > 1$) are depicted. Notice that the charging currents in b) are larger than those in a) as more charges are stored on the capacitor, which is indicated by the denser electric field lines. Also depicted is the stray field at the edges of the plate electrodes.

2.2 The Capacitance

The amount of charges Q ‘pushed’ onto the electrodes is linearly related to the applied voltage U . (Equation 2.1). The proportionality constant is the capacitance C , which is the amount of charge on the plate and expressed in Coulomb (C) per Volt (V). The unit of the electrical capacitance is by definition the Farad (F).

$$C = \frac{Q}{U} \quad (2.1)$$

The capacitance is determined by the absolute permittivity of the dielectric material (ϵ) and the geometric dimensions of the capacitor electrodes, *i.e.*, the area (A) and mutual distance (d). It can be shown that the capacitance is proportional to the area of the electrodes and inversely proportional to the distance between the plates. The larger the distance between the plates, the lower the Coulombic attractive electrostatic forces between the charges on the opposing plate electrodes. The charges accumulated onto the plate electrodes also experience mutual repulsive forces. For a capacitor with only vacuum between the plates, it can be shown that the proportionality factor is equal to 8.854 pF/m. This is the dielectric constant of vacuum (ϵ_0), also named the permittivity of free space, which is a physical constant. When a dielectric material is inserted between the plate electrodes, the capacitance rises to higher value. The factor by which the capacitance increases as compared to the vacuum is called the relative dielectric constant (ϵ_r). Hence, the proportionality constant is the dielectric constant or absolute permittivity (ϵ), for which $\epsilon = \epsilon_0 * \epsilon_r$, and the relative dielectric constant of vacuum is then by definition 1. Therefore, the Equation 2.1 can be rewritten as Equation 2.2:

$$C = \epsilon_0 \epsilon_r \frac{A}{d} \quad (2.2)$$

The reason why the capacitance increases upon insertion of a material is that the dielectric can polarize, that is charge displacements over the length of a single atom, ionic compound or molecule occurring within the material. There are no excess charges within the bulk of a polarized homogeneous dielectric material as the neighboring induced charges compensate each other electrostatically. At the surface of the material the charges are compensated by charges on the electrodes. Therefore, with a dielectric between the electrodes more charges can be accumulated as compared to vacuum.

2.3 Electronic Representation

As explained in the previous paragraph, in its simplest form, a capacitor can be constructed as a parallel-plate capacitor (Figure 2.2). In this case, it is assumed that all electrical circuit components are ideal and no current leakage across the capacitor and no voltage drop across the leads and connects occur. However, real capacitors (C) are subject to non-idealities. The materials involved, the leads, the connects, the plate electrodes, and the dielectric have an intrinsic resistance, which causes energy dissipation (R_S) or leakage currents between the plate electrodes (R_P). For high-frequency measurements, also the inductance (L_S) of, *e.g.*, the inductive loops between the leads can become significant. Figure 2.3a and 2.3b depict a common way of electronically representing an ideal and a non-ideal capacitor, respectively.

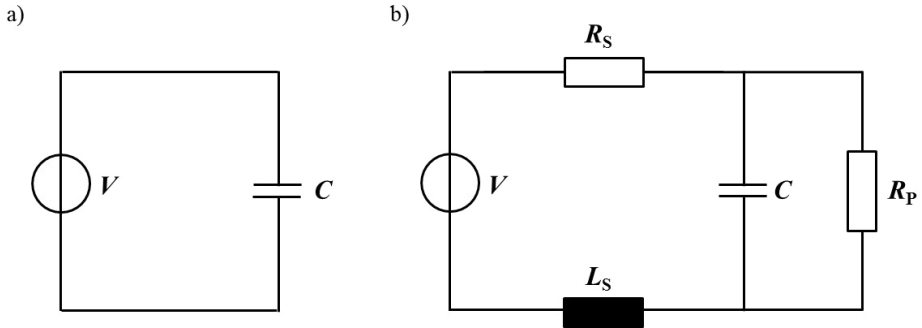


Figure 2.3. Equivalent electronic circuit of a) an ideal capacitor (C) and b) a non-ideal capacitor that is connected in series with an inductor (L_S) and an energy dissipation resistor (R_S) and in parallel with a leakage resistor (R_P).

At very high frequencies, an inductor has a very high impedance and prevents the capacitor in series from being charged. In contrast, at very low frequencies, a capacitor has a very high impedance while an inductor behaves like a short circuit. In addition, the polarized dielectric can dissipate energy itself, a process known as dielectric absorption. For further reading on the principles of capacitors, capacitance, and electronic representation, we recommend literature on electrical fundamentals.^{1,3,4}

2.4 Capacitance Measurements

Capacitors as electronic components can be purchased with high precision regarding their specification. These components can be assumed to be constant under the specified operation conditions of their common application. The task of capacitive sensor systems however is to measure changes in either the dielectric properties or the electrode dimensions of the capacitive transducer element as induced by a physical event. It is hence just desirable that the capacitance changes sensitively and if possible selectively to the event to be detected.

Capacitance measurements can be performed via different techniques, and the measurement accuracy and reliability are often linked to the price of the measurement instruments.⁵ As suggested, the capacitance can be determined from, *e.g.*, applying a direct voltage and measuring the charge flow or by applying a constant current source and measuring the voltage drop across the capacitor in its charged state. The latter principle is applied by a common multi-meter, probably the best-known example of a low-cost measurement device.⁵ A more accurate—but also more expensive—method is by using harmonic oscillators. These are modifiers capable of generating an alternating sinusoidal excitation signal (*e.g.*, voltage) of known frequencies and of synchronous detection of sine-shape signals (*e.g.*, current). By comparing the phase shift between the excitation and resulting *AC* signal, the capacitance can be derived. These instruments, that are said to work in the so-called frequency-domain, also allow the reduction of noise and interference effects.² An example is the Inductance-Capacitance-Resistance (*LCR*) meter or impedance analyzer. Yet, their electronic circuitry is far too complex to be integrated into low-cost chips.² Low-cost transducer interfaces typically work with simple block signals that can easily be generated from a direct voltage source, such as the voltage feed of a laptop.

In combination with various other techniques, including auto-calibration, chopping, dynamic element matching, and synchronous detection, measurement errors, drifts, noises, and interferences can be eliminated or reduced, and reliable and accurate measurements can be performed.⁶ An extended basic discussion of capacitance measurements can be found in recommended literature.⁷

2.5 Parasitic Effects and Noise

In capacitive measurements, it is of importance that the measurement currents remain unaffected by:

- a) Disturbing signals, such as interference and noise, which are not correlated with the excitation signals. The effect of such signals can be reduced by lowering the bandwidth while applying synchronous detection. As an alternative, many measurement results can be averaged over time so that the effect of the uncorrelated signals reduces with, for instance, the square root of the total measurement time. Examples of such disturbing signals are electromagnetic interferences (EMI), such as those coming from an external voltage source, and noise generated in the electronic components.
- b) Parasitic effects, which can cause systematic errors. Such effects will repeat every time when a measurement is repeated. In other words, repeating and averaging of the result will not improve the resolution. Examples of such parasitic effects are:
 1. electric-field bending, such as towards the shielded, *i.e.*, grounded sensor housing;
 2. parasitic capacitors as formed by the connection cables;
 3. shunting conductance due to contamination and water condensation.

For a measurement system, there are inherent noise sources, which are of low- and high-frequency origin. For instance, the electric power supply voltage and frequency of the domestic grid in Europe is 230 V and 50 Hz (and 120 V and 60 Hz in the United States), which can be a source for low-frequency interference while a microprocessor that operates at mega- or gigaHertz can be a source for high-frequency interference.

In the following sections it will be discussed how these disturbing signals and parasitics can be reduced or at least their effect can be reduced, and how the accuracy and reliability of the capacitive measurement can be enhanced by applying smart measurement techniques.

2.5.1 Shielding and Guarding

Shielding is a common technique to reduce external interferences as caused, for example, by an external voltage source (V_{int}) that induces parasitic currents (i_{int}). This is typically achieved by placing the sensing device into a grounded housing that fully encloses the sensor. However, this shield itself causes electric-field bending. Then, the application of so-called guarding electrodes can be a remedy. With guarding, *i.e.*, by surrounding the receiving (grounded) capacitor electrode with additional grounded electrodes, a part of the electric field originating from the transmitting electrode is sacrificed to the guarding electrodes. The residual electric sensing field is geometrically shielded off and is protected. Figure 2.5 shows a schematic representation of a parallel-plate capacitor that is fed by an alternating voltage source for the excitation signal (V_m). An electric current (i_1) flows to the transmitting electrode. An electric field is not only established with the receiving counter electrode but also with the shield and the guarding electrodes. The resulting induced currents (i_2 , i_G , i_S) are depicted. For sensing purposes, the current (i_2) is to be measured as it is not influenced by electric-field bending.

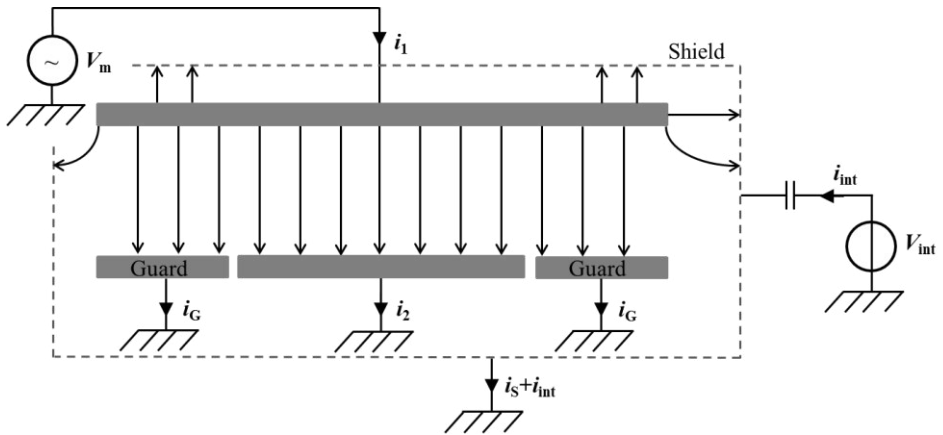


Figure 2.5. Schematic representation of a parallel-plate capacitor that is excited by an alternating voltage source (V_m). The dashed line indicates a grounded shield that prevents the current induced by external voltage sources (V_{int}) to reach the internal sensitive region. The guarding electrodes preserve a homogeneous electric sensor field that is not coupled to the shield. Also depicted are the resulting electric currents (i_1 , i_2 , i_G , i_S , i_{int}). Figure adapted.²

2.5.2 Two-Port Measurement Technique

For sensor transducer elements that are integrated into specific device holders, onto printed circuit boards, or in single-chip devices, it can generally be assumed that the impedances of other system parts, such as connectors and cables, are connected in parallel or in series with the sensing device. Therefore, their impedances also contribute and influence the overall electronic response. For long cables, for example, a so-called one-port measurement technique does not account for their electrical contributions. However, with the so-called two-port measurement technique, such problems can be solved. In capacitance measurements, application of the two-port measurement technique is essential as it eliminates the effect of parasitic capacitances of the cables that connect the sensing capacitor to the supply source and the current meter. In this configuration, the sensing capacitor (C_X) and the parasitic cable capacitors (C_{P1} , C_{P2}) form a so-called pi- (π) -network, as shown in Figure 2.6. The capacitor C_{P1} is connected in parallel to the voltage source V_m . The voltage source V_m should have a low impedance Z_{source} , so that the current through C_{P1} causes only a negligible voltage drop over Z_{source} . Consequently, it does not influence the measurement current i_m through C_X . On the other side of the capacitor, capacitor C_{P2} is “short-circuited” by the low-ohmic impedance of the current sensor and hence only a negligible voltage drop across C_{P2} and current through C_{P2} occur. Consequently, the current i_m is equal to the charge/discharge current of the capacitor C_X . For further reading on this measurement technique, we recommend following literature.^{2, 6, 8}

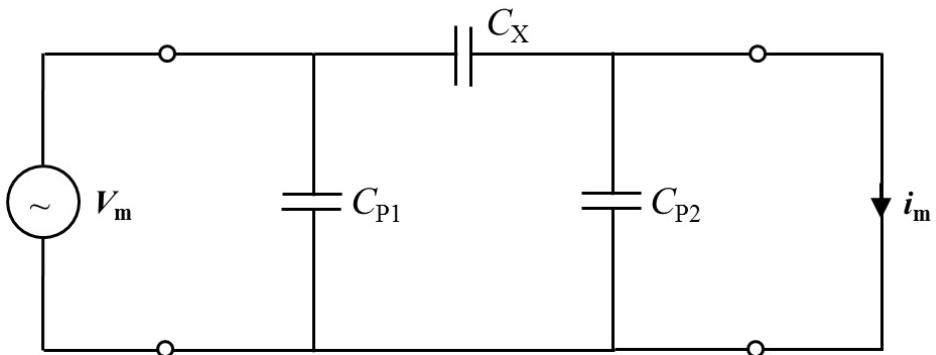


Figure 2.6. Equivalent electronic circuit of a sensor capacitor (C_X) and the parasitic cable capacitors (C_{P1} , C_{P2}) that are connected in a π -network, and representation of the measurement current i_m . Figure adopted.⁶

2.5.3 Three-Signal Measurement Technique

In capacitance measurements, it is common to compare the measured capacitance of the sensor capacitor with a reference capacitor. In order to get rid of unknown offsets and unknown gains in the system, the so-called three-signal measurement technique is applied.⁸⁻¹⁰ In addition to measuring the sensing capacitor, also a reference capacitor of known value and an offset capacitor are measured. The offset measurement is, *e.g.*, an open-circuit measurement. By performing the offset measurement, any parasitic parallel capacitance that is not attributed to the capacitor of interest is measured and can eventually be subtracted from the final capacitance measurement. For further reading on this measurement technique, we recommend following literature.^{2, 6, 8}

2.5.4 Sensor Packaging

Proper sensor packaging guarantees a good contact between the sensing element and the environment to be tested, while preserving it in that harsh environment.⁶ In this study, we investigate the detection possibility of polymer-coated interdigitated electrodes that are directly exposed to water containing the target compounds. As will be discussed in Chapter 3, it is a requirement that the polymer is both insulating and water repellent, allowing only the uptake of small amounts of water vapor. Good adhesion between the polymer layer and the transducer interface is a further requirement to prevent water settlement on and between the electrodes, thereby preventing the formation of shunt resistances. Yet, contamination remains an issue. Obviously, a sensing device made up of micro- or nanometer-sized electrodes covered with functional layers or receptors with dimensions on the same or even smaller size-scale cannot directly be exposed to harsh environments, such as natural water or waste water streams. Proper packaging of the sensing element will be necessary to establish a gentle contact between the fragile polymeric sensing layer and the water phase and to prevent the settlement of dirt and possible mechanical damage. A possible solution is the use of water-proof housings and the integration of filter elements or membranes,¹¹ depending on the matter to be kept outside of the sensing chamber. Hence, the packaging requirements depend strongly on the real composition and environment of the water under investigation.

2.6 Concluding Remarks

A capacitor stores energy within an electric field. Charges are electrostatically stored on the electrodes. The capacitance is defined as the amount of charges that can be stored on the electrodes per applied voltage across the capacitor. The capacitance is determined by the areas of the electrodes, by their mutual distance, and by the inserted (dielectric) material. In real systems a capacitor also possesses several non-ideal properties such as series resistance, causing energy dissipation, and parallel resistance, leading to further leakage currents. Further measurement problems can be caused by electromagnetic interferences (EMI), electric-field bending, parasitic capacitances, and shunt resistances as caused by contamination and water condensation. Electromagnetic interferences, such as induced by external voltage sources, can be diminished by shielding the capacitor from the surrounding by a grounded housing. Yet, shielding itself is a cause for electric-field bending. Fortunately, such bending can be remedied by the application of guarding electrodes. The influence of parasitic capacitances can be reduced by choosing the proper electronic measurement techniques. Two simple but powerful methods applied in capacitance measurements, which are also suited for low-cost systems, are the two-port measurement and the three-signal measurement technique. These methods reduce greatly the effect of parasitic capacitances for the sensor electrodes to ground, such as the cable capacitance, as well as capacitance offsets and unpredictable gain variations. Eventually, proper packaging guarantees good contact between the environment to be tested while keeping it from damage.

2.7 References

- 1 R. R. D. Halliday, J. Walker, Fundamentals of physics; Chapter 26 - Capacitance (New York, U.S.A.: John Wiley & Sons, Inc., 2001).
- 2 X. Li, Meijer, G. C. M., Capacitive sensors, in *Smart Sensor Systems*, ed. by G. C. M. Meijer (Chichester, U.K.: John Wiley & Sons, Ltd., 2008), pp. 225-248.
- 3 I. Wolff, Einführung in die Elektrotechnik (Aachen, Germany: Nellisen-Wolff GmbH, 1997).
- 4 G. M. P. A. Tipler, Physics for scientists and engineers; Part 4 - Electricity and magnetism (London, U.K.: W. H. Freeman & Co Ltd., 2007).
- 5 C. P. B. Coley, Using the right capacitance measurement technique, *EE Times-India* (2006), 1-3.
- 6 G. C. M. Meijer, Interface electronics and measurement technique for smart sensor systems, in *Smart Sensor Systems*, ed. by G. C. M. Meijer (Chichester, U.K.: John Wiley & Sons, Ltd., 2008), pp. 23-54.
- 7 G. C. M. Meijer, X. Li, B. P. Iliev, G. A. M. Pop, Z.-Y. Chang, S. N. Nihtianov, Z. Tan, A. Heidari, and M. A. P. Pertijs, Dedicated impedance-sensor systems, in *Smart Sensor Systems emerging technologies and applications*, ed. by M. A. P. Pertijs G. C. M. Meijer, K. Makinwa (Chichester, U.K.: John Wiley & Sons, Ltd., 2014), pp. 68-100.
- 8 F. M. L. Van der Goes, Low-cost smart sensor interfacing (Ph.D. Thesis, Delft University of Technology, 1996).
- 9 G. C. M. Meijer, J. van Drecht, P. C. de Jong, and H. Neuteboom, New concepts for smart signal processors and their application to PSD displacement transducers, *Sensors and Actuators A-Physical*, 35 (1992), 23-30.
- 10 M. J. S. Smith, L. Bowman, and J. D. Meindl, Analysis, design, and performance of micropower circuits for a capacitive pressure sensor IC, *IEEE Journal of Solid-State Circuits*, 21 (1986), 1045-1056.
- 11 C. K. Ho, and R. C. Hughes, In-situ chemiresistor sensor package for real-time detection of volatile organic compounds in soil and groundwater, *Sensors*, 2 (2002), 23-34.

DETECTION PRINCIPLES OF POLYMER-COATED INTERDIGITATED ELECTRODES

This chapter addresses the basics and the working principle of the polymer-coated interdigitated electrode (IDE) platform as a sensing device. Important design parameters of the transducer platform and the different detection mechanisms are discussed. This includes pollutant surface adsorption, bulk absorption, and resulting polymer swelling. A predestined polymer used for sensing application is the elastomeric silicone polydimethylsiloxane (PDMS), which is shortly introduced. Its visco-elastic and hydrophobic properties allow quick and reversible pollution absorption in combination with good sealing properties in water. Finally, it is explained how the system complexity is increased when these platforms are exposed directly to water.

3.1 IDE Platforms

Polymer-based capacitive sensors offer a polymeric sensing layer to the environment, into which chemical compounds can distribute. Within this concept, the polymer layer serves solely as a physical sorption phase without the involvement of a chemical reaction between the absorbed chemical compound and the polymer. That is the pollutants adsorb onto the polymer surface and are subsequently absorbed into the polymer bulk. Polymer-based interdigitated electrodes (IDEs) as transducer platforms for the capacitive detection of organic volatiles in the gaseous phase have been studied intensively by Igreja and Dias.¹⁻⁴ In this section, it will be discussed, which design parameters influence the capacitive response of the bare and polymer-coated IDE platform.

3.1.1 IDE Capacitance

In Chapter 2, the capacitance has been defined as the amount of charges stored on a capacitor per applied voltage. Briefly, the storage capacitance is thereby dependent on the dimensions and configuration of the capacitor electrodes and the dielectric properties of the insulating material that separates them. For polymer-coated IDEs, the sorption of chemical compounds onto and into the polymeric sensing layer results in a change of its dielectric constant ($\Delta\epsilon_r$) and hence in a change in the IDE capacitance (ΔC). If the two geometric dimensions electrode area (A) and electrode spacing or distance (d) are assumed to be constant, then the change in capacitance is solely determined by the change in the relative dielectric constant (Equation 3.1):

$$\Delta C = \epsilon_0 \Delta\epsilon_r \frac{A}{d} \quad (3.1)$$

where ϵ_0 is the dielectric constant of vacuum, which is a natural constant of value 8.854×10^{-12} F/m, and ϵ_r is the relative dielectric constant of the medium between the electrodes. For commercially available IDE sensors, it is usually documented how far—in units of length—the electric sensing field extends into the substrate, that is perpendicular from the IDE plane. The thickness of the inert support substrate, which represents the lower half of the electrode plane, is typically chosen as such that the

electric fringe field is constrained within the support substrate and only phenomena taking place on the upper half of the electrode plane lead to capacitance variations. This applies for the ideal case when the electric field is not submitted to interferences, such as electric-field bending. As capacitors form between two electrode fingers, two adjacent electrode fingers are necessary to form one capacitor. It can easily be calculated that for an IDE platform with N fingers, there are $N-1$ capacitors. These capacitors are all connected in parallel. Therefore, their capacitances add up and so do their changes (Equation 3.2):

$$\Delta C = \Delta C_1 + \Delta C_2 + \dots + \Delta C_{n-1} \quad (3.2)$$

Theoretically, this equation implies that by increasing the number of fingers and hence the number of parallel capacitors, any detection limit as determined by the noise level and by the resolution of the utilized measurement device can be reached. Yet, this would lead to very large IDE planes. The total capacitance and consequently the capacitive response upon a change in the dielectric constant is dependent on the relative dimensions of the sensor geometries area-to-distance rather than on the absolute dimensions. However, as this ratio has the dimension of length and minimization possibilities of IDE dimensions is often limited due to restrictions of the fabrication processes, small IDE planes mostly indicate small capacitance values. The calculation of the capacitance of the planar interdigitated electrodes with and without polymer layer is evidently not straightforward as for a simple parallel-plate capacitor. The inhomogeneous electric fringe field established between the interdigitated electrodes is approached in far more complex mathematical expressions, involving conformal mapping techniques,^{1,5} which goes beyond the scope of this study.

3.1.2 Design Parameters

Interdigitated electrodes have attractive features that allow optimizing the capacitance and its variations upon changes in the dielectric medium and hence tuning the sensitivity of the sensor device by manipulating its geometric dimensions.^{3, 6} In the previous section, it has already been addressed that the number of electrode fingers (N) determines the number of parallel connected capacitors, whose capacitances add up.

According to Equation 3.1, further increase in capacitance can be achieved by decreasing the so-called cell constant, which is the ratio of the electrode distance (d), usually denoted as the gap (G) between the electrodes, and the total electrode area (A) as determined by the electrode width (W) and length (L). It is to note that the height of the planar electrodes is often neglected and the structure is typically assumed to be two-dimensional. Also, as in contrast to a parallel-plate capacitor, for which the distance between the electrode plates is ideally equivalent to the electric field line length, the electric field for the planar IDE structure lies primarily bended out-of-plane. Therefore, its average electric field line length is considerably larger than the gap between the electrodes. Two important parameters, *i.e.*, the metallization ratio and the ‘ r^2 ’-ratio, have been defined by Igreja and Dias:¹⁻³

1. The metallization ratio η as defined in Equation 3.3 calculates the area fraction of metal of the electrode plane, where W is the width of the metal finger and G is the width of the spacing between the metal fingers (Figure 3.1),

$$\eta = \frac{W}{W + G} \quad (3.3)$$

The metallization ratio increases with increasing finger width (W), hence area (A), which automatically implies a decrease in the gap width (G). Thus, the higher the metallization ratio, the higher the IDE capacitance.

2. The dimensionless ratio r as defined in Equation 3.4,

$$r = \frac{h}{\lambda} \quad (3.4)$$

in which h is the thickness of the polymer layer and $\lambda = 2(G+W)$ is the spatial electrode wavelength.

The ratio r is an important parameter since the density of the electric field lines decreases with increasing perpendicular distance to the electrode plane. As reported by Igreja and Dias, the adimensional ratio r reaches a saturation value at $r = 0.5$.¹

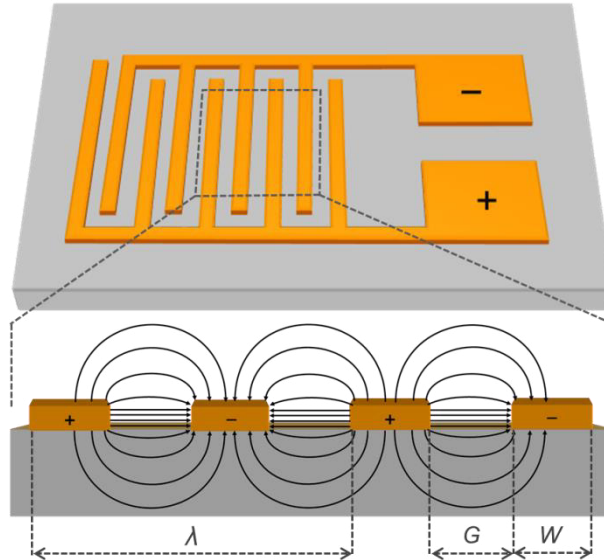


Figure 3.1. Schematic representation (not to scale) of an interdigitated electrode (IDE) sensor (top side view on top). The magnified side view (bottom) shows schematically the electric field between the finger electrodes of opposite electrical potential, and how it penetrates the surroundings on the top side and the substrate on the bottom side. Further indicated is the spatial electrode wavelength of the finger electrodes (λ), the electrode gap (G), and the electrode width (W). The finger length (L) is not indicated.

3.2 Polymeric Sensing Layers

The essential properties of polymeric sensing layers for gas phase applications have been summarized by Grate *et al.*⁷ In short, these sensing layers should have a high physical and chemical stability during operation. For polymeric sensing layers, the glass transition temperature should be well below the temperature of use. This will contribute to a rapid diffusion of molecules absorbed by the polymer due to the mobility of the random polymer chains.⁸ In particular, elastomers are suitable as sensing layers due to their visco-elastic behavior, which results in their excellent linearity of the sensor signal with the amount of absorbed molecules and their long-term stability.^{4, 9} In general, sorption in amorphous polymers, such as elastomers, is more favorable as compared to

partially crystalline materials.^{10, 11} Polymers in the glass state, as they lack mobility in their polymer chains, do also have a slower sensor response and recovery time. In addition, they are more prone to sensor irreversibility and possible hysteresis effects, and molecules are likely to adsorb in present micro-voids or micro-cracks and do not interact with the crystalline domains, which therefore represents dead volume.^{8, 12} Yet, in general, it is to conclude that polymers offer a good compromise between response time and reversibility.^{4, 13}

3.2.1 Polydimethylsiloxane

The elastomeric silicone polydimethylsiloxane, short PDMS, has been proven to be a suitable sensing layer material as for the capacitive detection of volatile organic compounds (VOCs) due to its apolar nature, its thermal and oxidative stability, and its visco-elasticity.¹⁴ A widely used commercially available PDMS is Sylgard®184, a product of the Dow Corning Company, U.S.A. It is delivered as a two component silicone elastomer kit, consisting of a base and a curing agent that are usually mixed in a weight or volume ratio of 10:1. The product already cross-links at room temperature and cross-links faster at higher temperatures.¹⁵ The base contains primarily vinyl-terminated dimethyl siloxane (> 60 wt.%) and dimethyl vinyl silylated and trimethyl silylated silica as filler material (30-60 wt.%),¹⁶ and the curing agent contains mainly methyl hydrogen siloxane (-Si(CH₃)H- units; 40-70 wt.%) as well as the dimethyl vinyl silylated and trimethyl silylated silica filler material (10-30 wt.%).¹⁷ By increasing or decreasing the weight ratio of the curing agent, one can prepare harder or softer PDMS, respectively. The vinyl-terminated groups of the base and the surface-modified silica undergo a hydrosilylation addition reaction to form a cross-linked PDMS network. Polydimethylsiloxane is a rather mechanically weak polymer¹⁸ that tears easily under stress. Therefore, the chemically end-capped silica is added to give sufficient mechanical strength to the final polymer product, which is beneficial for different application, including, *e.g.*, the fabrication of microfluidic PDMS devices.¹⁹

Several effective modification techniques for PDMS have been investigated and developed. Since the polymeric layer serves as a sorption layer, it is generally desirable to modify the bulk polymer and not only its surface. A well-known method for hydrogen-functional PDMS modification is by reaction with functional compounds having an alkene terminal group. As explained, an alkene- and an hydrogen-functional

PDMS couple via the hydrosilylation reaction. The modifier, which is an alkene with a certain functionality (R), such as allyl cyanide,²⁰ competes with the vinyl-terminated siloxane pre-polymer for the hydrogen-functional sites of the cross-linker (Figure 3.2).

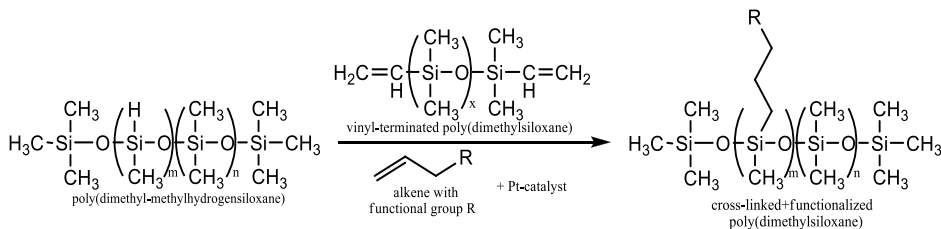


Figure 3.2. Schematic representation of the hydrosilylation cross-linking reaction of hydrogen-functional PDMS with a vinyl-terminated PDMS and the simultaneous functionalization with an alkene carrying the functional group R (Figure adapted²¹).

3.2.2 Preparation of Thin Polymeric Sensing Layers

There are various methods for depositing polymeric sensing films of controlled thicknesses onto a sensor substrate as, *e.g.*, casting, spraying, spin-coating, self-assembling, vacuum deposition processes, the Langmuir-Blodgett method, and even electrochemical polymerization for conductive and semi-conductive polymers.^{14, 22} The polymer layers can be established as thin monolayers of about 5 nm thickness to thin films of about 200 μm thickness to introduce chemical selectivity into solid-state sensor devices.²³

Thin films of PDMS are commonly prepared via spin-coating and a dipping technique. Spin-coating is probably the most common technique for the formation of uniform and thin polymeric layers of controlled thickness. Undiluted PDMS as, for instance, the commercially available Sylgard®184 product can be spin-coated down to a few micrometers.^{24, 25} Diluted PDMS can be spin-coated down to sub-micrometer scale. However, the minimum thickness of even diluted PDMS seems to approach a plateau value just below 100 nm.^{26, 27} A simple and fast method for obtaining PDMS films with controlled thickness from just a few nanometer (3.7 nm) up to 88 nm in glass capillaries was developed by using a filling technique based on oil-in-water PDMS emulsions of different concentrations.²⁸ The layer profile is further influenced by the chosen curing

temperature. Curing at room temperature gives convex surfaces, whereas curing at higher temperatures results in concave surfaces.²⁹

3.3 Principles of Pollution Detection

Polymer-based sensors work on the same principle as equilibrium sampling devices. That means they do not measure the actual concentration of freely dissolved compounds in the environment but in a reference phase, which was equilibrated with the sampling environment.^{30, 31} In this section, we address the basic principles of pollution partitioning into a polymer layer, the involved interaction mechanisms between the pollutant and the polymer network, and the mechanisms that are likely to contribute to a response change in the measured capacitance.

3.3.1 Pollutant Partitioning

A coated IDE platform offers a polymeric sensing layer to the pollutant to distribute or dissolve into. Each polymer is permeable to certain gases and vapors.³² Also, small molecular analytes can partition and dissolve from the environmental compartment into the polymer layer.³³ The affinity of a specific polymer layer for a pollutant follows hereby the rule of thumb “like dissolves like”.³⁴ A measure of the solvent behavior is the so-called Hildebrand solubility parameters of a given solvent or polymer.³⁵ The Hildebrand solubility parameter is defined as the square root of the cohesive energy density³⁴ and is thus related to the attractive strength among the molecules in the material.³⁵ It describes the degree of interaction forces among molecules that need to be overcome in order to separate those molecules from one another by the intrusion of another molecule and consequently to dissolve them.³⁴ The partition coefficient P , typically expressed as $\log P$, is another quantitative measure of the solvent behavior³⁵ and describes the equilibrium process of the analyte between the water phase (C_w) and in the polymer layer phase (C_p) as according to Equation 3.5. $\log P$ values are dependent on the solubility differences of the analyte in the two phases:^{36, 37}

$$\log P = \log \left(\frac{C_p}{C_w} \right) \quad (3.5)$$

The partition coefficient is a thermodynamic parameter that depends among others on temperature and pressure. Strictly speaking, the partition coefficient has to be determined experimentally for each specific system. The solvent n-octanol is often chosen to mimic the organic phase. The n-octanol-water partition coefficient (K_{OW}) or its logarithm ($\log K_{OW}$) is then applied to estimate the analyte distribution (Equation 3.6):³⁷

$$\log K_{OW} = \log \left(\frac{C_O}{C_W} \right) \quad (3.6)$$

with C_O the concentration of the compound in the n-octanol phase and C_W its concentration in the water phase.

In fact, over the last decades the role of the n-octanol-water partition coefficient for organic compounds has become of paramount importance in environmental studies, such as in the prediction of contaminant concentrations in the different environmental compartments.³⁸ Yet, there are also various factors that influence the fate, behavior, and metabolism of the compounds in the environment. For example, many organic compounds, such as pesticides, contain acidic or basic groups and can consequently easily dissociate in water. The extent of dissociation is fully determined by the solution pH and the respective pK_a and pK_b values of the acid and basic compounds. Non-dissociated analytes are less water soluble compared to their dissociated counterparts. Therefore, they have a higher $\log K_{OW}$ value.³⁹

3.3.2 Detection Mechanisms

The detection mechanism of polymer-coated IDE platforms in capacitive measurements is based on the relative change of the dielectric properties of the polymer layer upon interaction with the target compound, also referred to as the analyte or pollutant. In a first approximation, the change in dielectric constant is determined by the relative difference in the dielectric constant of the compound and the volume fraction of the host material, *i.e.*, the analyte after uptake.⁴⁰ For thin layers, for which the electrical sensing field extends beyond the polymer layer surface as shown in Figure 3.3 (for instance, $r = h/\lambda < 0.5$), the change in the environment, such as the replacement of the medium air by water or the introduction of an analyte into that medium, leads to a first response change (Figures 3.3a and 3.3b). Because the pollutant is often very diluted in the environmental

compartment, its volume fraction effect on the average dielectric constant of the medium is often negligible. It has been reported by Igreja and Dias¹⁻⁴ that for thin polymer layers three processes contribute to the capacitive response of the polymer-coated IDE platform: adsorption and absorption of the pollutant and subsequent swelling of the polymer layer (Figures 3.3c and 3.3d):

1. A quick adsorption process of the analyte onto the polymer surface can be viewed as a replacement of a layer of the surrounding medium (air or water) by a very thin layer or monolayer of that analyte.
2. A slow absorption process of the analyte into the polymer bulk changes the relative dielectric constant of the bulk material. In a first approximation, the average relative dielectric constant is again the sum of the relative dielectric constants of the polymer and analyte times their volumetric fractions.
3. The layer swells due to the absorbed analytes, which again can be viewed as a replacement of a layer of the surrounding medium by a layer of the polymer-analyte material.

If the electrical field lines do not extend beyond the polymer layer, then the transducer element is insensitive towards swelling, adsorption, and changes in the surroundings. For thick polymer layers —that measure at least about one half of the spatial electrode wavelength ($r = h/\lambda = 0.5$)—, the electric sensing field of the IDEs is restrained within the polymer layer and only dielectric changes within the polymer phase as caused by analyte absorption are observed.³

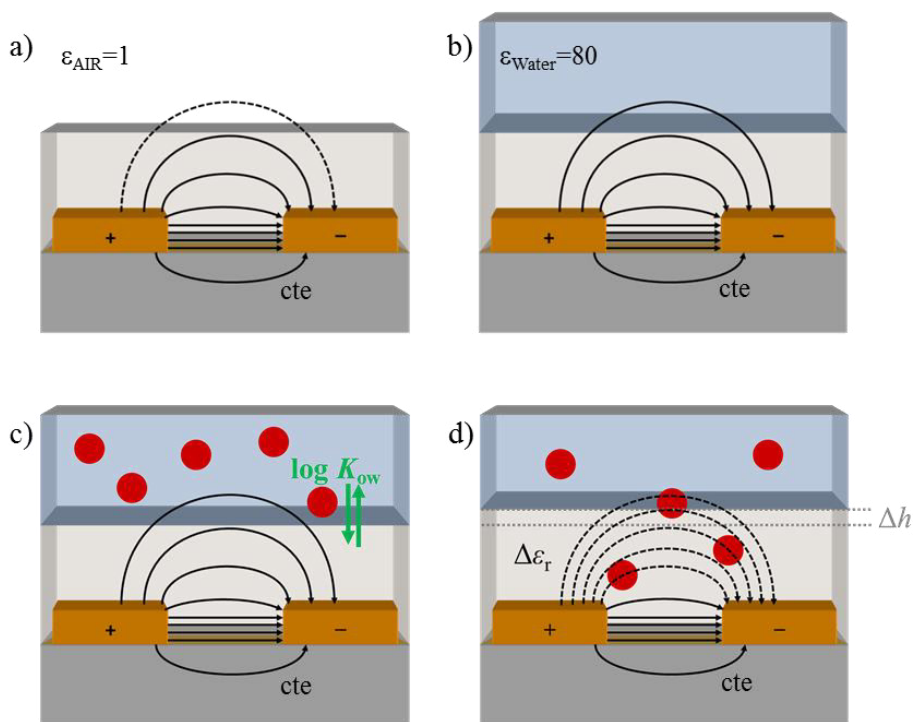


Figure 3.3. Schematic representation of the side view of a polymer-coated IDE sensor and the established electric field when being exposed to a) low dielectric air and b) high dielectric water. c) and d) show the schematic representation of the distribution process of a random pollutant (red sphere) into the polymeric sensing layer of the IDE sensor c) before and d) after interaction of the pollutant with the polymer layer and the electric sensing field. The green arrows in c) stand for the dynamic equilibrium of the pollutant over the environment and the polymer sensing layer and is estimated by the n-octanol-water partition coefficient (K_{OW}), typically expressed as its logarithm ($\log K_{OW}$). Electric field line changes upon changes of the relative dielectric constant ($\Delta\epsilon_r$) are represented by the dashed, bended arrows. Δh stands for the change in polymer thickness due to swelling upon pollutant absorption. The dielectric constant of the substrate remains constant (cte) throughout these processes. The schematic representation of the electric field on the substrate side was reduced to one electric field line for simplicity.

3.4 Complexity in Water Sensing Techniques

The challenge in performing electrical measurements in the gaseous phase mainly remains the variation of temperature and humidity.⁴¹ In the next sections, the environmental complexity of the water phase including the physico-chemical and

electrical properties of the system will be discussed, and it will be concluded, which requirements of the polymer layer must consequently be met.

3.4.1 Water-Enhanced Electrical Coupling

For a system of spatially arranged electrodes, not their potential but their presence already contributes to mutual capacitances.^{42, 43} The electrodes hereby share their area with several capacitors formed with other electrodes in their surroundings. For this reason, the capacitances between electrodes decrease upon the introduction of additional electrodes as a part of the overall electrode area is claimed by the additional electrodes. In other words, the effective electrode area of the capacitors is decreased. The capacitances increase with decreasing distance between the individual electrodes and with increasing dielectric constant of the inter-lying material. The potential of the electrodes plays a role when measuring the capacitance between two electrodes as it determines whether or not capacitors are electronically interconnected within the measuring circuitry. If an electrode is at no fixed potential within the measuring circuitry, it is considered a floating electrode. For any sensing device, such as a polymer-coated IDE platform, its capacitance may already be influenced by the near-by presence of grounded shielding areas and other system parts of the measuring system or in the environment. In fact, an electrical shield is a well-known cause for electric-field bending, for which the application of guarding electrodes can be a remedy as explained in Chapter 2, Section 2.5.1.⁴⁴

Figure 3.4a depicts schematically a PDMS-coated IDE platform deposited on a glass substrate mounted on an unshielded printed circuit board (PCB) and the ideally undisturbed capacitors formed between the IDE fingers on the lower glass plane and the upper PDMS plane. When a metallic bottom shield on the PCB and an in-plane guarding electrode on the IDE chip are introduced, capacitors (C_{shield} , C_{guard}) are formed as shown in Figure 3.4b. It should be noted that the introduction of guarding and shielding electrodes will reduce the IDE capacitance (C_{ide}) slightly. However, this reduction depends also on the distance from the IDE electrodes to the guarding and shielding areas as compared to the mutual distance between the electrodes.⁴⁵ The capacitive coupling effect to the shielding and to the guarding electrodes can be enhanced by the presence of a water layer that replaces the air above the PDMS layer surface. Air has a relative dielectric constant close to that of vacuum ($\epsilon_r \sim 1$). Water has

not only a high relative dielectric constant ($\epsilon_r \sim 80$) but also a relatively high conductivity as compared to air (especially when it contains salts). Therefore, the voltage drop over the water layer—with its very low specific impedance as compared to air, PDMS, glass, and PCB—is very low, so the water layer can be viewed as an equipotential layer and itself functions as an electrode. When the water layer exceeds the PDMS-coated IDE plane and extends over the shielding and guarding electrode as shown in Figure 3.4c and 3.4d, these areas are hence stronger electrically coupled to the IDEs than when being exposed to air. The more the water spreads over the shielding and guarding electrode area, the stronger the IDE sensing field is coupled to them. In the presence of a shielding and guarding electrode as shown in Figure 3.4d, it can be assumed that the water phase only enhances electrical coupling to the guarding electrode and not to the underneath-lying shielding electrode.

From an electrical point of view, situating a guarding electrode in the water phase right above the IDE plane at close distance to the PDMS layer instead of lying in-plane next to the IDE structure would be more effective. In case of high solution conductance, this externally applied guarding electrode, that we will shortly refer to as third electrode within this work, together with the inter-lying water layer will electrically behave as one electrode. If such a ‘third’ electrode is introduced as shown in Figure 3.4e, all capacitances are affected again. However, this arrangement of grounded electrodes will not influence the measurement as no potential drop—and hence no charge flow—to these capacitors occurs. If the water layer behaves like an ideal electrode, which is the case for high solution conductivity, then the impedance measured between the third electrode and the IDEs or guarding electrode approximates the capacitance that is formed across the PDMS layer (C_{PDMS}).

It is noted that different guarding approaches exist.⁴⁶ In this work we will demonstrate that the introduction of such a third electrode is an easy way to investigate the sensitivity for parasitic effects.

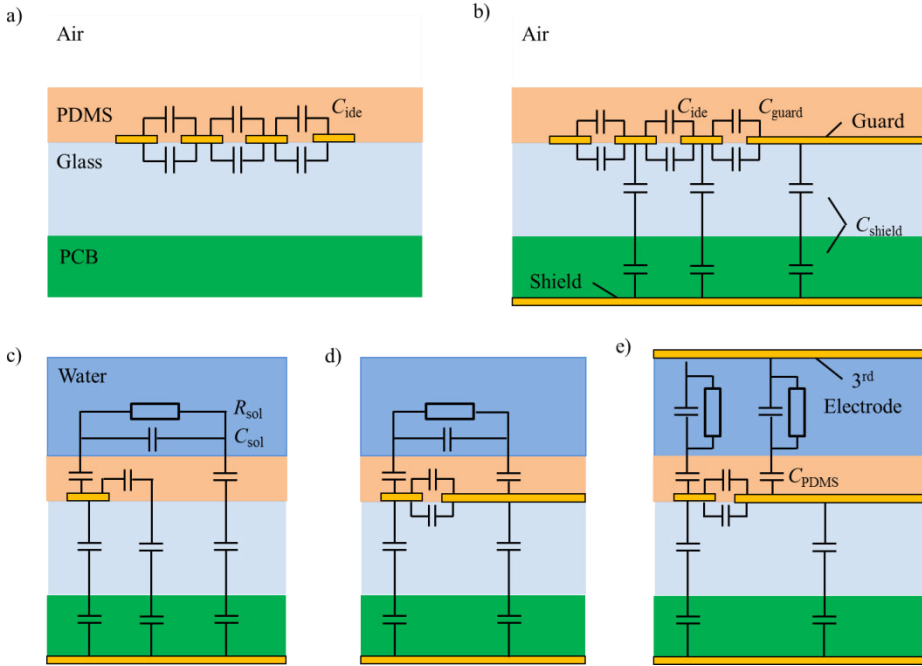


Figure 3.4. Schematic representation (not to scale) of the cross section of PDMS-coated IDEs deposited on a glass substrate on a PCB support a) without and b) with a shielding electrode on the PCB bottom side and an in-plane guarding electrode. Also shown are the possible capacitors formed between the IDE finger (C_{ide}), shielding (C_{shield}) and guarding electrodes (C_{guard}). Figure c) and d) demonstrate enhanced electrical coupling to the shielding and guarding electrode for the case that the air layer has been replaced by a water layer. The water impedance is electronically represented as a parallel connection of a resistor (R_{sol}) and a capacitor (C_{sol}). Figure d) shows the parasitic coupling effect to an additional third electrode in the water phase. The capacitance across the PDMS layer is denoted as C_{PDMS} .

Figure 3.5a to 3.5e show simplified equivalent circuits for an IDE capacitor that is coupled to the different electrodes and how these electrodes are interconnected within the circuitry, depending on the available terminals and connections. Figure 3.5a shows the simple case where the IDE capacitor between two terminals A and B is not electrically coupled to the surroundings. When a PCB bottom shield is introduced, it functions as a floating electrode when it is not connected to an external voltage source (Figure 3.5b). Figure 3.5c shows the equivalent circuit for the case that the shielding is connected to ground. Next, Figure 3.5d shows the equivalent circuit for the case that, in addition to the PCB shielding, a guarding electrode next to the IDE structure is added.

Finally, Figure 3.5e depicts the equivalent circuit for the case that an additional third electrode in direct contact with the water phase is introduced.

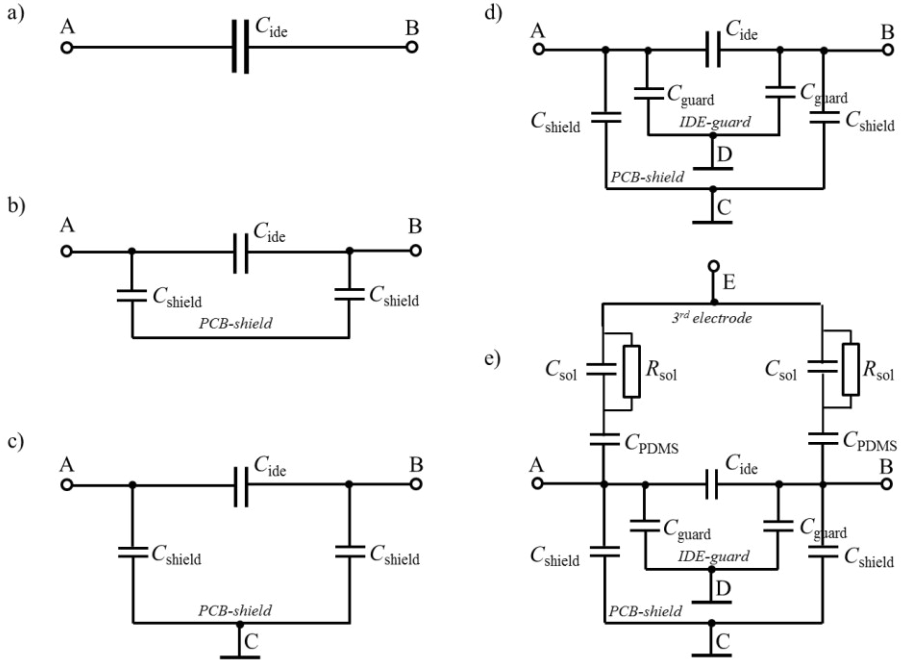


Figure 3.5. Idealized electrical equivalent circuits of a) an ideal IDE capacitor (C_{ide}) between the terminals A and B; an IDE capacitor in the presence of b) a floating PCB shielding electrode; c) a PCB shielding electrode that is connected to ground terminal C; d) in the additional presence of an IDE guarding electrode that is connected to ground terminal D, corresponding to Figure 3.4b. In this case, two parasitic capacitors, that is C_{shield} and C_{guard} , are formed; e) additional capacitances formed by the presence of a third electrode in the surrounding, corresponding to Figure 3.4e, at a yet undefined terminal E, to which parasitic coupling through the PDMS and the water layer (C_{PDMS} , R_{sol} , C_{sol}) occurs. Note that only water-enhanced coupling to the third electrode is shown for simplicity.

For a simple IDE capacitor (Figure 3.5a), measuring the capacitance between terminals A and B, of which one is excited with an alternating signal while the other one is held at ground potential, will give the true C_{ide} value. If the introduced shielding area is not at a fixed potential as shown in Figure 3.5b, *i.e.*, it serves as a floating electrode, the capacitors C_{shield} themselves are connected in series but both parallel to the IDE

capacitor C_{ide} . Therefore, the capacitances formed with the shielding area contribute to the total capacitance that is measured between the two terminals A and B of the IDE capacitor. Yet, this contribution is not useful as the information to be extracted is only found within the PDMS layer on the top-side of the IDE plane. Because the capacitor values are independent of their potentials, grounding of the shield (Figure 3.5c) does not affect the value of the capacitor C_{ide} . However, when the measurement is performed correctly, the grounded parasitic capacitors C_{shield} do not affect the measurement anymore. The introduction of a guarding electrode in the IDE plane, next to the outer electrodes, leads to enhanced parasitic capacitive coupling (Figure 3.5d). Due to the very small distance between the outer IDEs and the guarding electrode, the values of the corresponding capacitances (C_{guard}) can be significant, especially in the presence of water that enhances the electrical coupling effect as explained in Figure 3.4. Fortunately, also in this case, with a proper measurement setup, the effect of these capacitances can be eliminated. Finally, as depicted in Figure 3.5e, the introduction of a third electrode causes further electrical coupling (C_{PDMS} , R_{sol} , C_{sol}), which again affects all capacitors within the system. The effect of the introduction of this third electrode on the capacitive response thereby depends on whether or not and to what extent the electric sensing field of the IDEs—that is prone to electric-field bending—has already been coupled to shielding and guarding electrodes.

3.4.2 The Role of Swelling

In air, swelling may be viewed as a replacement of a thin layer of air by a thin layer of the (higher dielectric) polymer within the electric sensing field.³ Therefore, the response contribution of swelling to the capacitive response change will always be an increase in capacitance. However, when exposed to water, swelling may be viewed as a replacement of a thin layer of the higher dielectric water phase by the relative lower dielectric polymer layer. Hence, the response contribution of swelling to the capacitive response change will be a decrease in capacitance. As discussed in Section 3.3.2 and 3.4.1, the thickness of the polymer layer determines not only the sensitivity of the platform towards surface adsorption, swelling, and changes in the surrounding media, but also its sensitivity towards interferences of charged particles and the presence of other electrodes present within the system and in the surrounding. It can be concluded that for thin polymer layers layer swelling in an aqueous phase and in the presence of a

third electrode will lead to two counteracting response changes: swelling causes a decreased IDE capacitance and a reduction of the electrical coupling effect to the third electrode as described in Section 3.4.1. That is, the reduction of the parasitic electrical coupling effect increases the IDE capacitance. At a sufficient layer thickness, the capacitance between the IDEs and the parasitic electrode becomes negligibly small and an increase in layer thickness will have no additional effect on the observed capacitive response.

Swelling ratios of PDMS samples immersed in pure organic solutions have been determined by measuring changes in their dimensions⁴⁷ and of thin PDMS layers exposed a gaseous phase containing volatile compounds have been measured by light reflective spectroscopy.⁴⁸

3.4.3 Polymer Layer Requirements

When the polymer layer is allowed to come into direct contact with the aqueous phase, water vapor will distribute into it until an equilibrium is reached. Water vapor uptake can be tolerated to a certain degree, depending on the resulting change in the electrical properties of the polymer layer. However, the infiltration of liquid water must be prevented at all costs as it will lead to a drastic increase in the dielectric constant of the layer, simultaneously lowering its electrical resistance. Eventually, mechanical instability of the polymer layer, polymer aging, and polymer wear are factors that can promote further water uptake with time and use. In water, the polymeric film does not only serve as a sensing layer, but ideally it also acts as a water repellent and electrically insulating coating. This will probably limit the choice of applicable polymers to more hydrophobic (water-fearing) ones but not to hydrophilic (water-loving) ones. As addressed in Section 3.2.2, PDMS is a predestinated material for the detection of organic pollutants in aqueous phases. Firstly, it is an inert and hydrophobic polymer that readily absorbs in organic solvents but is compatible with water, preventing the infiltration of liquid water and allowing the absorption of water vapor and of small molecules.⁴⁹⁻⁵³ Secondly, it has a high electrical resistivity, preventing electrical leakage currents.⁵⁰ Thirdly, as a sensing layer, the visco-elastic behavior of PDMS ensures quick and fully reversible diffusion processes and hence sensor responses.⁷ Furthermore, we expect that the system stability is enhanced by the good adhesion of the silicone rubber to the glass substrates^{25, 54} as swelling events can cause mechanical stress on the

substrate-polymer interface. Good adhesion further minimizes water leakage to and on the electrode plane. Finally, PDMS is of interest as its wetting and dielectric properties can be tuned via hydrosilylation chemistry to achieve chemical diversity within a multi-array sensor.⁵⁵

3.4.4 The Physico-Chemical Complexity

As compared to the gaseous phase application of polymer-coated IDEs, the physico-chemical complexity of the system is further increased when applying these sensing platforms in water. This is among others due to variation in the pH and the redox-potential, which can change the speciation of the pollutants. This means pollutants may be ionized, occur in their reduced or oxidized state, or form chemical complexes. In addition, the polymer layer itself can retain chemical groups on its surface and in its bulk that may ionize when being exposed to liquid water. As PDMS is water repellent, dissociation of PDMS silanol groups is expected to occur only at the polymer surface that is directly exposed to the liquid water phase. Also, silanol groups originating from the silica filler material might contribute to dissociation processes at the polymer surface. In fact, at $\text{pH} > \text{p}K_a \sim 4$ most silanol groups are expected to be dissociated, leaving negatively charged surface silanolate moieties on the PDMS surface.⁵⁶ Though the polar siloxane backbone is properly shielded with non-polar methyl groups, the $-\text{Si}-\text{O}-\text{Si}-$ unit is capable of bending by $\sim 130^\circ$,⁵⁷ thereby exposing the electron-rich oxygen atoms of the PDMS backbone to the outside. Reorientation of the polymer chains at a PDMS surface that had been exposed to a water phase has been reported.⁵⁸ It was found that the presence of hydrogen-bonds between water molecules with silanol groups or the siloxane units ($\text{Si}-\text{O}-\text{Si}$) was of minor importance. Yet, it is noteworthy that in addition to the weak dispersion interaction forces also strong electrostatic interaction forces are likely to occur between the pollutants and the PDMS layer and this both at its surface and in its bulk. When a charged or polarized surface is in contact with an electrolyte solution, an electrical double layer establishes that forms an interfacial capacitor. In an alternating field, electrical double layers can polarize typically at frequencies up to ~ 10 kHz⁵⁹ and the polymer/water interface is expected to behave more as a contact resistance at higher signal frequencies. Although it is understood that interfacial polarization effects are complex and system characteristic, they have been neglected in the current study as the applied frequency was as high as 30 kHz.

3.5 Concluding Remarks

The interdigitated electrode structure is a highly interesting transducer platform for chemical sensing applications. First of all, sensitivity is among others determined by the IDE capacitance, which can be easily tuned via proper dimension design. The planar and robust IDE structure can further be cost-effectively fabricated by common IC technology and offers a large interaction area to the analyte environment to be probed. Polymer coatings can be easily deposited with thicknesses in the millimeter down to nanometer range. The polymers should have low glass transition temperatures for fast and reversible sensing processes. In addition, good water repellency and electrical insulating properties are needed if the polymer layer is directly exposed to water. The polydimethylsiloxane based on the commercial two-component product Sylgard®184 is a very good polymer choice to fulfil these requirements. The sensing of small organic compounds proceeds likely via adsorption and absorption of the compounds, and concomitant swelling of the sensing layer. The environmental complexity in aqueous media differs from the gas phase, creating new challenges for capacitive sensing techniques. This is among others due to the high dielectric constant of the water and the presence of ions in it. The electrical properties of the water phase also contribute to enhanced parasitic electrical coupling to the surrounding and other system parts, which requires more care in the interpretation of the observed capacitive response.

3.6 References

- 1 R. Igreja, and C. J. Dias, Analytical evaluation of the interdigital electrodes capacitance for a multi-layered structure, *Sensors and Actuators A-Physical*, 112 (2004), 291-301.
- 2 R. Igreja, and C. J. Dias, Capacitance response of polysiloxane films with interdigital electrodes to volatile organic compounds, *Advanced Materials Forum II*, 455-456 (2004), 420-424.
- 3 R. Igreja, and C. J. Dias, Dielectric response of interdigital chemocapacitors: The role of the sensitive layer thickness, *Sensors and Actuators B-Chemical*, 115 (2006), 69-78.
- 4 R. Igreja, and C. J. Dias, Organic vapour discrimination using sorption sensitive chemocapacitor arrays, *Advanced Materials Forum Iii, Pts 1 and 2*, 514-516 (2006), 1064-1067.
- 5 M. W. den Otter, Approximate expressions for the capacitance and electrostatic potential of interdigitated electrodes, *Sensors and Actuators A-Physical*, 96 (2002), 140-144.
- 6 D. Roy, J. H. Klootwijk, N. A. M. Verhaegh, H. H. A. J. Roosen, and R. A. M. Wolters, Comb capacitor structures for measurement of post-processed layers, *Microelectronic Test Structures, 2008. ICMTS 2008. IEEE International Conference on* (2008), 205-209.
- 7 J. W. Grate, and M. H. Abraham, Solubility interactions and the design of chemically selective sorbent coatings for chemical sensors and arrays, *Sensors and Actuators B-Chemical*, 3 (1991), 85-111.
- 8 C. E. Rogers, Permeation of gases and vapours in polymers, in *Polymer Permeability*, ed. by J. Comyn (London, U.K.: Elsevier Applied Science, 1985), pp. 11-73.
- 9 D. S. Ballantine, White, R. M., Martin, S. J., Ricco, A. J., Frye, G. C., Zellers, E. T., Wohltjen, H., Acoustic wave sensors: theory, design, and physico-chemical applications (San Diego, U.S.A.: Academic Press, 1997).
- 10 J. E. Guillet, Purnell, J. H., Advances in analytical chemistry and instrumentation gas chromatography (New York, U.S.A.: John Wiley and Sons, Inc., 1973).
- 11 C. H. M. Jacques, and H. B. Hopfenberg, Vapor and liquid equilibria in glassy polyblends of polystyrene and poly(2,6-dimethyl-1,4-phenylene oxide) Part I, *Polymer Engineering & Science*, 14 (1974), 441-448.
- 12 H. B. Hopfenberg, Stannet, V. B. , The diffusion and sorption of gases and vapours in glassy polymers. ed. by R. N. Hayward, *The Physics of Glassy Polymers* (London, U.K.: Applied Science Publishers Ltd., 1973).
- 13 G. Harsanyi, Polymer films in sensor applications (Basel, Switzerland: Technomic Publishing, 1995).
- 14 G. Harsanyi, Polymer films in sensor applications: a review of present uses and future possibilities, *Sensor Review*, 20 (2000), 98-105.
- 15 Product datasheet: Sylgard184 silicone elastomer, *Dow Corning Corporation* (2012).
- 16 Material safety datasheet: Sylgard184 silicone elastomer base, *Dow Corning Corporation* (2005).
- 17 Material safety datasheet: Sylgard184 silicone elastomer curing agent, *Dow Corning Corporation* (2004).

- 18 A. Camenzind, W. R. Caseri, and S. E. Pratsinis, Flame-made nanoparticles for
nanocomposites, *Nano Today*, 5 (2010), 48-65.
- 19 I. A. M. Ibrahim, Zikry, A. A. F, Sharaf, M. A., Mark, M. J. E, Jacob, K.,
Jasiuk, I. M., Tannenbaum, R., Dielectric behavior of
Silica/Poly(dimethylsiloxane) nanocomposites. nano size effects, *IOP
Conference Series: Materials Science and Engineering*, 40 (2012), 2001-2011.
- 20 M. Rutnakornpituk, Modification of epoxy–novolac resins with polysiloxane
containing nitrile functional groups: synthesis and characterization, *European
Polymer Journal*, 41 (2005), 1043-1052.
- 21 M. L. van Poll, Khodabakhsh, S., Brewer, P. J., Shard, A. G., Ramstedt, M.,
Huck, W. T. S., Surface modification of PDMS via self-organization of vinyl-
terminated small molecules, *Soft Matter*, 5 (2009), 2286-2293.
- 22 B. Adhikari, and S. Majumdar, Polymers in sensor applications, *Progress in
Polymer Science*, 29 (2004), 699-766.
- 23 M. Josowicz, Janata, J., Organic polymer films for solid-state sensor
applications, *Solid State Ionics*, 28-30 (2008), 1625-1630.
- 24 W. Y. Zhang, Ferguson, G. S., Tatic-Lucic, S., Elastomer-supported cold
welding for room temperature wafer-level bonding, in *MEMS 2004 Technical
Digest* (Maastricht, The Netherlands, 2004).
- 25 J. H. Koschwanez, R. H. Carlson, and D. R. Meldrum, Thin PDMS films using
long spin times or tert-butyl alcohol as a solvent, *PLoS ONE*, 4 (2009), e4572.
- 26 A. L. Thangawng, Ruoff, R. S., Swartz, M. A., Glucksberg, M. R., An ultra-
thin PDMS membrane as bio/micro-nano interface: Fabrication and
characterization, *Biomedical Microdevices*, 9 (2007), 587-595.
- 27 A. L. Thangawng, Swartz, M. A., Glucksberg, M. R., Ruoff, R. S., Bond-
detach lithography: A method for micro/nanolithography by precision PDMS
patterning, *Small*, 3 (2007), 132-138.
- 28 A. E. Niotis, C. Mastichiadis, P. S. Petrou, A. Sifaka-Kapadai, I. Christofidis,
K. Misiakos, and S. E. Kakabakos, Ultra-thin poly(dimethylsiloxane) film-
coated glass capillaries for fluoroimmunosensing applications, *Microelectron.
Eng.*, 86 (2009), 1491-1494.
- 29 A. W. Feinberg, A. Feigel, S. S. Shevkoplyas, S. Sheehy, G. M. Whitesides,
and K. K. Parker, Muscular thin films for building actuators and powering
devices, *Science*, 317 (2007), 1366-1370.
- 30 T. P. Rusina, F. Smedes, J. Klanova, K. Booij, and I. Holoubek, Polymer
selection for passive sampling: A comparison of critical properties,
Chemosphere, 68 (2007), 1344-1351.
- 31 P. Mayer, Tolls, J., Hermens, J. L. M., Mackay, D., Equilibrium sampling
devices, *American Chemical Society*, 37 (2003), 184A-191A.
- 32 R. Waack, N. H. Alex, H. L. Frisch, V. Stannett, and M. Szwarc, Permeability
of polymer films to gases and vapors, *Industrial & Engineering Chemistry*, 47
(1955), 2524-2527.
- 33 S. A. Stern, and J. Fried, Permeability of polymers to gases and vapors, in
Physical Properties of Polymers Handbook, ed. by James E. Mark (New York,
U.S.A.: Springer Verlag, 2007), pp. 1033-1047.
- 34 J. Burke, Solubility parameters: Theory and application, *The Book and Paper
Group Annual*, 3 (1984), 13-58.
- 35 M. P. Eastman, R. C. Hughes, G. Yelton, A. J. Ricco, S. V. Patel, and M. W.
Jenkins, Application of the solubility parameter concept to the design of

- chemiresistor arrays, *Journal of The Electrochemical Society*, 146 (1999), 3907-3913.
- 36 M. Bertoldo, and F. Ciardelli, Water extraction and degradation of a sterically hindered phenolic antioxidant in polypropylene films, *Polymer*, 45 (2004), 8751-8759.
- 37 U. Gasslander, A. Arbin, and A.-C. Albertsson, Polymer-water partition coefficients of extended range measured by using organic modifiers in the aqueous phase, *Polymer*, 48 (2007), 7523-7530.
- 38 A. Finizio, M. Vighi, and D. Sandroni, Determination of n-octanol/water partition coefficient (Kow) of pesticide critical review and comparison of methods, *Chemosphere*, 34 (1997), 131-161.
- 39 K. Chamberlain, A. A. Evans, and R. H. Bromilow, 1-Octanol/water partition coefficient (Kow) and pKa for ionisable pesticides measured by apH-metric method, *Pesticide Science*, 47 (1996), 265-271.
- 40 S. Bosch, J. Ferré-Borrull, N. Leinfellner, and A. Canillas, Effective dielectric function of mixtures of three or more materials: A numerical procedure for computations, *Surface Science*, 453 (2000), 9-17.
- 41 D. Rivera, M. K. Alam, C. E. Davis, and C. K. Ho, Characterization of the ability of polymeric chemiresistor arrays to quantitate trichloroethylene using partial least squares (PLS): Effects of experimental design, humidity, and temperature, *Sensors and Actuators B-Chemical*, 92 (2003), 110-120.
- 42 G. W. de Jong, Smart capacitive sensor - physical, geometrical and electronic aspects (Ph.D. Thesis, Delft University of Technology, 1994).
- 43 A. M. Thompson, The precise measurement of small capacitances, *IEEE Transactions on Instrumentation*, 1-7 (1958), 245-253.
- 44 X. Li, Meijer, G.C.M., Capacitive sensors, in *Smart Sensor Systems*, ed. by G. C. M. Meijer (Chichester, U.K.: John Wiley & Sons, Ltd., 2008), pp. 225-248.
- 45 F. N. Toth, A design methodology for low-cost, high-performance capacitive sensors (Ph.D. Thesis, Delft University of Technology, 1997).
- 46 W.-C. Heerens, Application of capacitance techniques in sensor design, *Journal of Physics E: Scientific Instruments*, 19 (1986), 897.
- 47 J. N. Lee, C. Park, and G. M. Whitesides, Solvent compatibility of poly(dimethylsiloxane)-based microfluidic devices, *Analytical Chemistry*, 75 (2003), 6544-6554.
- 48 M. Kitsara, D. Goustouridis, E. Valamontes, P. Oikonomou, K. Beltsios, and I. Raptis, Polymer based chemical sensor array fabricated with conventional microelectronic processes, *Journal of Optoelectronics and Advanced Materials*, 12 (2010), 1147-1152.
- 49 M. W. Toepke, and D. J. Beebe, PDMS absorption of small molecules and consequences in microfluidic applications, *Lab on a Chip*, 6 (2006), 1484-1486.
- 50 J. Park, H. S. Kim, and A. Han, Micropatterning of poly(dimethylsiloxane) using a photoresist lift-off technique for selective electrical insulation of microelectrode arrays, *Journal of Micromechanics and Microengineering*, 19 (2009).
- 51 J. N. Lee, C. Park, and G. M. Whitesides, Solvent compatibility of poly(dimethylsiloxane)-based microfluidic devices, *Anal. Chem.*, 75 (2003), 6544-6554.

- 52 E. Favre, P. Schaetzel, Q. T. Nguyen, R. Clément, and J. Néel, Sorption, diffusion and vapor permeation of various penetrants through dense poly(dimethylsiloxane) membranes: A transport analysis, *Journal of Membrane Science*, 92 (1994), 169-184.
- 53 S. J. Harley, E. A. Glascoe, and R. S. Maxwell, Thermodynamic study on dynamic water vapor sorption in Sylgard-184, *The Journal of Physical Chemistry B*, 116 (2012), 14183-14190.
- 54 A. Plecis, and Y. Chen, Improved glass-PDMS-glass device technology for accurate measurements of electro-osmotic mobilities, *Microelectronic Engineering*, 85 (2008), 1334-1336.
- 55 J. W. Grate, Nelson, D. A., Kaganove, S. N., Polymers for chemical sensors using hydrosilylation chemistry, (Richland, U.S.A.: Pacific Northwest National Laboratory, 2001).
- 56 G. Z. Garyfallou, L. C. P. M. de Smet, and E. J. R. Sudholter, The effect of the type of doping on the electrical characteristics of electrolyte-oxide-silicon sensors: pH sensing and polyelectrolyte adsorption, *Sensors and Actuators B-Chemical*, 168 (2012), 207-213.
- 57 I. Van Reeth, Wilson, A., Understanding factors which influence permeability of silicones and their derivatives, *Cosmetics & Toiletries*, 109 (1994), 87-92.
- 58 A. E. Ismail, G. S. Grest, D. R. Heine, M. J. Stevens, and M. Tsige, Interfacial structure and dynamics of siloxane systems: PDMS-vapor and PDMS-water, *Macromolecules*, 42 (2009), 3186-3194.
- 59 W. D. Brown, Hess, D., Desai, V., Deen, M. J., Dielectric science & technology, *The Electrochemical Society's Interface*, 15 (2006), 28-31.

MEASUREMENT SETUP AND TECHNIQUE

The experimental setup as used throughout all experiments reported in this thesis is described. Shortly, micro-sized interdigitated electrode (IDE) platforms are deposited onto the centre of 1 cm² sized borosilicate glass chips with diagonally arranged leads to the contact pads. IDE structures have been designed with and without in-plane guarding electrodes. Polydimethylsiloxane (PDMS) films of controlled thickness are deposited via a spin-coating technique. A printed circuit board (PCB), which is integrated into a holder device, provides the necessary electronic connects to the LabVIEW supported universal transducer interface (UTI), the electronic readout device. Aqueous solutions of tuneable composition are supplied via a two-drive syringe pump to the self-designed flow cell system.

4.1 Interdigitated Electrode Platform

During the design phase of the interdigitated electrode (IDE) platform, several aspects, such as the specification of the fabrication process, the availability of the experimental methods, and the possibility for later (flow cell) system integration, had to be accounted for. One technical limitation was set by the photolithographic fabrication process for IDE fabrication, whose bottom resolution was $3\ \mu\text{m}$ as according to the information provided by the cooperating company, LioniX B.V., Enschede, the Netherlands. It is realized that smaller features at nanometer scale could be fabricated by advanced lithography and other techniques.¹ However, it was anticipated that the given resolution was good enough for the scope of the initial work, that is to study the detection principles and to show the proof-of-concept.

Further, the IDE chips should be large enough for manual handling, and hence chip size dimensions of $1\ \text{cm} \times 1\ \text{cm}$ were chosen. The electrode structures were deposited onto borosilicate glass wafers of $1.1\ \text{mm}$ in thickness. All electrode structures and leads measure a height of $50\ \text{nm}$, consisting of $40\ \text{nm}$ thick gold on a $10\ \text{nm}$ thick chromium adhesion layer. The contact pads were reinforced by an additional $500\ \text{nm}$ aluminum layer for wire-bonding purposes. Gold was chosen as electrode material for two reasons: first, it has a low degree of oxidation; second, gold can be surface-functionalized via thiol-chemistry,² which meets other research interests of ours than discussed in this work.

For the experiments described in this work, the IDE structure with the following dimensions was used: The IDE plane consists of 221 fingers, resulting in a total number of 220 parallel connected capacitors. The electrode finger width W and gap G are $6\ \mu\text{m}$ and $3\ \mu\text{m}$, respectively. This results in a spatial wavelength of $\lambda = 18\ \mu\text{m}$ and a metallization ratio of $\eta = 0.667$. The minimal distance was set, as said, by the resolution of the fabrication process. The total electrode finger length L is $2\ \text{mm}$, and the total electrode plane covers an approximate area A of $\sim 4\ \text{mm}^2$. The most important parameters are listed in Table 4.1.

Table 4.1. Geometric parameters of the IDE platform used in this work.

W (μm)	G (μm)	L (mm)	N	λ (μm)	η
6	3	2	221	18	0.667

The contact leads to the contact pads are arranged in a diagonal fashion to decrease the capacitive contribution between them. The leads are of the same width as the electrode fingers to further minimize this contribution. Though lead arrangement is typically done in a parallel fashion to avoid self-induction,³ it was experimentally confirmed by impedance measurements that no induction peak occurred within the 1 kHz up to 110 MHz range (Appendix A, Section A.1, Figure A.1). In addition, it was confirmed that the lead resistance of ~ 3.5 kOhm (Appendix A, Section A.1, Figure A.2), though higher than theoretically expected, was acceptable for the measurement frequency of 30 kHz of the applied measurement technique, which will be introduced in Section 4.6. IDE platforms with and without in-plane guarding electrodes were designed and fabricated. These guarding electrodes cover the unused area on the chip surface and lie at 3 μm distance on both sides of IDE layout, which includes the IDE structure at the chip centre, the diagonal arranged leads, and the contact pads.

The purpose of the presence of the grounded metallic areas is threefold. First, due to their proximity to the IDE structure, they primarily function as guarding electrodes. Second, due to their large areas, they also provide additional shielding against external sources. Third, they also diminish surface effects caused by the settlement of moisture and charged dust particles as electrostatic interaction of these charged species with the large guarding electrode is more likely to occur. The guarding area has the same metallic build-up as the IDE structure, that is 40 nm thick gold on a 10 nm aluminium adhesion layer. Figure 4.1 depicts a schematic representation of the IDE platform without and with in-plane guarding electrodes.

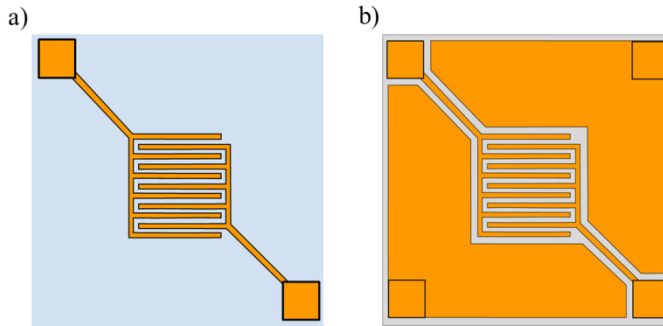


Figure 4.1. Schematic representation (not to scale) of the top-view of the layout of the IDE structure under study with diagonally arranged leads a) without and b) with in-plane guarding electrodes.

The capacitance of the bare IDE platforms measures ~ 15 pF. After the deposition of a PDMS layer (see Section 4.2), that has a larger thickness than the spatial wavelength of $18 \mu\text{m}$, and after chip integration into the printed circuit board—as will be described in Section 4.2 and 4.3, respectively—the capacitance measures about 4.5 pF more, that is ~ 19.5 pF, for the unguarded IDE structure. The PDMS-coated guarded IDE structure measures ~ 19 pF. The lower capacitance baseline is due to capacitive coupling of the IDEs to the grounded in-plane guarding electrodes as explained in Chapter 3, Section 3.4.1. As will be shown in Section 4.6, the capacitance of the chosen geometry further fits within the operating ranges of the proposed universal transducer interface, which we can therefore utilize.

4.2 Polydimethylsiloxane Layer

The properties of the silicone rubber polydimethylsiloxane (PDMS) layer have been discussed in Chapter 3. In this section, we describe the preparation of the PDMS layer. The commercial two-kit product Sylgard®184 by the Dow Corning Company was used for all experiments. The base and the curing agent were mixed in a weight ratio of 10:1 as recommended by the supplier on the product information sheet.⁴ No solvent was added. The mixture was degassed in a desiccator under reduced pressure for about 15 min, using an oil pump that generated a pressure of ~ 0.4 mbar. Subsequently, the degassed mixture was spin-coated onto the sensor chip. The polymer layer was cured at ambient conditions for at least 48 h before further processing and testing of the IDE

chip started. By adjusting the spin-coater (type Spin150 by SPS) settings, that is the angular acceleration, the spinning velocity, and the spinning time, the layer thickness could be controlled. To have a comparative study on the layer thicknesses, the methods and spin-coating settings as reported⁵ were applied with the only difference that the prepared samples were dried at room temperature rather than in an oven. The layers were spin-coated at different rotational speeds. The angular acceleration was initially set to 85 rpm/sec and the spin-coating time to 90 sec. A calibration curve was established by increasing the spin-coating rate for a fixed acceleration rate and spinning time (Figure 4.2). The layer thicknesses at the center of the prepared test samples were experimentally determined by Scanning Electron Microscopy (FEI-Philips XL30 FE-SEM) measurements as shown by two examples given in Figure 4.3.

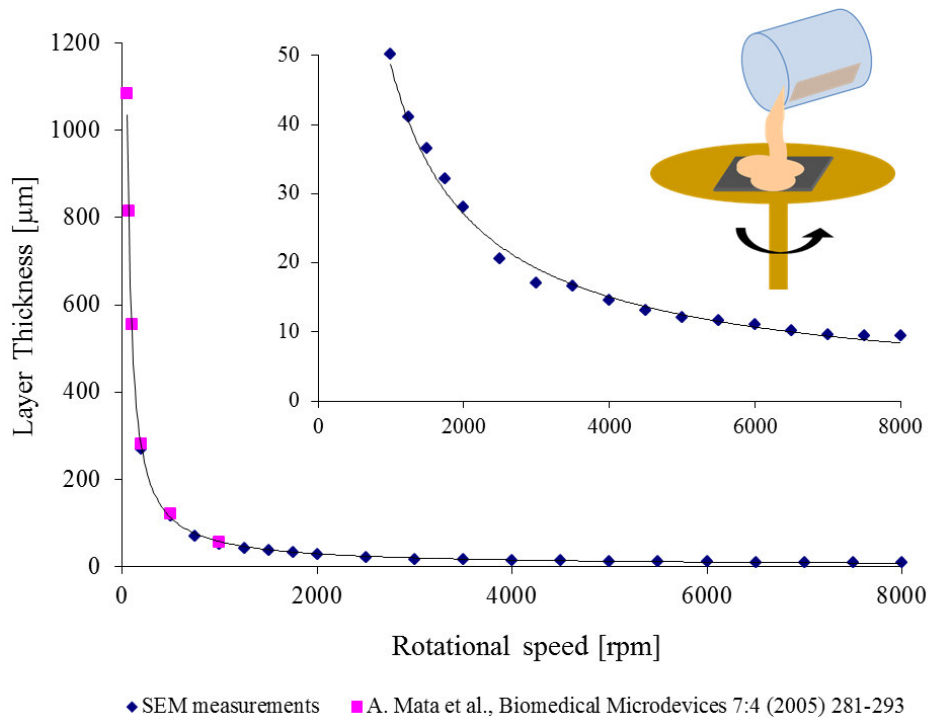


Figure 4.2. Calibration curve of the polymer thickness versus the spin-coating rate. The acceleration rate was fixed at 85 rpm/sec and the spinning time at 90 s. Note that some literature values (pink squares) have been added for comparison. The insert shows the values for the range 1000 to 8000 rpm and a simplified schematic representation of the spin-coating technique. The data points were approximated with the power function fit.

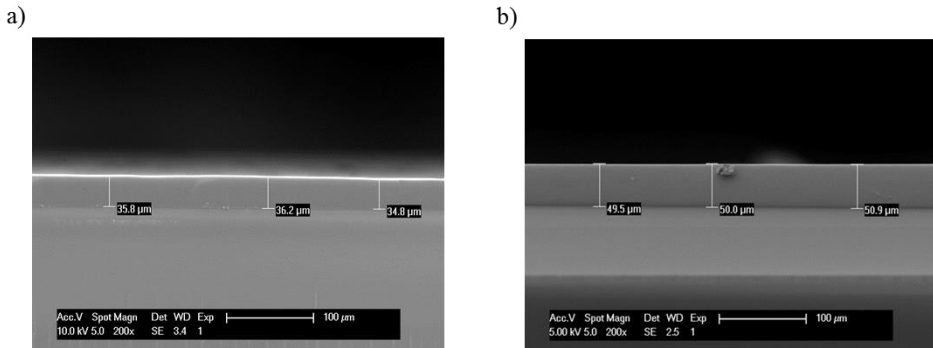


Figure 4.3. SEM images of PDMS layers spin-coated onto supporting glass substrate. The rotational speed was 1500 and 1000 rpm, resulting in layer thicknesses of a) $\sim 35 \mu\text{m}$ and b) $\sim 50 \mu\text{m}$, respectively.

4.3 Printed Circuit Board

After the PDMS layer had cross-linked and hardened, the IDE chip was placed and glued with pine tree resin (melting point: $160 \text{ }^\circ\text{C}$) into a fitted milling hole that is provided on a printed circuit board, short PCB. The PDMS was carefully scratched off from the contact pads, which were then wire-bonded (Wire bonder Type 827X by Mech-EI Industries Inc.) with $25 \mu\text{m}$ gold threads to the provided contact pads of the PCB. Pin connectors are soldered to the outlying contact pads of the PCB to make further connections to the electronic readout. A schematic representation of the top-side of the PCB containing the PDMS-coated IDE chip is shown in Figure 4.4.

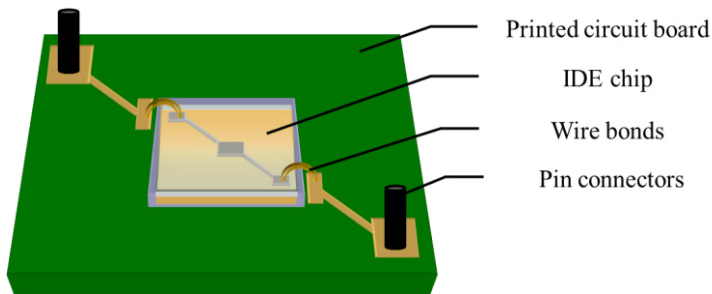


Figure 4.4. Schematic representation (not to scale) of the top-side view of the PDMS-coated IDE chip that is placed into the fitted milling hole and wire-bonded to the contact pads of the PCB.

The printed circuit boards were designed with Eagle Layout Editor 6.4.0 and ordered at Eurocircuits N.V. in Belgium. The PCB dimensions are 30 mm × 30 mm × 1.55 mm ($l \times b \times h$). The milling hole of 13 mm × 13 mm × 1.1 mm ($l \times b \times h$) is centred on the PCB. All free areas of the top and bottom side of the PCB are provided with shielding areas, which lie at 0.3 mm distance from the circuitry pattern. Note that the representation of the top shielding area of the PCB has been omitted in Figure 4.4 for matters of clarity. Hence, for 1.1 mm thick glass dices, that is the thickness of the 1 cm × 1 cm large IDE chips, about 1.55 mm of insulating material lies between the IDE structure and the grounded bottom shielding area of the PCB, and about 4.15 mm lie between the outer electrode plane and the top shielding area. The thickness of the glue between the glass chip and the PCB is neglected. Detailed information on the dimensions and dielectric constants of the materials of the IDE chip and the PCB are provided in Figure 4.5.

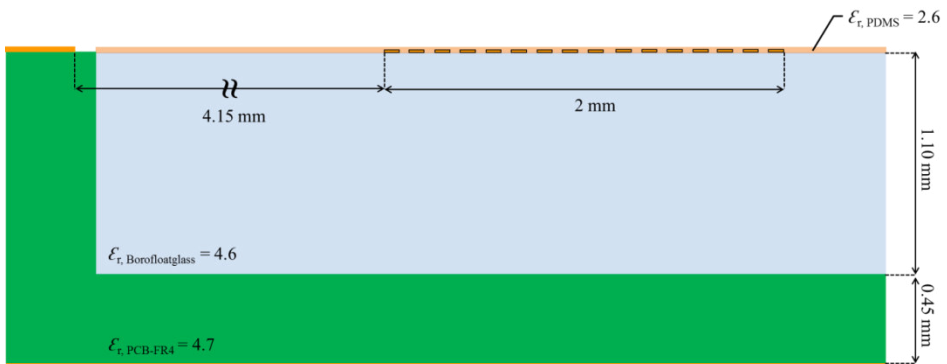


Figure 4.5. Schematic representation of the PDMS-coated IDE chip placed into the PCB with the grounded top and bottom shields and the approximate system part dimensions and the relative dielectric constants of the materials. All dimensions, except for the distance between the IDE glass chip and the PCB top shield, are to scale.

4.4 Electric Connectors

The PCB containing the PDMS-coated IDE chip is placed into a fitted milling hole provided on a metallic holder element as shown in Figure 4.6. The pin connectors are connected via standard cables to SubMiniature Version B (SMB) connectors that are integrated in the metallic holder. The holder element is equipped with four SMB connectors to make the required connections via coax-cables to the electronic readout,

the universal transducer interface as will be explained in Section 4.6. One SMB connector (1) is connected to the transmitting electrode of the IDE chip and another SMB connector (2) to the transmitting electrode of the reference capacitor of 32.2944 pF, which is also integrated within the metallic holder. A third SMB connector (3) lies open for performing the offset measurement. The fourth and last SMB connector (4) represents the common virtual ground pole that all capacitors are connected with. The metallic holder is simultaneously grounded via the SMB connectors for shielding purposes. Grounding of both the top and bottom shield of the PCB is achieved by placing the PCB into the grounded metallic flow cell holder. This is because the PCB has two metallic through holes for screwing purposes that connect the bottom and top shielding areas and that get in direct contact with the grounded metallic holder. The two screws ensure stable connection and fixation of the PCB in the metallic holder element. Figure 4.6 shows the described metallic holder element, into which the PCB containing the IDE chip is placed and screwed tight to. Also shown is a deposited drop of water on top of the IDE structure centred on the glass chip. Two cables connect the SMB connectors to the transmitting electrode (bottom-right, red) and to the receiving electrode (top-left, black).

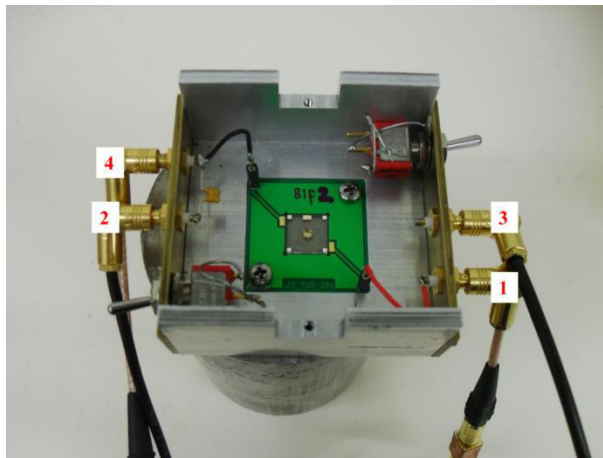


Figure 4.6. Photograph of the metallic holder element containing the PCB with the PDMS-coated IDE chip, onto which a drop of water has been deposited. The flow cell holder is put at ground potential via the four SMB connectors that connect the transmitting electrodes of the target capacitor (1), the reference capacitor (2), the offset capacitor (3), and the common ground terminal (4) to the universal transducer interface.

4.5 Flow Cell System

The flow cell system was designed to allow measurements in water under continuous flow conditions while controlling the water flow rate and composition at any time. Solutions were delivered to the flow cell through polytetrafluoroethylene (PTFE) tubing by a Harvard Pump 33 Twin Syringe Pump that is equipped with two individual syringe drives. The individual liquid streams were merged in a 3-way-valve followed by a polyether ether ketone (PEEK) tee, from which the two inlet streams lead into the flow cell chamber. The design of the Teflon flow cell is based on a mixing chamber with two diagonal inlets and one centred vertical outlet. Though the composition of both inlet streams is the same, the turbulent flow reassures that no concentration gradient occurs within the chamber and that the transport of the target compound to the sensor surface is enhanced by convection. This is in contrast to laminar-flow-type microfluidic cells, where convection occurs only in direction of the fluid flow and the chemical transport perpendicular to the fluid flow is diffusion limited.⁶

The chamber volume measures less than 30 μl . The flow cell is equipped with a metallic bar that fits and is screwed into the metallic holder element to ensure right positioning. By doing so, the flow cell is pressed against the underlying substrate, which is the PDMS-coated IDE chip. When mounted, the flow cell chamber is centred over and encloses the entire electrode plane. An inter-lying Viton O-ring of 5 mm in diameter reinsures that the flow cell is sealed off. Flushing a polar liquid over a hydrophobic surface, *e.g.*, the PDMS sensing layer, leads initially to an entrapped air layer between the aqueous and the polymeric phase. The air dissolves slowly into the liquid, leading to potential bubble formation. The dome-shaped top of the chamber functions as a bubble-trap, supporting a quick flush out of air bubbles. Teflon was chosen as flow cell material due to its insulating and chemically resistant properties. A schematic representation of the flow cell system is shown in Figure 4.7. The diagonally entering fluid streams create turbulent flow directly over the electrodes as depicted in Figure 4.8.

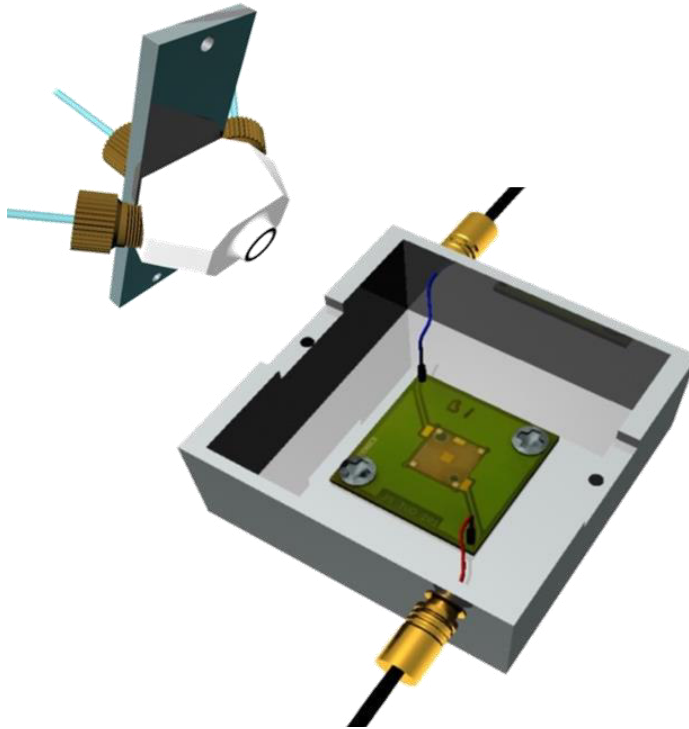


Figure 4.7. Schematic representations of the Teflon flow cell system and the sensor platform containing the PCB, onto which the IDE sensor chip is placed and wire-bonded to. Electronic connections are made to the metallic holder that is grounded by the external SMB connectors of the universal transducer interface. Note that in this graphical figure the two SMB connectors necessary for performing the measurement of the reference capacitor and the system offset are omitted for simplicity. With courtesy of Isabelle M. Aerts, MSc.

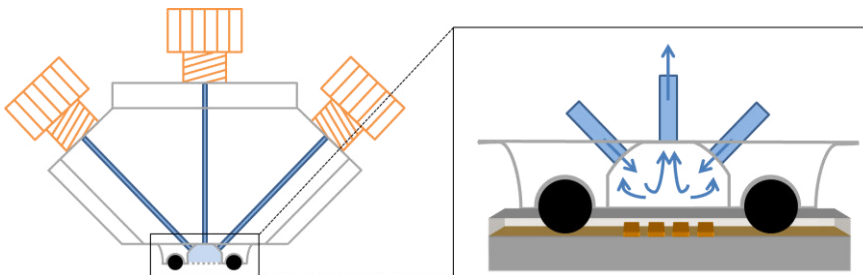


Figure 4.8. Schematic representation of the Teflon flow cell. The magnification view shows the arrangement of the two diagonal inlets, the vertical outlet, and the created turbulent flow within the chamber. The dome-shaped top of the chamber functions as a bubble-trap. Adopted from graphical figure made by Isabelle M. Aerts, MSc.

4.6 Universal Transducer Interface

In Chapter 2, it has been summed up that capacitive sensors are prone to electromagnetic interferences, electric-field bending, parasitic capacitors, and shunting resistors. If the parasitic impedances behave differently on frequency and phase of the applied excitation signal, then it is possible to eliminate or reduce them to single out the measurand. This can be achieved by means of laboratory equipment, such as impedance analysers and LCR-meters (Figure 4.9), that apply harmonic sine-shaped excitation signals. By smart signal choice and frequency scans, also small capacitances can be measured accurately. Yet, as further explained in Chapter 2, the required electronic circuitry is by far too complex to realize them into low-cost sensor interfaces.⁷ These low-cost sensor interfaces typically apply block or ramp signals, which can be realized by simple electric circuitry. The Universal Transducer Interface, short UTI, is commercially available by Smartec B.V. in the Netherlands and has originally been developed at the Department of Micro-Electronics and Computer Engineering at the Delft University of Technology (Figure 4.9).⁸

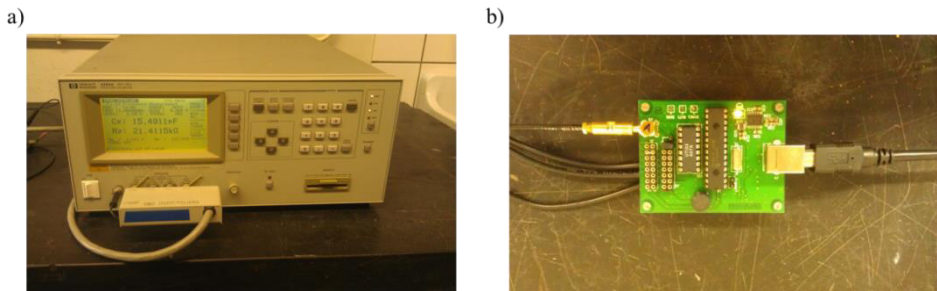


Figure 4.9. Photograph of a) a precision LCR (inductance-capacitance-resistance) meter Type HP Agilent 4284A and b) the Smartec universal transducer interface (UTI) developed at the Delft University of Technology.

The measurement circuitry of the UTI is based on the two-port measurement system, which has been explained in Chapter 2. The UTI is connected via USB to and powered by a common laptop, which supply voltage is a 5 V DC. The UTI board generates the excitation block signal with a frequency of about 30 kHz and a top-top voltage of 5 V. Depending on the measurement mode, a voltage divider has to be integrated and the resulting signal is applied to the transmitting electrode of the IDE capacitor from a low-

ohmic source, while holding the receiving electrode at (also low-ohmic) virtual ground by means of an amplifier with so-called shunt feedback (Figure 4.10). This way all parasitic capacitances lying parallel to the excitation source, such as C_{P1} , as well as all capacitances parallel to the amplifier input, such as C_{P2} , do not affect the measurement of the target capacitor C_S . Parasitic capacitances parallel to the target capacitor (C_{P3}) are eliminated with an offset measurement. As also discussed, the UTI performs a three-signal measurement, that is, it measures in turns the target capacitance and the reference capacitance and performs an offset measurement.

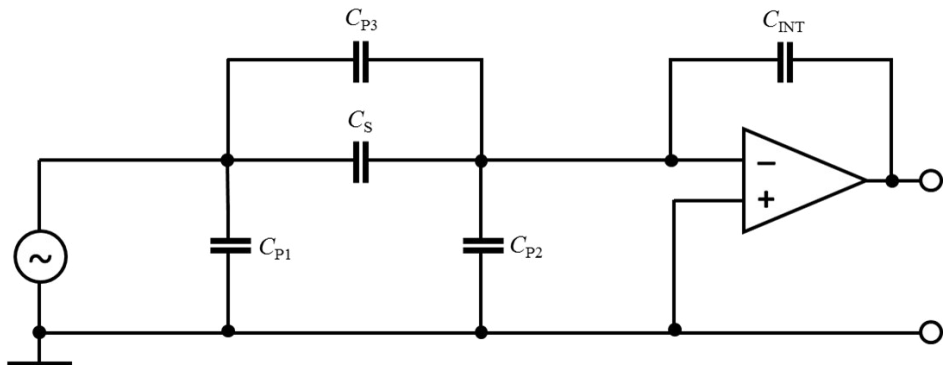


Figure 4.10. Simplified circuit diagram of the 2-port method as applied by the UTI to measure the target capacitor (C_S) independent of parasitic capacitance effects parallel to ground (C_{P1} , C_{P2}). Parasitic capacitances parallel to the target capacitor, such as C_{P3} , are eliminated via an offset-measurement. Figure adopted.⁷

For the measurement mode 12 - 300 pF, a voltage divider has to be integrated as according to the data sheet of the UTI⁹ and shown in Figure 4.11. The excitation voltage V_{ex} between node E and F can be calculated according to the Equation 4.1 to be 0.38 V.

$$V_{ex} = \frac{R_2}{R_1 + R_2} V_{DD} \quad (4.1)$$

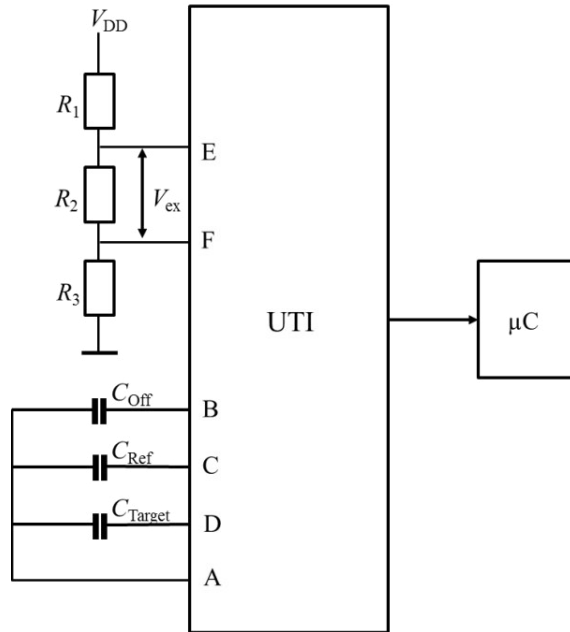


Figure 4.11. Connections of the voltage divider with $R_1 = 27$ kOhm, $R_2 = 2.2$ kOhm, and $R_3 = 0$ kOhm, and the capacitors with $C_{Ref} = 32.2944$ pF, $C_{Off} =$ offset, and $C_{Target} \sim 20$ pF to the UTI in the 300 pF mode and $V_{DD} = 5V$. Figure adapted from literature.⁹

The UTI is set to an operation range of 300 pF at slow mode, *i.e.*, the output data of the evaluation board is generated at a rate of ~ 15 samples per second resulting in measurement times of ~ 70 ms. As according to the production sheet provided by Smartec B.V., the UTI has a resolution down to 500 aF when operating in the 300 pF mode, and the resolution increases to higher values with increasing capacitances to be measured. In real-time measurements, it was found that for capacitances of ~ 20 pF the resolution of the UTI amounts to a values of about 2 fF. In order to improve the resolution, the measurement points were averaged over 100 data points, which yielded a resolution of about 0.5 fF at measurement times of 7 s. According to the obtained measurements, the high frequency noise of the real-time value is mainly attributed to thermal noise. Averaging as done over 100 points leads to a noise with lower amplitude. It was observed that further increasing the index of averaging does not result in much less noise. In terms of capacitance, this resolution determines the limit of detection. Recently, similar interfaces have been fabricated with better noise specifications.¹⁰

However, the current resolution was acceptable for the presented experiments in this work.

4.7 LabVIEW Program

Read-out and processing is performed with the UTI-supporting LabVIEW software Version 8.5. With this programme, all measurement settings are controlled. The original LabVIEW file as provided by Smartec B.V. was extended and modified to meet the needs of the experiments performed in this work. This is, *e.g.*, allowing time-based measurements and displaying the data for long or short measurement periods. Both the real-time measurements and the averaged measurements are displayed. For the latter, the average index can be set. The generated data, that is the time, the measurement times, the real-time capacitance, and the averaged capacitance, is stored in '.txt' files from where it can then be transferred into a programme of choice for further processing. In the current work, further processing was done using Microsoft Excel. For long-term measurements, which exceeded 2^{16} (65536), data points, the data was compressed by a data converter programme. Depending on the total amount of measurement points stored in the '.txt' file, the data converter programme calculated the data points that could be transferred to fit into the column of the Excel-file.

4.8 Temperature Dependency

Fully developed chemical sensor systems are calibrated or/and conditioned for any other parameter, such as humidity or temperature, that can influence the system response.¹¹ The designed measuring system is neither calibrated nor conditioned, so the influence of external influencing parameters have to be accounted for and the ambient temperature must be stabilized. Since the PDMS-coated IDE platform will be directly exposed to the aqueous phase in the next described experiments, the polymer layer is first saturated with water vapour. Therefore, variations in humidity that may cause drastic capacitive changes in the response do not occur. Yet, it was found that the system responses sensitively to temperature changes. In order to study the system dependency on temperature more closely, the entire sensor system was placed into an air-conditioned room, where we measured the ambient room temperature and the sensor capacitance simultaneously. The temperature sensor was located close to the Teflon flow cell that was mounted onto the PDMS-coated IDE chip as described in the previous section. The

system was filled with water and the recording of both the capacitance as measured with the UTI and the ambient temperature was started. The temperature was recorded with the XL100 Portable Data Station by Yokogawa. The total measurement series extended over a period of 5 hours. The results are depicted in Figure 4.12.

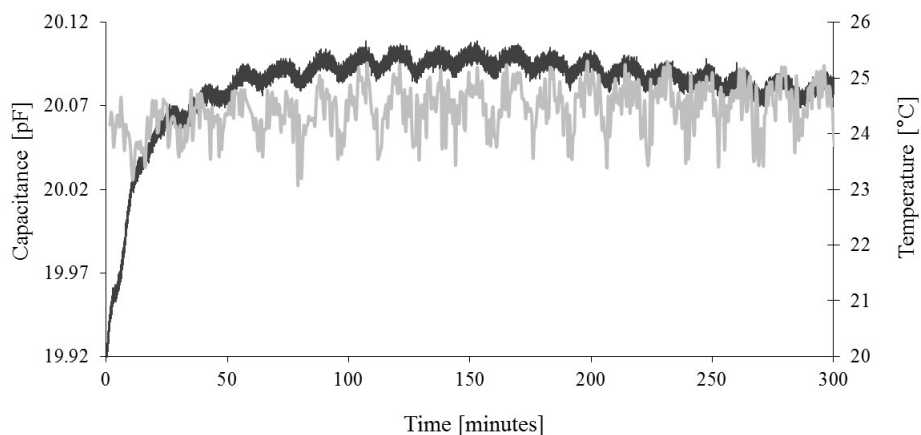


Figure 4.12. Simultaneous recording of the capacitance (dark grey) of a PDMS-coated IDE-chip and the ambient temperature (light grey) close to the flow cell over a 5 hour measurement period.

As can be seen from the graph, the capacitance (dark grey) follows the temperature profile (light grey). Both are oscillating with a period of ca. 20 minutes, which is about the regulating period of the air conditioning system. From the graph it can be derived that the sensor system has a positive temperature coefficient of ~ 13 fF per degree Celsius. The increase in capacitance occurring within the first hour as shown in this diagram after starting the measurement has also been observed in other measurements in closed aqueous systems during the start-up phase but not for gas phase measurements. It is related to the uptake of water into the polymer layer until full saturation under the given conditions. Over longer time periods and depending on the experimental phases that the polymer layer had to go through, the uptake of water as indicated by the rising capacitance baseline continued and accelerated. This could be related to the gradual wear and eventual breakdown of the polymer layer. A second overlaying drift may be attributed to the actual temperature of the IDE device. In closed rooms with regular heating systems and in the absence of air drafts and daylight exposure, it was found that for short measurement periods the system response was stable enough for enabling

measurements with detection limits at the mentioned resolution of 500 aF. All experiments described in Chapter 5 and 6 were performed under such conditions.

4.9 Concluding Remarks

The developed interdigitated electrode (IDE) platform is made up of a 1 cm² sized borosilicate glass chip with a centred IDE plane, consisting of 221 parallel golden electrode fingers of 6 μm width and 3 μm distance between them. The leads are arranged diagonally to the contact pads. IDE structures have been designed with and without in-plane guarding electrodes, lying at 6 μm distance from the IDE structure. The IDE platforms are coated with polydimethylsiloxane (PDMS) films of controlled thickness as obtained via a spin-coating technique similar to a method described in literature.⁵ The obtained PDMS thicknesses were in good agreement with this reference work. The PDMS-coated IDE chip is placed onto a printed circuit board (PCB) and integrated within a metallic holder device, containing the necessary electronic connects. By means of a self-designed flow cell system, of which the PDMS-coated IDE chip forms the bottom part, measurements under continuous water conditions can be performed. Solutions are supplied and their composition is controlled via a two-drive syringe pump. Electronic readout is performed with a low-cost and LabVIEW-supported universal transducer interface (UTI), that had originally been designed at the Delft University of Technology for Smartec B.V. located in the Netherlands. The UTI measuring principle is based on the two-port and three-signal measurement technique, which allows to eliminate parasitic capacitances to ground, offsets, and gains. Real-time measurements revealed a resolution in the low fF range. Yet, by averaging over 100 data points, a resolution of ~500 aF can be achieved. Averaging over more data points, *i.e.*, time periods, does not enhance the resolution, which can be related to thermal effects. Due to the high temperature sensitivity of ~13 fF/°C, stable temperature conditions in the lab environment are required.

4.10 References

- 1 L. H. D. Skjolding, C. Spegel, A. Ribayrol, J. Emnéus, and L. Montelius, Characterisation of nano-interdigitated electrodes, *Journal of Physics: Conference Series*, 100 (2008), 052045.
- 2 J. C. Love, L. A. Estroff, J. K. Kriebel, R. G. Nuzzo, and G. M. Whitesides, Self-assembled monolayers of thiolates on metals as a form of nanotechnology, *Chemical Reviews*, 105 (2005), 1103-1170.
- 3 G. C. M. Meijer, Elektronische implementatiekunde (Delft, The Netherlands: Delft University Press, 1998).
- 4 Product datasheet: Sylgard184 silicone elastomer, *Dow Corning Company* (2012).
- 5 A. Mata, Fleischman, A. J., Roy, S., Characterization of polydimethylsiloxane (PDMS) properties for biomedical micro/nanosystems, *Biomedical Microdevices*, 7 (2005), 281-293.
- 6 T. Gervais, and K. F. Jensen, Mass transport and surface reactions in microfluidic systems, *Chemical Engineering Science*, 61 (2006), 1102-1121.
- 7 X. Li, Meijer, G. C. M., Capacitive sensors, in *Smart Sensor Systems*, ed. by G. C. M. Meijer (Chichester, U.K.: John Wiley & Sons, Ltd., 2008), pp. 225-248.
- 8 F. M. L. Van der Goes, Low-cost smart sensor interfacing (Ph.D. Thesis, Delft University of Technology, 1996).
- 9 Datasheet: Universal transducer interface (UTI), *Smartec B.V.* (2012).
- 10 A. Heidary, A low-cost universal integrated interface for capacitive sensors (Ph.D. Thesis, Delft University of Technology, 2010).
- 11 D. Rivera, M. K. Alam, C. E. Davis, and C. K. Ho, Characterization of the ability of polymeric chemiresistor arrays to quantitate trichloroethylene using partial least squares (PLS): Effects of experimental design, humidity, and temperature, *Sensors and Actuators B-Chemical*, 92 (2003), 110-120.

WATER-ENHANCED GUARDING OF POLYMER-COATED IDE PLATFORMS

The detection limit of a measuring system is dependent on its noise level and on systematic physical non-idealities. To achieve a high sensitivity, all parasitic impedance effects must be eliminated to not interfere with the information carrying signal. In comparison to ‘closed’, three-dimensional structures, the electrical sensing field of the ‘open’, planar IDE structure is geometrically difficult to guard. Direct exposure to aqueous solutions may cause unpredictable parasitic coupling to the surrounding, which results in device sensitivity to changes in environmental conditions, such as salt concentration and pH. In this work, we demonstrate how water-enhanced electrical coupling to guarding electrodes is a key mechanism in achieving response immunity to parasitic electric-field bending without impairing the detection performance of the polymer-coated IDE platform.

A slightly modified version of this chapter has been accepted for publication:

Staginus, J.; Chang, Z.-Y.; Sudhölter, E.J.R.; de Smet, L.C.P.M.; Meijer, G.C.M., *Sensors & Actuators A-Physical* (2015).

5.1 Introduction

Capacitive sensing is used frequently to obtain spatial-related information (*e.g.*, proximity, position, displacement, acceleration) or to obtain information based on dielectric constants as an indirect method to measure humidity, fluid levels or chemical compositions.¹⁻⁴ Much effort has been spent on the study of polymer-based capacitive interdigitated electrode (IDE) platforms for the detection of chemical compounds.⁵⁻⁷ The polymer layer that is deposited on the IDEs serves as a chemical filter, that extracts selectively and concentrates the target compound. Thereby it enhances the desired information from the water or from the air phase, which is the type of pollutant and its environmental concentration. At the same time, the polymeric sensing layer insulates the IDEs, which is of essence when performing capacitive measurements in aqueous media. Embedding IDEs into polymers that act as support, sensing, and also insulation material, could present a further design option for chemical capacitive sensing techniques. Such sensing elements could be based on recent advances in the development of flexible electrodes on flexible polymer substrates, such as carbon nanotube-based IDEs on polydimethylsiloxane supports as developed for capacitive sensing of mechanical deformation.⁸ As we introduced in Chapter 3, the interdigitated electrode platform is a popular transducer platform for chemical detection, because it consists of a robust structure that can cost-effectively be fabricated by common IC technology.^{9, 10} Furthermore, it offers a large interaction surface, which chemical properties can easily be modified by various deposition techniques.¹¹⁻¹³

Polydimethylsiloxane, short PDMS, is an inert and hydrophobic polymer that readily absorbs and swells in organic solvents but is compatible with water and only prone to water-vapor absorption.¹⁴⁻¹⁶ Therefore, it is a predestinated material for the detection of organic pollutants in aqueous phases. In our previous work,¹⁷ we demonstrated the capability of PDMS-coated IDE platforms to detect capacitively organic pollutants in water by direct exposure to the spiked aqueous phases. Yet, we further reported on the presence of a parasitic coupling effect to the surroundings as induced by the water phase. In fact, one major challenge is the proper guarding of the out-of-plane electric sensing field of the IDEs as depicted in Figure 5.1, which affects negatively the detection performance. In this work, we demonstrate how the water-enhanced coupling effect to in-plane guarding electrodes as described in Chapter 4 and to ‘third’ guarding electrodes as described in Chapter 3 can be exploited to reduce this

negative effect significantly. In combination with optimization of the polymer layer thickness, this yields a significant improvement of the IDE system.

A schematic representation of a PDMS-coated interdigitated electrode structure is shown in the insert of Figure 5.1.

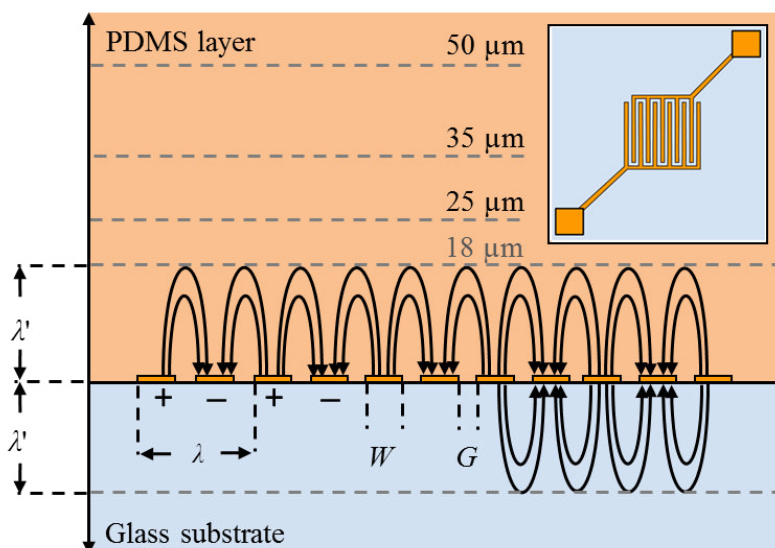


Figure 5.1. Schematic representation of the side-view of polymer-coated IDEs (here: polydimethylsiloxane, PDMS) on a glass substrate, showing the electric sensing field established between the finger electrodes (dimensions to scale except for finger thickness, which is typically in the nm range). Depicted are the width (W) of the finger electrodes, the gap (G) between them, and the spatial wavelength (λ). Also shown are the penetration depth of $18\ \mu\text{m}$ (λ') of the electrical field into the PDMS layer and the glass substrate and an indication of three layer thicknesses ($25\ \mu\text{m}$, $35\ \mu\text{m}$, and $50\ \mu\text{m}$). The penetration depth has theoretically been derived for the case of absence of parasitic electric-field bending.^{5, 18} The insert shows a schematic representation of the top-view of an IDE structure with diagonally arranged leads (top-right, not to scale).

5.2 Materials and Methods

5.2.1 Chemicals

Milli-Q water ($0.35\text{-}0.75\ \mu\text{S}/\text{cm}$) was tapped from a Millipore system (type AFS-3D). NaCl (99%) was purchased from Sigma Aldrich and used as received. The conductivities of the Milli-Q water and salt solutions were measured with a

conductometer (Metrohm 712). For the preparation of the PDMS layer, the commercial two-component product Sylgard®184 of the Dow Corning Company was used as described in Chapter 3, Section 3.2.1 and Chapter 4, Section 4.2.

5.2.2 IDE Platform

The IDE design is as described in Chapter 4, Section 4.1. That is, IDE platforms with diagonally arranged leads and with and without in-plane guarding electrodes were used.

5.2.3 PDMS Layer

The PDMS layers of approximate thicknesses of 25 μm , 35 μm , and 50 μm were deposited via a spin-coating technique as described in Chapter 4, Section 4.2.

5.2.4 Universal Transducer Interface

For electrical readout, a Universal Transducer Interface (UTI) with the specifications as described in Chapter 4, Section 4.6 was used.

5.2.5 Drop Experiment

For the experiments performed with Milli-Q water, the water drops were deposited manually onto the PDMS-coated IDE structure with in-plane guarding electrodes by means of a pipette. By depositing drops of increasing volumes (*i.e.*, 8 μl , 20 μl , 50 μl , and 100 μl), the size effect on the capacitive read-out was studied. As larger drops would risk contact with the contact pads, which are not covered and sealed by the PDMS layer, and hence present a risk of electrical shortage, the maximum drop volume was chosen to be 100 μl . The water drops also served for making electrical connection to additional ‘third’ electrodes in the environment. After fixed periods of times, that is 1 min of water deposition and absorption, the water drop was penetrated right above the center of the IDE plane by means of a metallic shaft to simulated the effect of an additional ‘third’ electrode. A flat-tipped metallic thin and pointed shaft of 3 mm maximal width was chosen, which does not disturb the droplet upon introduction as to cause further spreading. The metallic shaft is grounded via physical contact with the grounded metallic flow cell holder element. The shaft tip was held at a perpendicular distance of about 2 mm to 3 mm from the center of the IDE plane (Appendix B, Section B.1, Figure B.1). The contact was repeated after ca. 10 s of relief. Between single

measurements, the water drops were carefully removed from the PDMS surface with a dust-free tissue, and the IDE chip was left to dry until the capacitance baseline returned to the original dry-state value.

5.2.6 Continuous Flow Experiment

An aqueous 20 mM NaCl solution was prepared using Milli-Q water. The flow cell system as described in Chapter 4, Section 4.5 was used. Solutions were delivered to the flow cell through PTFE tubing by a Harvard Syringe Pump 33 that is equipped with two individual syringe drives. One syringe was filled with Milli-Q water and the other one with a stock solution. The individual liquid streams were merged in a 3-way-valve followed by a PEEK tee, from which the two inlet streams lead into the flow cell. The sensor was first allowed to stabilize in the pure aqueous phase for at least 1 h to achieve a stable baseline before the measurements were started. The salt concentration delivered to the measuring cell was increased stepwise from 1 to 20 mM by applying different flow rates of stock solutions and Milli-Q water. A calibration curve of the solution conductivity as function of NaCl concentration for the molar range studied is given in the Appendix B, Section B.2, Figure B.2. The total flow rate was kept at 600 $\mu\text{L}/\text{min}$ at all times to avoid pressure differences and to ensure a refreshment rate of the measurement chamber ($\sim 20 \mu\text{l}$) of about 18 times per minute and of the entire flow cell system including pipes and connectors ($\sim 600 \mu\text{l}$) of about 1 time per minute. The capacitive responses of the IDE chips with and without in-plane guarding electrodes and 25 μm , 35 μm , and 50 μm thick PDMS layers to increasing solution salinity were studied.

5.3 Experimental Investigation

Capacitive sensors based on planar, polymer-covered IDE platforms are interesting for a wide range of applications. Independent of whether the measuring system is open or closed, under stationary or continuous-flow conditions, it is of great importance to properly guard the electric sensing field. The direct contact of the polymer surface with the water phase, which contains the chemical species, *e.g.*, as pollutant, can electrically couple the sensing device to the environment or to other system parts. In the following experiments, we will first demonstrate how for a droplet detector water-enhanced electrical coupling to guarding electrodes provides a simple but effective mechanism in

achieving response immunity for influences of coupling with the water phase or its environment (Section 5.3.1). We will then show how for the designed flow detection system the response sensitivity to changes in the solution conductivity as induced by changes in salinity further depends on the polymer layer thickness (Section 5.3.2). It will be shown that, with proper care, the water phase can be considered as being an electrode itself, that can protect our sensitive device from being influenced by changes in the environment, the effects of interfering signals, and from variations in the conductivity of water and this without impairing the detection performance of the polymer-coated IDE device.

5.3.1 Droplet Detector

In this section, we present an easy method to demonstrate for the designed droplet-detector platform the effect of water-enhanced guarding on the response sensitivity to further electrical coupling effects as caused by the introduction of a third electrode. To do so, water drops of increasing volumes and hence increasing areas are deposited onto the polymer-coated IDE structure with in-plane guarding electrodes. In this way, an enhanced electrical coupling effect to the guarding electrodes is achieved. Then, it is demonstrated that when the droplet is contacted with an additional grounded "third" electrode, that together with this third electrode the droplet itself can very well function as a guarding electrode. Once such an arrangement is realized, the IDE sensor is rather immune for further environmental effects, such as parasitic coupling to the metal parts in the environment. As a summary of the performed experiments, the following will be shown:

- a) Upon the moment of drop deposition, the IDE sensing field is electrically coupled to the in-plane guarding electrodes, which will be observed as an instant decrease in capacitance. This water-enhanced guarding effect increases for larger droplets.
- b) When the droplets are electrically floating, so not directly contacted with a grounded electrode, then the measured capacitance is rather sensitive to parasitic coupling to the environment. This sensitivity is demonstrated by the effect of introducing a grounded third electrode. This sensitivity decreases for larger droplets.

- c) When the droplets are in contact with a grounded third electrode, the droplet size is not that important anymore as the water-enhanced guarding effect is dominated by the presence of the grounded third electrode. Then, a ‘new’ baseline value is reached, and it is expected that with such a third electrode also variations in the salinity does not have much influence anymore.

Figure 5.2 depicts the capacitive response of an IDE platform with a 50 μm thick PDMS coating, which is larger than the spatial wavelength of 18 μm , and in-plane guarding electrodes surrounding the IDE structure upon the deposition moment of Milli-Q water drops of increasing volumes (8 μl , 20 μl , 50 μl , and 100 μl) onto its center. Then, after absorption times of ~ 60 s and ~ 80 s the center of the deposited water drop was brought in direct contact with a grounded metal shaft, the third electrode, for ~ 10 s. The insertion figures give a schematic representation of the top-view of the guarded version of the IDE chip and an idea of the relative sizes of the deposited water drops.

As shown in Figures 5.2a-d, upon the moment of a water drop deposition at ~ 25 s, the capacitance initially decreases abruptly within 1-2 s before increasing gradually to higher values. This is because water-enhanced coupling to the guarding electrodes occurs instantly during the time of drop deposition, leading to the abrupt reduction in IDE capacitance while the simultaneous occurrence of slow water vapour absorption into the PDMS layer causes a gradual positive change in capacitance. Water vapor absorption occurs until full saturation of the PDMS layer. Then, a capacitance value is reached that represents the baseline value. As approximated by the dashed tangent and horizontal line, the reduction in IDE capacitance due to water-enhanced guarding increases for larger water drops. Hence, for larger drops also this baseline value decreases. In Figures 5.2e-h, it can be clearly seen that the additional negative capacitance change, upon the introduction of a third (grounded) electrode, diminishes significantly for bigger droplets. This is because big droplets already have a better coupling effect with the grounded guarding electrodes due to their large areas. The total capacitance decrease caused by water-enhanced electrical coupling to the guarding electrodes plus to the third electrode always amounts to about 200 fF, which is just above 1 % of the total IDE capacitance of ~ 18.89 pF. Therefore, a ‘new’ baseline capacitance value of ~ 18.82 pF is reached, which is now *independent* of the droplet size.

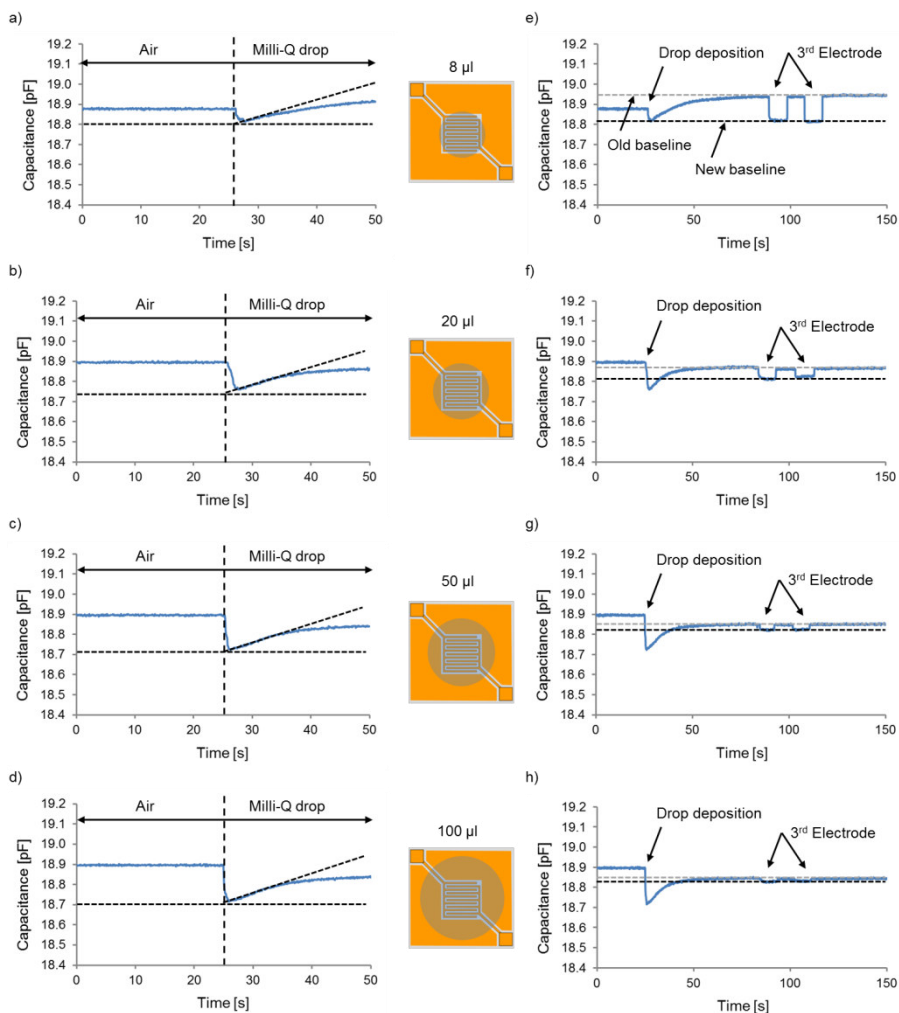


Figure 5.2. Real-time capacitive response upon the deposition of a a), e) 8 μl , b), f) 20 μl , c), g) 50 μl , and d), h) 100 μl drop of Milli-Q water onto the PDMS-coated and guarded IDE structure and the two events of a parasitic third electrode effect. Figures 5.2 a-d show the initial 50 s of the measurement. Depicted with the dashed vertical line is the moment of depositing the drop of Milli-Q water (*i.e.*, ~ 25 s). The dashed tangent and horizontal line approximate the capacitance decrease due to water-enhanced guarding. Figure 5.2 e-h show the full measurement including the event of drop deposition and the two events of contacting the droplet with a grounded third electrode at ~ 60 s and ~ 80 s. Also depicted are the highest (old) and the lowest (new) capacitance baselines. The schematic representations (not to scale) show the top-view of the PDMS-coated IDE chip with guarding electrodes and the deposited water drops of increasing volume (not to scale).

For example, upon the deposition of a 8 μl droplet the capacitance decreases by ~ 75 fF and the introduction of the third electrode leads to a further reduction of ~ 125 fF, amounting to a total reduction in IDE capacitance by ~ 200 fF. For a 100 μl drop, the electrical coupling effect to the guarding electrodes is much larger and measures ~ 185 fF, however, the residual response effect upon the introduction of a third electrode measures only ~ 15 fF, again resulting in a total IDE capacitance reduction by ~ 200 fF. As these capacitance changes due to electrical coupling effects are rather small, it will require a high system resolution (possibly as close as the resolution of the electronic readout device) to achieve pollutant detection at low aqueous concentration.¹⁷ It is hence of interest in sensing techniques that the sensor operates at this ‘new’ baseline that represents the capacitance of a guarded IDE sensing field.

Further, it has been found that due to the reduction in IDE capacitance as caused by water-enhanced guarding, the sensitivity of the IDE sensing device is not significantly reduced (Appendix B, Section B.3, Figure B.3). This is plausible, as only the electric field that lies at the largest distance from the IDE plane and closest to the water layer, where the electric-field density and thus sensitivity is the lowest, is affected by water-enhanced guarding. The low impact on the device sensitivity is further supported by the observation that the positive change due to water-vapor absorption is not significantly influenced by the enhanced initial coupling to the guarding electrode and measures about ~ 125 fF for all cases. It has to be noted that electric-field bending occurs instantly, which is also shown by the jump-like response behavior upon the introduction and removal of the third electrode. In other words, upon the introduction of the additional third electrode into the water layer, both the IDE capacitance (C_{ide}) and the guard capacitance (C_{guard}) are affected instantly. As described in Chapter 3, Section 3.4.1, theory suggests that the electrical coupling effect to the third electrode through the water layer is most influential. The results let to conclude that if the coupling effect to the guarding electrodes was enhanced to ~ 200 fF, that is when the old and the new baseline coincide, the introduction of the third electrode could not be observed anymore, because the enhanced guarding effect by the water layer was already very effective. This will happen by using a larger droplet and/or by using droplets with a higher conductivity. This way the detection performance could be increased to achieve a detection resolution close to the resolution of the UTI, which measures ~ 500 aF. Under environmental conditions the conductivity of the water phase is significantly increased

due to the presence of dissolved ions. Fresh water streams such as rivers typically have a conductivity up to ~ 2 mS/cm. This means, the electrical coupling effects to the guarding electrode and to the third electrode are expected to be larger due to the lower impedance of the water phase. To reveal this impact, a comparative study with an aqueous 20 mM NaCl solution, that is ~ 2.1 mS/cm solution conductivity (see Figure **B.2**), was performed. It was found that the total electrical coupling effect to the guarding electrodes and to a third electrode is enhanced by ~ 10 %, which is ~ 0.1 % of the total capacitance, when performing the drop experiment with a 20 mM NaCl solution. The coupling effect to the third guarding electrode depends on its distance to the IDE plane and its area, in particular the wetted electrode area. The latter increases for larger droplets when a perpendicular distance of about 2 mm to 3 mm from the center of the IDE plane is maintained. However, it was found that variations in the penetration depth of the flat-tipped head of the third electrode —and hence its resulting distance down to about 2 mm to 3 mm from the IDE plane— have a negligible response effect. This demonstrates that water itself already functions pretty well as an electrode, especially when it contains salts. Finally, depending on the measurement frequency also the electrode material plays a role as the impedance of electric double layers may become significant. Yet, due to the high measurement frequency of the excitation voltage as applied by the UTI (> 25 kHz), their influence is negligible.¹⁹ From the results obtained here, the following is to conclude: the application of in-plane guarding electrodes is a simple but powerful tool to achieve response immunity to parasitic electric-field bending. From an electrical point of view, it would be even better to apply a porous guarding electrode right above the IDE plane at the shortest possible distance from the polymer surface and to ground that electrode, so that the sensor ground is in direct contact with the liquid to be tested. However, such a sensor structure would significantly increase the complexity and costs of device fabrication.

5.3.2 Flow Detector

The response sensitivity to salinity changes also depends on the absolute solution conductivity as well as on the polymer layer thickness, which will be discussed in this subsection. As discussed and demonstrated in Chapter 3, Sections 3.1, the water phase that is in direct contact with a grounded third electrode may best function as a guarding electrode. The presence of the third electrode could easily be integrated within a flow

detector as part of the fluidic system. However, it is not yet implemented in our current setup. In this section, we demonstrate the impact of polymer layer thickness on the sensitivity of the response to increasing salinity and hence solution conductivity for PDMS-coated IDE platforms with and without in-plane guarding electrodes. The test was performed under continuous flow conditions within a closed Teflon-based flow system as described in Chapter 4, Section 4.5. Guarded and unguarded IDE platforms with PDMS layer thicknesses of 25 μm , 35 μm , and 50 μm were exposed to water solutions with increasing salt (NaCl) concentration and corresponding solution conductivity (Figure 5.3). Because of the different baseline capacitance of the IDE chips, the capacitance change, that is the difference in baseline capacitance C_{IDE} as measured in Milli-Q water and in salt water, is depicted. The PDMS area covered by water is determined by the size of the O-ring of the flow cell chamber and is comparable to the area taken in by a 50 μl drop. Thus, residual response sensitivity to a parasitic electrode and consequently to changes in solution conductivity has to be expected. Parasitic coupling of the flow cell environment was also reported on in previous work.¹⁷ In that case, IDE chips without in-plane guarding electrodes were used and negative response changes could partly be linked to parasitic coupling effects to the PCB bottom shield area. For comparison reasons, the IDE chips without in-plane guarding electrodes were included in this study. As a summary of the performed experiments, the following will be shown:

- a) Thicker polymer layers increase the distance towards the water phase, thereby decreasing parasitic coupling effects to other system parts and the surroundings. Since only the most outer part of the electric sensing field is affected by parasitic coupling effects, a saturation value is expected to be approached for higher solution conductivities. Furthermore, it is expected that the salinity effect will decrease with increasing layer thickness.
- b) As the out-of-plane electric sensing field decreases for increasing distance from the IDE plane, the relative impact of increases in polymer layer thickness will also decrease.
- c) For the IDE chip without in-plane guarding electrodes, the same qualitative observations will be made, but the salinity effect on the capacitive response change will be significantly larger.

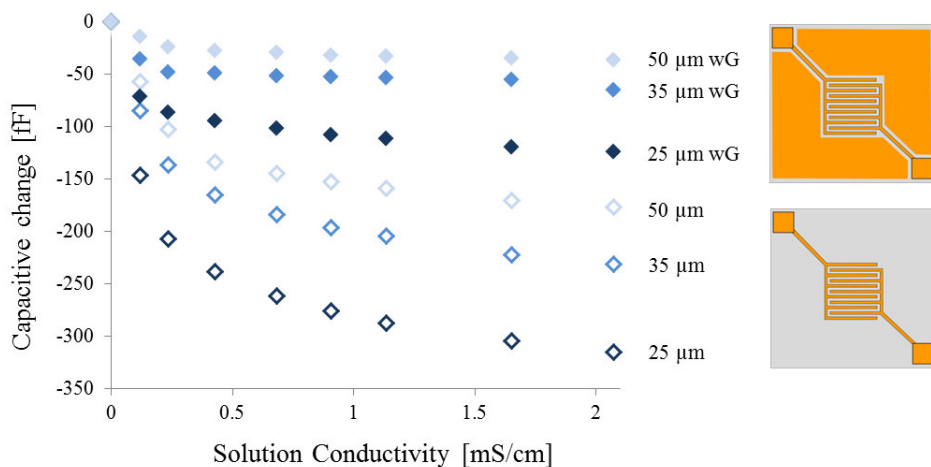


Figure 5.3. Capacitive change as function of solution conductivity of the NaCl solutions for IDE chips without and with (wG) in-plane guarding electrodes and different PDMS-layer thicknesses (25 μm , 35 μm , and 50 μm) under flow conditions. In these experiments, the liquid was not in contact with a grounded third electrode. The schematic representations of the two different IDE devices is shown on the right. For the guarded IDE chip, the result of a single measurement is represented, and for the unguarded IDE chip, the average of two subsequent measurements is displayed. Further information is found in the main text.

As can be seen in Figure 5.3, for increasing solution conductivity, the capacitance change is negative for all IDE platforms and shows a saturation behaviour. Upon increasing salt concentration the aqueous phase behaves increasingly more as a conductor than a capacitor. This may be viewed as a transition from a non-ideal to an ideal electrode. Consequently, electrical coupling to other electrodes is enhanced until the maximal coupling effect is reached. It is to be noted again that the liquid was not brought in direct contact with a grounded third electrode. As expected, the coupling effect decreases for thicker PDMS layers. For a guarded IDE platform with 50 μm thick PDMS coating, changes in capacitive response due to changes in water conditions above 8 mM are close to the resolution of the applied UTI, which is ~ 500 aF. As further expected, the reduction in sensitivity of the response to changes in water salinity is less when increasing the layer thickness by 15 μm from 35 μm to 50 μm than when increasing it by only 10 μm from 25 μm to 35 μm . This is of importance as the optimal polymer layer thickness must be chosen as such that the system becomes non-

responsive to swelling effects. As expected, the negative response changes to increasing solution salinity and corresponding conductivity is significantly less for the guarded IDE platform than for the unguarded version. As can be seen in Figure 5.3, the effect of placing in-plane guarding electrodes next to the IDE structure coated with a 25 μm thick PDMS layer is much more effective than doubling the PDMS layer thickness, saving valuable response time. In contrast to the unguarded IDE platform as also used in previous work for a flow-detection system,¹⁷ it was found that the guarded IDE platforms were prone to instability of the capacitance baseline under the same operation conditions. This could be linked to poor adhesion between the PDMS layer and the much larger gold electrode area, which however can be successfully enhanced by a gold-surface-modification technique based on thiol-chemistry as reported elsewhere.²⁰ However, this matter was outside the scope of the current project. So far, it can be concluded that the presence of a guarding electrode situated over the IDE plane will significantly contribute the response immunity to solution conditions, likely allowing further reduction of the polymer layer as also suggested by the results obtained in Section 5.3.1.

5.4 Concluding Remarks

Capacitive sensors utilizing polymer-coated IDE structures are highly suited to implement simple systems for the detection of organic pollutants in water. To enable the detection of small amounts of pollutants, such systems should have a high immunity for other effects that can cause small capacitance changes. A high immunity for parasitic effects can be obtained by completely surrounding the IDE sensors with guarding electrodes. However, such a closed structure will disable or degrade the required open contact between the sensor and the water to be analysed, unless the water phase itself can be used as a guarding or also shielding electrode. Experimental results obtained with a droplet detector show that after contacting the droplet with a grounded “third” electrode, the water droplets indeed act as electrodes that can be used for water-enhanced guarding. The salinity of water in a natural environment will help to lower the water impedance and to realize low-impedance contact with the grounding (third) electrode. Even when a grounding electrode is not available, the ungrounded water layer has still some shielding/guarding properties. These properties are enhanced by capacitive coupling with a grounded electrode. For instance, for a droplet detector with

an IDE sensor in combination with in-plane guarding electrodes, it is shown that with larger droplet sizes, a better guarding for environmental effects is obtained, which is due to the better “electrical contact” between the droplet and ground. Similarly, for a flow detector that did not have a special electrode for grounding the water flow, it has been experimentally shown, that the flow system is acting as an electrode, where the quality of guarding depends on the salinity of water and of the admittance of electrical contact between water and the in-plane guarding electrode on the IDE sensor.

5.5 References

- 1 J. H. Huijsing, Smart sensor systems: Why? Where? How?, in *Smart Sensor Systems*, ed. by G. C. M. Meijer (Chichester, U.K.: John Wiley & Sons, Ltd., 2008), pp. 1-22.
- 2 F. Reverter, X. Li, and G. C. M. Meijer, Liquid-level measurement system based on a remote grounded capacitive sensor, *Sensors and Actuators A-Physical*, 138 (2007), 1-8.
- 3 R. V. Jones, and J. C. S. Richards, The design and some applications of sensitive capacitance micrometers, *Journal of Physics E: Scientific Instruments*, 6 (1973), 589-600.
- 4 Z.-Y. Chang, B. P. Iliev, J. F. de Groot, and G. C. M. Meijer, Extending the limits of a capacitive soil-water-content measurement, *IEEE Transactions on Instrumentation and Measurement*, 56 (2007), 2240-2244.
- 5 R. Igreja, and C. J. Dias, Dielectric response of interdigital chemocapacitors: The role of the sensitive layer thickness, *Sensors and Actuators B-Chemical*, 115 (2006), 69-78.
- 6 S. Dimopoulos, M. Kitsara, D. Goustouridis, S. Chatzandroulis, and I. Raptis, A chemocapacitive sensor array system for gas sensing applications, *Sensor Letters*, 9 (2011), 577-583.
- 7 M. Kitsara, D. Goustouridis, S. Chatzandroulis, M. Chatzichristidi, I. Raptis, T. Ganetsos, R. Igreja, and C. J. Dias, Single chip interdigitated electrode capacitive chemical sensor arrays, *Sensors and Actuators B-Chemical*, 127 (2007), 186-192.
- 8 W. Jhih-Yu, H. Chih-Fan, H. Chitsung, S. Wang-Shen, and F. Weileun, Development of 3D CNTS interdigitated finger electrodes on flexible polymer for bending strain measurement, in *Micro Electro Mechanical Systems (MEMS), 2011 IEEE 24th International Conference on*, (2011), pp. 408-411.
- 9 M. Paeschke, U. Wollenberger, C. Kohler, T. Lisec, U. Schnakenberg, and R. Hintsche, Properties of interdigital electrode arrays with different geometries, *Analytica Chimica Acta*, 305 (1995), 126-136.
- 10 R. de la Rica, C. Fernandez-Sanchez, and A. Baldi, Polysilicon interdigitated electrodes as impedimetric sensors, *Electrochemistry Communications*, 8 (2006), 1239-1244.
- 11 G. Harsanyi, Polymer films in sensor applications: a review of present uses and future possibilities, *Sensor Review*, 20 (2000), 98-105.
- 12 G. Eranna, B. C. Joshi, D. P. Runthala, and R. P. Gupta, Oxide materials for development of integrated gas sensors - A comprehensive review, *Critical Reviews in Solid State and Materials Sciences*, 29 (2004), 111-188.
- 13 B. Adhikari, and S. Majumdar, Polymers in sensor applications, *Progress in Polymer Science*, 29 (2004), 699-766.
- 14 J. N. Lee, C. Park, and G. M. Whitesides, Solvent compatibility of poly(dimethylsiloxane)-based microfluidic devices, *Analytical Chemistry*, 75 (2003), 6544-6554.
- 15 E. Favre, P. Schaetzel, Q. T. Nguyen, R. Clément, and J. Néel, Sorption, diffusion and vapor permeation of various penetrants through dense poly(dimethylsiloxane) membranes: A transport analysis, *Journal of Membrane Science*, 92 (1994), 169-184.

- 16 S. J. Harley, E. A. Glascoe, and R. S. Maxwell, Thermodynamic study on dynamic water vapor sorption in Sylgard-184, *The Journal of Physical Chemistry B*, 116 (2012), 14183-14190.
- 17 J. Stagnus, I. M. Aerts, Z.-Y. Chang, G. C. M. Meijer, L. C. P. M. de Smet, and E. J. R. Sudhölter, Capacitive response of PDMS-coated IDE platforms directly exposed to aqueous solutions containing volatile organic compounds, *Sensors and Actuators B-Chemical*, 184 (2013), 130-142.
- 18 R. Igreja, and C. J. Dias, Analytical evaluation of the interdigital electrodes capacitance for a multi-layered structure, *Sensors and Actuators A-Physical*, 112 (2004), 291-301.
- 19 B. Brown, D. Hess, V. Desai, and M. J. Deen, Dielectric science and technology, *Electrochemical Society - Interface* (2006).
- 20 I. Byun, A. W. Coleman, and B. Kim, Transfer of thin Au films to polydimethylsiloxane (PDMS) with reliable bonding using (3-mercaptopropyl)trimethoxysilane (MPTMS) as a molecular adhesive, *Journal of Micromechanics and Microengineering*, 23 (2013), 085016.

CAPACITIVE RESPONSE OF PDMS-COATED IDES TO VOLATILE ORGANIC COMPOUNDS AND THEIR AQUEOUS SOLUTIONS

In this chapter, the capacitive response of interdigitated electrodes (IDEs) covered with a thin (~50 μm) polydimethylsiloxane (PDMS; Sylgard®184) film is reported. The electrodes were exposed to 1) drops of pure chloroform, methyl tert-butyl ether, 1-hexanol, toluene, m-xylene, and n-hexane; and 2) to aqueous solutions of these volatile organic compounds (VOCs, up to 1 mM) under continuous flow conditions. It is observed that the capacitive response changes are in line with their relative dielectric constants in relation to the dielectric constant of the thin PDMS layer. All response changes were fully reversible. Chloroform, methyl tert-butyl ether, and 1-hexanol were measured reproducibly with a detection limit down to the resolution of the transducer interface. For toluene, m-xylene, and n-hexane the response reproducibility was strongly impaired due to their low water solubility. In the case of n-hexane, an overshoot seemed to be responsible for the observed additional features of the response profile before reaching equilibrium.

A slightly modified version of this chapter has been published:

Staginus, J.; Aerts, I.M.; Chang, Z.-Y.; Meijer, G.C.M.; de Smet, L.C.P.M.; Sudhölter, E.J.R., *Sensors & Actuators B-Chemical*, 184 (2013), 130-142.

6.1 Introduction

An important class of water pollutants is the one of volatile organic compounds (VOCs). VOCs of great interest are, for example, chlorinated compounds contained in boat paints and solvents, gasoline oxygenates, such as methyl *tert*-butyl ether (MtBE), and other fuel hydrocarbons, such as toluene, benzene, and m-xylene.¹ Gasoline spills occur frequently at gasoline stations or from leakage points of underground tanks and pipe systems. After some time, a pollution plume, that is a chemical pattern, will form around the spilling point. This is due to the different affinities of the gasoline components for the water and soil phase. The more water-soluble compounds, such as the oxygenates as MtBE, will dissolve and migrate easily with the ground water, and hence their plumes will be spread further out. This increases the risk of reaching drinking water supplies. MtBE, for instance, is known to give an offensive taste to water already at low ppb level.² In contrast, the non-polar and more hydrophobic organic compounds, such as the aromatics, will have higher affinity for the organic soil phase and hence reside closer to the spilling spot. In this chapter, we report on the capacitive response of interdigitated electrodes (IDEs) covered with a ~50 μm thin polydimethylsiloxane (PDMS) layer to, firstly, the deposition and evaporation of drops of pure volatile organic compounds, and secondly, the *direct* exposure to aqueous solutions of these VOCs (up to 1 mM) under continuous flow conditions. The investigated VOCs were chloroform, methyl *tert*-butyl ether, 1-hexanol, toluene, m-xylene, and n-hexane, to have a spectra of compounds of increasing hydrophilicity/-phobicity and of relative dielectric constants as compared to the PDMS layer.

6.2 Materials and Methods

6.2.1 Chemicals

MtBE (99% purity), chloroform, 1-hexanol, toluene, m-xylene, and n-hexane (all at analytical grades) were obtained from Sigma Aldrich and used as received. Milli-Q water (0.35-0.75 $\mu\text{S}/\text{cm}$) was tapped from a Millipore system (type AFS-3D). For the preparation of the PDMS layer, the commercial two-component product Sylgard®184 of the Dow Corning Company was used as described in Chapter 3, Section 3.2.1 and Chapter 4, Section 4.2.

6.2.2 IDE Platform

The IDE design is as described in Chapter 4, Section 4.1. Two IDE platforms with diagonally arranged leads without in-plane guarding electrodes were used.

6.2.3 PDMS Layer

The PDMS layer of approximate thickness of 50 μm was deposited via a spin-coating technique as described in Chapter 4, Section 4.2.

6.2.4 Universal Transducer Interface

For electrical readout, the Universal Transducer Interface (UTI) with the specifications as described in Chapter 4, Section 4.6 was used.

6.2.5 Drop Experiment

Drops (4 μL) of pure volatile organic compounds (VOCs) and Milli-Q water were pipetted in series onto the PDMS-coated IDE platform. The capacitance changes were recorded from the moment of deposition until complete evaporation of the compounds, except for 1-hexanol.

6.2.6 Continuous Flow Experiment

Aqueous 1 mM solutions were prepared for all organics using Milli-Q water. For n-hexane, which has a solubility limit of ~ 0.11 mM, an oversaturated solution of 1 mM was prepared. The aqueous concentrations are derived from the theoretical water solubility of those compounds and reported as such. The flow cell system as described in Chapter 4, Section 4.5 was used. For solution preparation and delivery, one syringe of the twin-drive pump was filled with Milli-Q water and the other one with the VOC stock solution. The individual liquid streams were merged in a 3-way-valve followed by a PEEK tee, from which the two inlet streams lead into the flow cell. The sensor was first allowed to stabilize in the clean aqueous phases for at least one hour to achieve baseline stabilization before the measurements were performed. The water composition was controlled via flow-rate setting and the pollutant concentration was decreased from 1 mM to 0.1 mM, *i.e.*, from 0.11 mM to 0.009 mM for n-hexane. Due to very long absorption times of chloroform, the measurement recordings were done at fixed time intervals. The total flow rate was kept at 200 $\mu\text{L}/\text{min}$ at all times to avoid pressure

differences and to ensure a refreshment rate of the measurement chamber ($\sim 20 \mu\text{l}$) of about 6 times per minute.

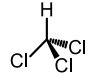
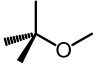
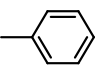
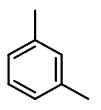
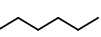
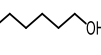
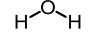
6.3 Experimental Investigation

To learn more about the capacitive responses of pure VOCs, first drops of these compounds were deposited directly onto the PDMS-coated IDEs. These results are presented and discussed in Section **6.3.1**. Then, changes in the capacitance of aqueous solutions containing VOC using the flow cell and operating under continuous flow conditions are reported and discussed in detail in Section **6.3.2**.

6.3.1 Drop Experiment

First, we studied the effect of the deposition, adsorption, and subsequent evaporation of $4 \mu\text{L}$ drops of the pure VOCs MtBE, chloroform, 1-hexanol, toluene, m-xylene, and n-hexane onto the PDMS-covered IDEs as a function of time (Figure **6.1**). Table **6.1** lists some relevant physical properties and their reported values for these compounds (columns **1-6**) as well as data obtained from the drop-based analysis (column **7-9**). In Figure **6.1**, a positive change in capacitance upon drop deposition implies that the relative dielectric constant of the applied VOC is higher than the one of the PDMS layer. This is the case for MtBE, chloroform, and 1-hexanol, whereas the changes in capacitance for toluene, m-xylene, and n-hexane are negative because their relative dielectric constants are lower than the one of the PDMS layer. The relative dielectric constants of all compounds involved are listed in Table **6.1** (third column).

Table 6.1. Chemical structure, relative dielectric constant (ϵ_r), partial vapor pressure, n-octanol-water partition coefficient ($\log K_{OW}$), and water solubility of the organic compounds used in this study. The seventh column lists the results of drop contact angle measurements (as derived from Appendix C, Section C.1, Figure C.2). The last two columns summarize data from the drop-based measurement (as derived from Figure 6.1).

Chemical compound	Chemical structure	Relative dielectric constant (ϵ_r)	Partial vapor pressure (mmHg) ^c	Partition coefficient ($\log K_{OW}$)	Water Solubility @ 25 °C (mass %) ^b	Drop contact angle after 10s (°) ^f	Absolute change in capacitance (pF) ^g	Δt (s) ^g
Chloroform (1)		4.81 ^b	153	1.97 ^e	0.80	46	2.3	~350
MtBE (2)		2.60 ^a	202	1.24 ^d	3.62	0	1.15	~450
Toluene (3)		2.38 ^b	28	2.73 ^e	0.053	37	0.3	~450
m-Xylene (4)		2.36 ^b	8	3.20 ^e	0.016	37	0.41	~1200
n-Hexane (5)		1.89 ^b	151	4.00 ^e	0.0011	0	0.7	~250
1-Hexanol (6)		13.3 ^b	0.84	2.03 ^e	0.6	48	1.2	>>
Milli-Q Water (7)		80.1 ^b	18	-	-	112	0.23	>2700

Extracted from (a) ref³, (b) ref⁴, (c) ref⁵, (d) ref², (e) ref⁶, (f) Figure C.2, (g) Figure 6.1.

The data of Figure 6.4 indicates that the dielectric constant for the PDMS layer is between 2.36 (m-xylene) and 2.60 (MtBE). This is slightly lower than the reported values for Sylgard®184 (between 2.68 and 2.7 as measured at signal frequencies of 100 Hz and 100 kHz, respectively).^{7, 8} This deviation might be related to the difference between electrical properties of thin layer PDMS and bulk PDMS as also observed by others.⁹

Next, we address the magnitude of the change in capacitance when the drops are deposited. Apart from n-hexane and 1-hexanol, the absolute changes in the capacitive response (Table 6.1, column 6) are in line with the magnitudes of their relative dielectric properties as compared to the PDMS layer. Based on its relative dielectric constant, a larger response for n-hexane was expected. Upon the moment of deposition of a 4 μL drop of the VOCs onto the PDMS layer, that measures about a 5 μL volume, a liquid phase was observed for all organics, except for the n-hexane drop, which seemed to be instantly fully absorbed by the PDMS layer. The high affinity of n-hexane for the hydrophobic PDMS phase is also suggested by its relatively high partitioning coefficient ($\log K_{\text{OW}} = 4$) (Table 6.1, column 3).

It is further observed that in all cases the capacitive response returns to its original value, showing the full reversibility of the PDMS-coated IDE platform. This is not demonstrated for 1-hexanol in this measurement series as this compound does practically not evaporate over comparable time periods and can only be removed over comparable time periods by heating the substrate. The last column of Table 6.1 gives an overview of the time needed for complete recovery of the PDMS-covered IDEs. The differences in the recovery times cannot be solely explained by the vapor pressures of the VOCs. For the desorption process of VOCs from the polymer structure, also the strength of the electrostatic interaction forces will be a determining factor for the retention times. Finally, higher PDMS affinities, as indicated by either higher partition coefficients or similar dielectric constant, will lead to increased absorption. The drops of high-affinity compounds spread more over the polymer surface, promoting the evaporation process.

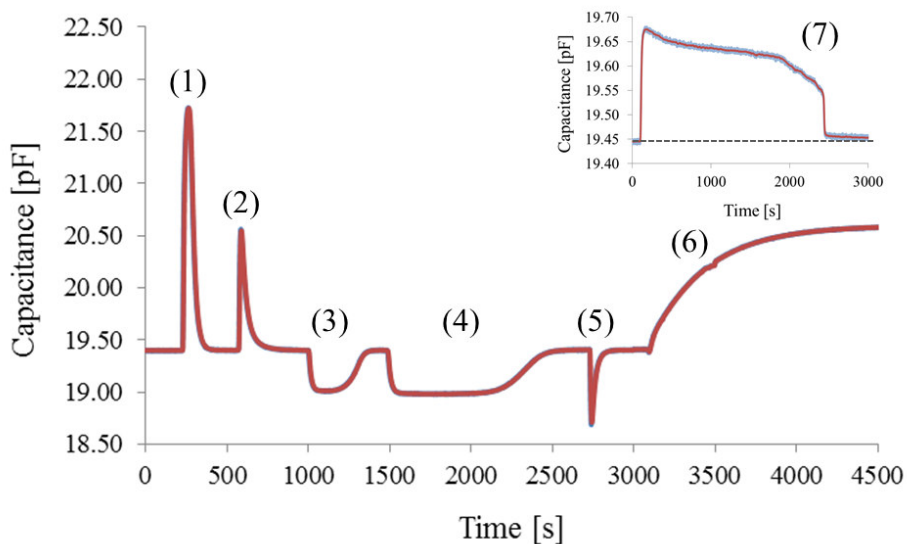


Figure 6.1. Real-time (blue) and averaged over 100 points (red) capacitive response upon the deposition and subsequent evaporation of a 4 μL drop of the organic liquids chloroform (1), MtBE (2), toluene (3), m-xylene (4), n-hexane (5), and 1-hexanol (6) onto an IDE coated with a PDMS layer that is 50 μm in thickness. Insert: capacitive response to the deposition and subsequent evaporation of a 4 μL drop of Milli-Q water (7). Note that in the main graph at larger scale the real-time value overlaps to a large extent with the average value.

The insert in Figure 6.1 shows the capacitive response of the PDMS-covered IDE chip to the deposition of a 4 μL water drop and the subsequent evaporation. In this cases it took ~ 2700 s before the capacitive response was returned to its initial value. Striking is that the capacitance change of ~ 230 fF upon drop deposition is the smallest when taking into consideration that the dielectric constant of water is on average about 40 times higher than for the other volatile organic compounds or about 6 times higher than for 1-hexanol. This can be explained by the low affinity of the apolar PDMS layer for the polar compounds water and 1-hexanol. The low affinity of water for PDMS is also reflected by the contact angle of water onto the Sylgard®184 surface that was measured to be $> 112^\circ$ (Appendix C, Figure C.1, Section C.1). For the organic compounds the initial drop contact angle directly after deposition was found to be significantly lower and —except for 1-hexanol— changed quickly with time due to absorption and evaporation (Appendix C, Section C.1, Figure C.2). With respect to the reversibility of water ad-/absorption, it was found that after ~ 2000 s the observed response is still $\sim 2\%$

of the maximal response change. Such very long retention times may be indicative of the presence of strong polar, hydrogen-bonding, or even ionic interaction forces between the water molecules and the polymer layer.¹⁰ Though the dielectric constant of 1-hexanol is much higher than those of the other VOCs, its lower affinity for the PDMS layer is represented by its relatively slow absorption as suggested by the capacitance response profile as well as by its stable drop contact angle over time. As discussed in Chapter 3, Section 3.4.4, an reorientation of the polymer chains and a consequent interaction with the (rather polar) siloxane backbone is expected. Also, the presence of silanols and other polar groups originating from imperfectly end-capped silica particles or from an incomplete synthesis reaction cannot be excluded. As mentioned for the drop test with water, possible polar-polar or hydrogen interaction forces can be a plausible explanation for relatively long response tailings until complete desorption. To conclude, the drop experiments provide significant information for further underwater experiments as the relative dielectric constant of the PDMS layer can now be approximated. Though it has to be accounted for that the response changes and times depend strongly on the ambient conditions, they clearly follow a qualitative trend.

6.3.2 Continuous Flow Experiment

The following experiments were performed under continuous flow conditions using Milli-Q water that was spiked with different VOCs. Before applying the VOC-containing water, the IDE platform was first allowed sufficient time to stabilize its capacitance baseline response in the aqueous phases under continuous flow. The flow cell chamber was then flushed with aqueous solutions containing different VOC concentrations (Figure 6.2).

It was found again that all results are in agreement with the relative dielectric constants of the organic compounds as compared to the PDMS layer. Positive changes in capacitance are observed for MtBE uptake from the water into the polymeric phase and negative changes for toluene, m-xylene, and n-hexane. Due to the low concentration ranges, the effect of changes in the electrical properties of the solution on the sensor response is assumed to be negligible. Significant changes in solution conductivity could not be measured. We further reason that all organic compounds have both significant lower dielectric constants and conductivities than water and that their addition to the aqueous phase will result in a decrease of both solution permittivity and conductivity.

Therefore, similar response changes would be expected for all pollutants. The results show that the system responds reproducibly for aqueous solutions of the rather hydrophilic compounds chloroform, MtBE, and 1-hexanol in the concentration range of ~0.1 mM - 1 mM. Furthermore, the responses are in agreement with their PDMS affinity as observed for the gas phase. For toluene, m-xylene and n-hexane the lowest measured concentrations as derived from their water solubility were found to be ~0.2 mM, ~0.2 mM, and ~0.009 mM, respectively. However, it was found that the response reproducibility was strongly impaired, which we attribute mainly to the low solubility of these compounds leading to concentration issues within the system. However, the measured response changes follow a qualitative trend, *i.e.*, except for the 1 mM concentration solution, the results for toluene and m-xylene are very much comparable and the largest response was recorded for the saturated solution of n-hexane, having the highest deviation of dielectric constant within this series of VOCs. Yet, based on the differences in K_{OW} (Table 6.1, column 5), it must be accounted for that the concentration of n-hexane in the polymer layer can be assumed to be about ten times larger than for toluene and m-xylene and about a thousand time larger than for example the one of MtBE.

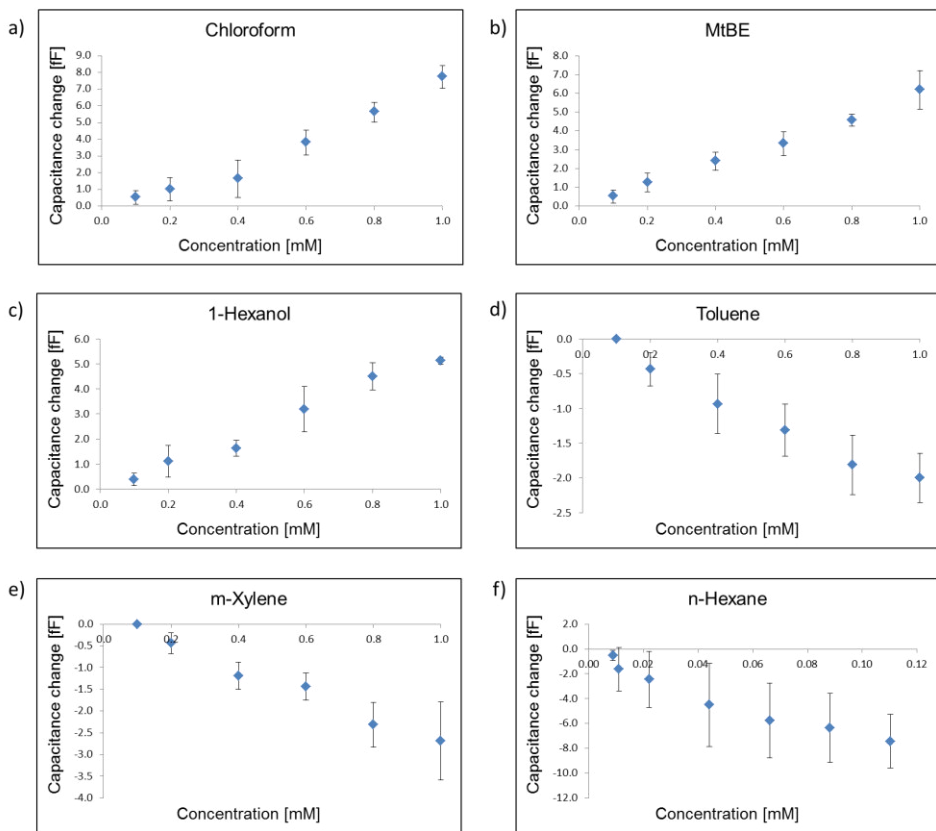


Figure 6.2. Changes in the average capacitance as function of increasing concentrations of a) chloroform, b) MtBE, c) 1-hexanol, d) toluene, and e) m-xylene, and f) n-hexane in Milli-Q water. The error bars of chloroform, MtBE, and 1-hexanol are based on the standard deviation of 4 measurements with 2 measurements performed on 2 individual devices. The error-bars of toluene, m-xylene, and n-hexane are based on 4 measurements with the largest response changes as achieved on 2 individual devices. More information on this matter is provided in the text.

More information can be extracted from the individual sorption profiles of the different pollutants that are shown in Figure 6.3. For the hydrophobic compounds, the measurement series with the highest response changes was taken as example.

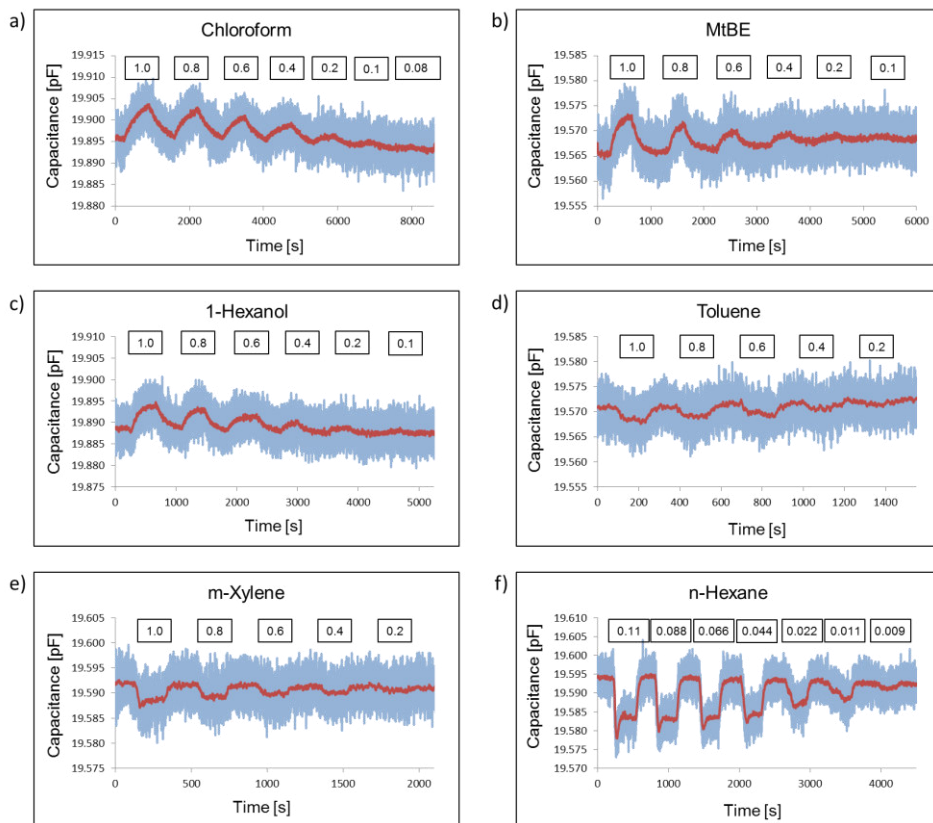


Figure 6.3. Real-time (blue) and averaged over 100 points (red) capacitive response upon alternating exposure to Milli-Q water and different concentrations of a) chloroform, b) MtBE, c) 1-hexanol, d) toluene, e) m-xylene, and f) n-hexane in Milli-Q water.

The capacitive response profiles clearly reveal the occurrence of ad-/absorption and desorption processes with individual sorption times and intensities for each compound. In the case of n-hexane a striking feature at the initial uptake is observed (Figure 6f). In more detail, for concentrations down to 0.044 mM, the capacitive response shows quick characteristic dips followed by a gradual and slight increase back to higher capacitance values. Both the steep decrease and the following increase in the signal diminish for lower concentrations and the dip characteristic is hardly observable at concentrations below 0.022 mM anymore. For concentrations of 0.11 mM down to 0.066 mM, the total capacitance changes at equilibrium are almost equal. However, the sorption profiles before reaching equilibrium are distinct. Also, for the 1.0 mM m-xylene solution a similar response feature was observed but much less pronounced. Saturation values are reached for all compounds except chloroform, for which recording was done after fixed time intervals in order to limit the effect of interfering drifts that are encountered over longer measurement periods as also shown in Figure 6.3.

As discussed in Chapter 4, it was found that the IDE chip is highly temperature sensitive with a positive temperature coefficient of ~ 13 fF/ $^{\circ}$ C. Over longer time periods, an additional positive drift of the baseline was observed in the aqueous phase indicating increased absorption of water molecules into the PDMS layer. Such an overlapping positive drift was not observed in measurements performed in open air, where the baseline was quasi stable and only prone to temperature deviations. The profiles of the capacitive response changes upon adsorption/absorption and desorption of the VOCs from the 1 mM (and 0.11 mM saturated) solution are represented more detailed in Figure 6.4 and the extracted times are listed in Table 6.2.

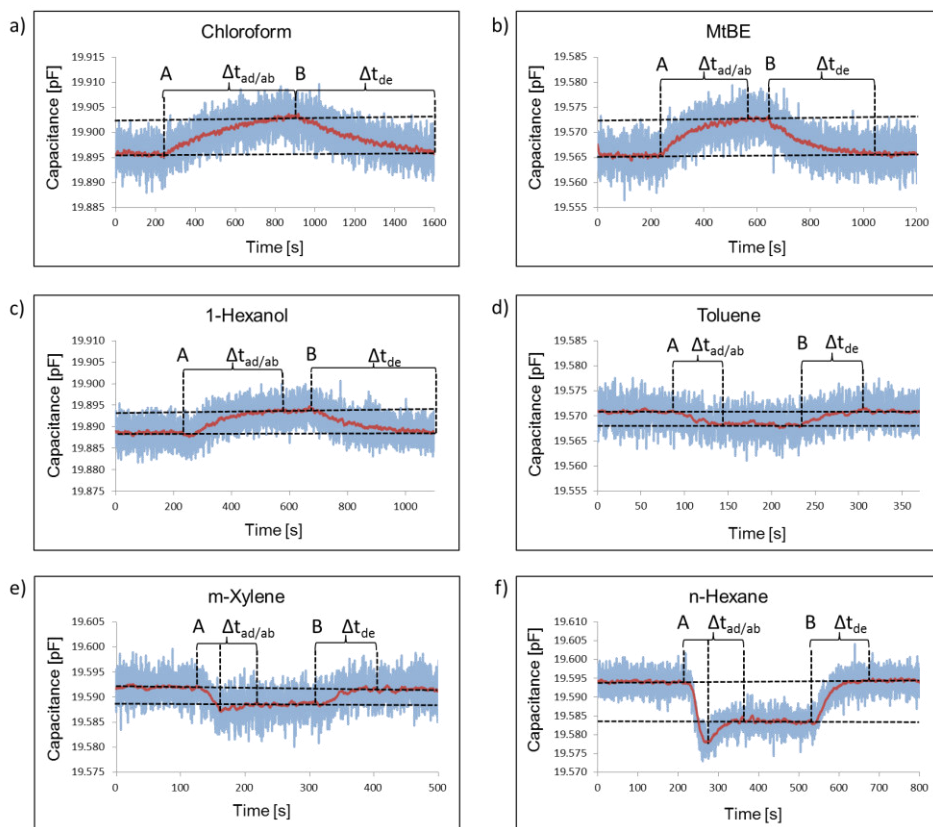


Figure 6.4. Real-time (blue) and averaged over 100 points (red) capacitive response upon substitution (event A) of the water phase by a 1.0 mM a) chloroform, b) MtBE, c) 1-hexanol, d) toluene, e) m-xylene solution, and f) a saturated 0.11 mM n-hexane solution and subsequently back to pure Milli-Q water (event B). The black dashed line approximates the overlapping drift probably caused by further uptake of water into the polymer layer with time.

Table 6.2. Response change times upon adsorption/absorption of chloroform, MtBE, toluene, m-xylene, and 1-hexanol for a 1 mM solution and of n-hexane for a saturated 0.11 mM solution. Desorption was performed using Milli-Q water for flushing.

	Chloroform	MtBE	1-Hexanol	Toluene	m-Xylene	n-Hexane
Adsorption/ absorption time [s]	>600	350	200	50	100	150
Desorption time [s]	>600	400	250	70	100	150

For m-xylene and n-hexane, the characteristic dip occurs after 30 s and after 70 s, respectively. For the n-hexane measurement a 17 fF dip is followed by a 7 fF increase in capacitance. For m-xylene this characteristic increase is indicated after a 5 fF dip but is with 1-2 fF less pronounced. During desorption of the n-hexane and m-xylene out of the polymer layer, the dip does not reoccur (or much less pronounced with ~1 fF as for the saturated 0.11 mM n-hexane solution) but the capacitance gradually returns to its original value. Based on the shape of the sorption profile the characteristic dip observed during the n-hexane and m-xylene measurements is a strong indication on the occurrence of temporary VOC overshoot, which is a sudden increase in uptake value before reaching the true equilibrium.¹¹ This overshoot behavior has already been observed for n-hexane vapor absorption by a rubbery polymer.¹²

As discussed in Section 6.2, also swelling plays a significant role in aqueous phases if a parasitic coupling effect to the environment or other system parts is involved. The observed recovery of capacitance might also be explained by a reduction in the parasitic coupling effect through swelling. Since this effect is only observed for aqueous m-xylene and n-hexane solutions and not for aqueous solutions of chloroform, MtBE, 1-hexanol, and toluene, we exclude the uptake of water as the origin. Further investigations into this matter are under progress.

6.4 Concluding Remarks

Using an interdigitated electrode platform covered with a thin film of Sylgard®184 polydimethylsiloxane (PDMS, ~50 μm in thickness), we have investigated the reversible change of electrical capacitance upon exposure to drops of pure volatile organic compounds (VOCs) and to continuously flowing aqueous solutions of these compounds at mM concentrations. Under both conditions, a capacitance increase is observed for the VOCs having a dielectric constant larger than PDMS, *i.e.*, for chloroform, MtBE, and 1-hexanol, and a capacitance decrease is observed for the VOCs having a lower dielectric constant than PDMS, *i.e.*, toluene, m-xylene, and n-hexane. Once the platform is stabilized under aqueous conditions, further changes in capacitance due to the additional absorption of water vapor are low as compared to the changes caused by the uptake of VOCs. Larger response deviations were attributed to the high temperature sensitivity of the system (13 fF/°C). The system responded reproducibly for aqueous chloroform, MtBE, and 1-hexanol solutions in the range of 0.1-1 mM. For toluene, m-xylene, and n-hexane, the response reproducibility is greatly impaired and the lowest measured concentrations as derived from their theoretical water solubility so far were 0.2 mM, 0.2 mM, and 0.009 mM, respectively. As the reproducibility decreases with decreasing water solubility of these compound, it is evident that this issue is strongly related to concentration issues. Especially the environmental temperature seems to play a significant role in this regard. For n-hexane and m-xylene solutions a strong capacitance decrease followed by a rise to an equilibrium value was observed. It is proposed that this effect is a result of a temporary overshoot of absorbed molecules into the PDMS film, although the effect of swelling cannot be ruled out. The designed measurement system allows to study qualitative trends, yet a more advanced and fully controlled system will be necessary to study the absorption and desorption kinetics of the different compounds, *e.g.*, the long sorption times of chloroform. In addition to system calibration and conditioning such as stabilizing the temperature of the IDE substrate, further response optimization can be achieved by utilizing recent UTI technology with enhanced signal-to-noise ratios and by tailored polymer-design as will be discussed in Chapter 7.

6.5 References

- 1 J. S. Zogorski, J. M. Carter, T. Ivahnenko, W. W. Lapham, M. J. Moran, B. L. Rowe, P. J. Squillace, and P. L. Toccalino, The quality of our nation's waters: Volatile organic compounds in the nation's ground water and drinking-water supply wells (Reston, Virginia, U.S.A.: U.S. Geological Survey, 2006).
- 2 WHO, Methyl tertiary-butyl ether (MTBE) in drinking-water, *Background document for development of WHO Guidelines for Drinking-water Quality* (2005).
- 3 Product information: ARCOPURE® high purity MTBE, *Lyondell Chemical Company* (2004).
- 4 D. R. Lide, ed., Handbook of chemistry and physics - 81st Edition (2000-2001) (Boca Racon, Florida, U.S.A.: CRC Press, 2000).
- 5 C. L. Yaws, P. K. Narasimhan, and C. Gabbula, Yaws' handbook of Antoine coefficientents for vapor pressure - 2nd Electronic Edition (2009), Knovel, www.knovel.com, 2012.
- 6 C. L. Yaws, Chemical properties handbook: Physical, thermodynamics, environmental transport, safety & health related properties for organic & inorganic chemicals (New York, U.S.A.: McGraw-Hill Education, 1999).
- 7 Product datasheet: Sylgard184 silicone elastomer, *Dow Corning Corporation* (2012).
- 8 Product information: Dow Corning brand silicone encapsulants, *Dow Corning Electronics Solution* (2000, 2001, 2003, 2005).
- 9 J. Sun, S. K. Vajandar, D. Xu, Y. Kang, G. Hu, D. Li, and D. Li, Experimental characterization of electrical current leakage in poly(dimethylsiloxane) microfluidic devices, *Microfluidics and Nanofluidics*, 6 (2009), 589-598.
- 10 G. Eranna, B. C. Joshi, D. P. Runthala, and R. P. Gupta, Oxide materials for development of integrated gas sensors - A comprehensive review, *Critical Reviews in Solid State and Materials Sciences*, 29 (2004), 111-188.
- 11 T. M. Aminabhavi, and H. T. S. Phayde, Transport kinetics and diffusion of monocyclic aromatic liquids in polymeric blends of ethylene-propylene random copolymer and isotactic polypropylene, *Polymer-Plastics Technology and Engineering*, 36 (1997), 369-390.
- 12 A. Alentiev, M. Sanopoulou, N. Ushakov, and K. G. Padadokostaki, Melting and recrystallization processes in a rubbery polymer detected by vapor sorption and temperature-modulated DSC methods, *Polymer*, 43 (2002), 1949-1952.

OUTLOOK

In the previous chapters, we introduced the theoretical basics of polymer-coated interdigitated electrodes (IDEs) as capacitive sensing platforms for applications in aqueous solutions and we demonstrated a proof-of-principle for volatile organic compound (VOC) detection in water. The chapters form a systematic guide for understanding the mechanisms of this type of sensor platform in a step-by-step approach, and they show the relevance of system integration as, *e.g.*, in droplet detectors and flow cell detectors. This final chapter recaptures the main issues and challenges encountered throughout the study. It addresses in particular the necessary system requirements to be met in order to achieve a reliable detection and measuring system. It further points out future research and engineering tasks to be tackled to promote the development of water-resistant and stable polymer-coated capacitive multi-array sensors with well-guarded electric sensing fields.

7.1 Challenges and Future Prospects

Multi-array based sensor systems utilize partially selective sensing elements that each interact to a different extent with the target compounds. With smart pattern recognition techniques, a qualitative and quantitative interpretation of the multivariate response can be achieved already with a relatively small amount of sensing elements with chemical diversity.¹⁻³ This project aimed on studying and understanding the response mechanisms of the polymer-coated interdigitated (IDE) electrode structures. The electronic aspects of reading out the multivariate response and analyzing it with an appropriate algorithm has not been addressed. Throughout the stages of research and development of this project, a diverse range of expertise has been gained and various technical and physical challenges have been encountered. As many of these aspects do not lie within the main focus of this project and could not be investigated, they will be highlighted in this chapter as they might be of great interest for future research work. This includes in particular knowledge acquisition on the following system levels: the polymer layer (Section 7.1.1), the polymer/transducer interface (Section 7.1.2), the transducer platform including the IDE structure (Section 7.1.3), the leads (Section 7.1.4), and finally the flow cell and measuring system (Section 7.1.5).

7.1.1 Polymer Design

One major challenge encountered is the identification and design of polymers that are suitable for capacitive sensing applications in water. When performing capacitive measurements with polymer-coated IDE platforms that are directly exposed to the aqueous phase, the polymer layer must meet additional requirements as compared to gas-phase applications. As pointed out in Chapter 3, the polymer layer functions in principle as a ‘filter’ that ideally concentrates selectively the target compound by absorption. Then, the change in the dielectric constant of the polymer layer can be detected capacitively. In addition to serving as a sensing layer, the polymer layer also has to act as a sealant against water infiltration to isolate the electrodes. Therefore, the polymeric sensing layer must be physically and chemically stable and hydrophobic (water-fearing) in nature. The more hydrophilic (water-loving) a polymer is, the higher will be the uptake of water vapor. This will lead to drastic chemical and electrical modifications of the polymer layer. If liquid water infiltrates the polymer layer, it will eventually lose its chemical filtering function. Further research will have to be done to

investigate what degree of water vapor uptake into the polymer layer and hence what degree of hydrophilicity is acceptable for capacitive sensing applications.

An additional possibility to insulate and isolate the electrodes is to deposit an extra thin insulating layer, such as an oxide layer,⁴ on top of the IDEs before depositing the polymeric sensing layer (Figure 7.1).

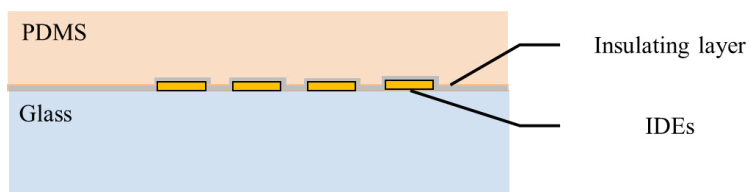


Figure 7.1. Schematic representation (not to scale) of the side view of PDMS-coated IDEs on a glass substrate with an insulating layer.

In order to achieve chemical diversity within a multi-array, it is consequently of interest to chemically modify the bulk of a predestined polymer, such as that of polydimethylsiloxane (PDMS). By doing so, the basic and indispensable properties of the polymer for applications in aqueous environments can be preserved to a great extent while the affinity of the polymer layer for chemical compounds can be tuned.⁵

As discussed in Chapter 3, the detection principle of polymer-coated transducer platforms is based on the rule-of-thumb “like dissolves like”, which is linked to similar interaction forces between the chemical compounds and the polymer network.⁶ One measure for this likeness is also the dielectric constant of the compounds. *Ironically, something which has a high affinity to dissolve or distribute into the polymer layer will not necessarily lead to the greatest changes in capacitance due to closest resemblance with the dielectric constant of the polymer layer.* Eventually, valuable information for the identification of compounds is also obtained from not only the absolute capacitance changes but also the absorption and desorption times, hence the total sorption profile.

The bulk modification of a polymer requires a thorough review of the basic formulation of the polymer synthesis. The introduction of functional monomers into the network will typically affect with the actual cross-linking reaction. In case of the hydrosilylation reaction of PDMS, vinyl-terminated or hydrogen-functional monomers containing a functional group to be introduced compete for the hydrogen-functional or

vinyl-terminated group, thereby affecting the cross-linking degree.^{5, 7} For example, if a vinyl-terminated functional monomer is introduced, then more of the siloxane (typically the curing agent) that carries the hydrogen-functionality must be added or a curing agent with higher loading of the hydrogen-functionalities must be chosen for achieving a sufficient cross-linking degree. There is a variety of bulk modification techniques to achieve an enhanced polymer affinity for the target compound. In the previous example, the monomer containing the functionality was cross-linked, *i.e.* covalently bound, to the polymer network. This bulk modification technique is referred to as functionalization. Further bulk modification techniques include blending and copolymerization of polymers and the formation of interpenetrating networks.⁸ Interpenetrated networks (IPNs) consist of at least two different polymer networks that are formed by synthesizing and/or cross-linking at least one polymer in the presence of the other polymer and this without the formation of covalent bonds between them.⁹ Other advanced modification techniques include, *e.g.*, molecularly imprinted polymers (MIPs) and solvent-impregnated resins (SIRs). MIPs contain cavities as artificial receptors that have a high selectivity and affinity to the predetermined target molecule.^{10, 11} They have shown potential in wastewater treatment applications for the extraction of various biomolecules.¹² Also the solvent-impregnated resins that contain complex-forming agents have primarily found use for the extraction of organic compounds. Successes are reported on the removal of the water pollutants phenol and methyl tetra-butyl ether by SIRs.¹³⁻¹⁵ Hence, MIPs and SIRs are modification techniques for increasing the affinity of a polymer layer for target pollutants that could inspire the investigation of advanced polymer designs for sensing applications, including those based on IDE technologies.

Within a flow cell system under continuous flow, the polymer layer is exposed to increased pressure conditions as in comparison to a steady state system. This puts further requirements on the mechanical properties of the polymer layer. As introduced in Chapter 3, pristine PDMS has poor mechanical properties.¹⁶ Yet, the addition of a filler material, such as surface-modified silica that cross-links to the PDMS network and hence cannot be extracted, is a possible method to increase the mechanical strength of the final polymer product.¹⁷ In our research work done on polymer design, we found that the self-prepared pristine PDMS layers were mechanically instable with time under the given operation conditions. This could be investigated by exposing the layers to water under continuous flow conditions within our designed flow cell system and by

measuring the capacitive response of the PDMS-coated IDE platform over time. It was found that after short time of use the IDE capacitance rose quickly to high values with simultaneously increasing noise amplitude. The suddenly occurring rise in capacitance as shown in Figure 7.2 is linked to water infiltration as consequence of the layer breakdown.

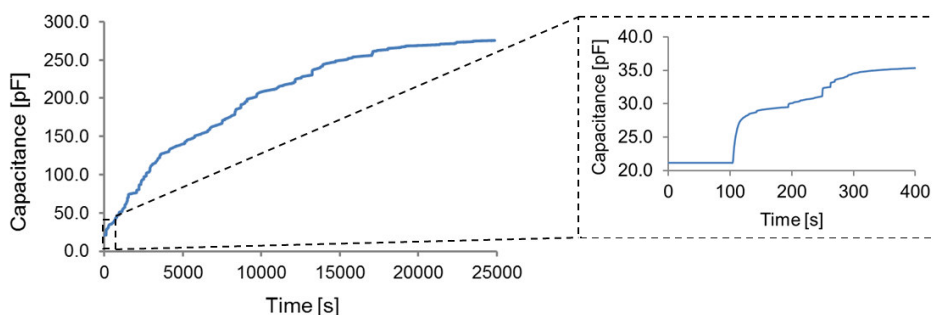


Figure 7.2. Real-time capacitive response as measured over a period of ~7 hours under continuous flow condition with Milli-Q water at a flow rate of 200 ml/min for an IDE chip with a pristine PDMS coating. The magnified view shows the first 400 s of the measurement and the moment of breakdown at ~100 s.

As can be seen from the magnified view, there is a moment of breakdown, after which the capacitance rises rapidly to a value of approximately 300 pF. For comparison, it was found that when exposing a bare IDE sensor, *i.e.*, without a polymer layer, to Milli-Q water, the capacitance rises to values above 600 pF. Therefore, such a rapid rise in response is very likely due to uptake of water into the polymer layer. Sudden and rapid response changes were also occasionally observed for IDE chips covered with the commercial and silica-filled PDMS product Sylgard®184. In that case, the breakdown could be linked to entrapped bubbles or settled dust particles within the polymer layer. Evidently, besides being mechanically strong and chemically stable, further important layer requirements are that the polymer layer is homogeneous and defect-free. These factors will also determine the life-time of the polymer layer under the conditions of operation, *e.g.*, whether the sensor is suitable for only one-time or repetitive use or whether it can even work on-line and continuously for longer periods.

A further common problem that is encountered over long-time use of polymer-based devices in water is (bio-)fouling as caused by the settlement of large bio-organic

molecules and microorganisms onto and within the polymer layer. As addressed in Chapter 2, Section 2.5.4, proper packaging that include filter elements is a method to retain undesired matter including macro-molecules from the polymer surface. Yet, filter elements are prone to clogging, although reverse-flow schemes can be used to flush out the materials that has built up. Another possibility to prevent (bio-)fouling is to graft, that is to chemically modify, the surface of a polymer with anti-fouling and anti-microbial polymers.¹⁸ Although exceptions exist, there is consensus among scientists that these antifouling polymers should be electrically neutral, hydrophilic, and may possess hydrogen bond acceptors but no hydrogen bond donors.¹⁹⁻²¹ It remains to investigate how these grafted antifouling polymers can be used as protective layers on the polymeric sensing layers and how they influence the polymer partitioning process.

7.1.2 Polymer/Transducer Interface Design

In addition to the required polymer properties as outlined in the previous section, the quality of the polymer/transducer interface is of equal importance in order to achieve system and hence response stability. If the polymer layer does not adhere well, there is a risk of detachment, creating space between the electrode platform and the sensing layer. Furthermore, if the underlying substrate is hydrophilic, such as in case of glass supports, interfacial water vapor that promotes adhesion loss of the polymer layer can become an additional issue.²²

Interfacial deposition of water or other matter is a problem that does not only affect the physical stability but also the electronic response. A possible method to be insensitive to such surface effects is the integration of guarding electrodes in between the sensing electrodes.²³ That way, the nearby electric sensing field of the IDEs is coupled to the guarding electrodes and only the outer electric field of the IDEs functions as electric sensing field as depicted in Figure 7.3. Another positive side effect of this electrode arrangement is that the response time may be reduced.

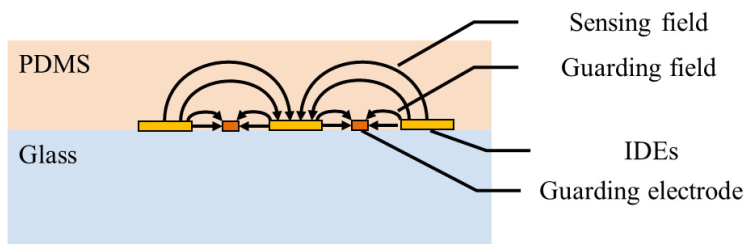


Figure 7.3. Schematic representation (not to scale) of a side view of PDMS-coated IDEs on a glass substrate and the guarding electrodes placed between the IDE fingers. The electric field on the lower electrode half, which penetrates the glass substrate, is omitted for simplicity.

If the adhesion of the polymer on the underlying substrate is poor, then chemical modification of these surfaces can be a remedy. For example, PDMS does chemically bond well to glass but not to gold electrodes. If in addition large golden in-plane guarding electrodes are provided next to the IDE structure, then the PDMS layer can easily be peeled off as found in experimental work. Gold surface modification by means of thiol-chemistry is a possible solution to tightly link the elastomeric silicone to the gold electrodes²⁴ as shown in Figure 7.4. Such modification techniques rely on the self-assembly of thiolates on the metal surface.²⁵ If these monomers, with a thickness of a few nanometers only, are terminated with vinyl groups, then these vinyl groups can compete for the hydrogen-functionality in the PDMS and quasi cross-link the polymer layer to the electrodes. In case oxides are used as an interlayer (as discussed in Section 7.1.1), then silanes can be used instead to react with the surface silanol groups (Si-OH).²⁶

Another technical solution is to fabricate a support substrate with ‘openings’, such as in the in-plane guarding electrode area, that allow polymer access to the glass substrate as depicted in Figure 7.5. In this way, the PDMS can partially bond on the large surface, while sufficient guarding electrode area remains. However, the additional edges may also result in the presence of voids formed during the spin coating process. This may then be solved by embedding the gold IDE fingers into the glass to form a flat gold/glass surface, facilitating the spin coating process, possibly supported by silane and/or thiol chemistry.

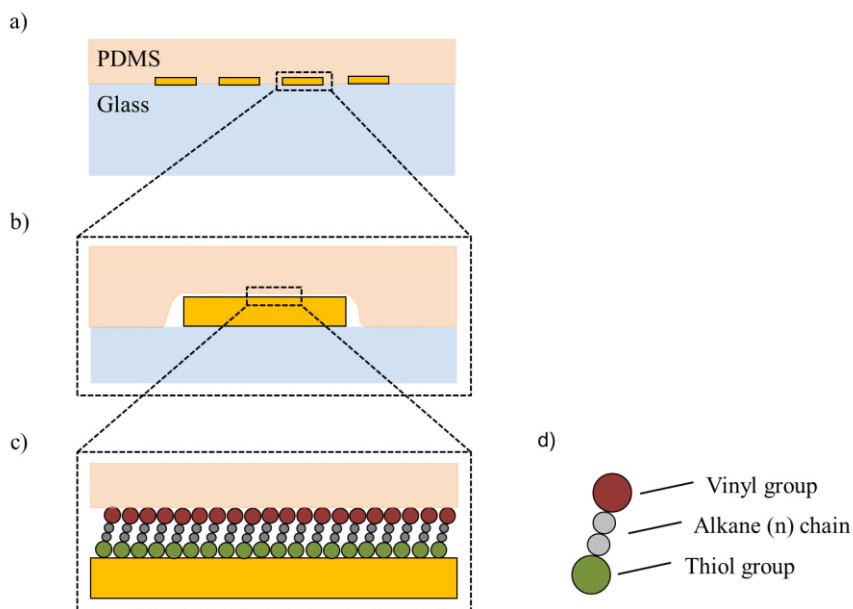


Figure 7.4. Schematic representation (not to scale) of the side view of a) PDMS-coated IDEs on a glass substrate, and b) a magnified view of a single finger electrode to demonstrate the deposition of the PDMS layer and the good adhesion to the glass and the lacking adhesion to the gold surface, and c) a magnified view of the interface between gold and PDMS, which has been chemically modified with a thiol- and vinyl-functional alkane to achieve semi-covalent bonding between the PDMS layer and the gold surface, and d) generalized molecular structure of the chemical linker.

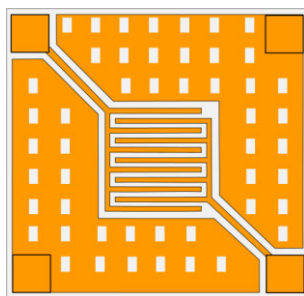


Figure 7.5. Schematic representation (not to scale) of the top view of an IDE structure on a glass substrate with in-plane guarding electrodes that is provided with openings, allowing PDMS access to the underlying glass substrate.

A further technology trend is device miniaturization towards the development to nanoscale electrode platforms.²⁷ The miniaturization trend puts new requirements on the device design and brings up new challenges for the fabrication process, requiring amongst others the invention and development of new surface modification and/or deposition techniques. This is because device minimization results in smaller spatial wavelengths of the electrodes and hence thinner polymer layers will be required with the benefit of shorter response times. When using electrode structures in the submicrometer and nanometer range, the question arises whether the polymer can still adopt the required features, *e.g.*, fill in the spacing between the electrodes. Again, good contact of the polymeric sensing layer with the transducer interface is a requirement for good adhesion and consequently for the stability of the polymer/transducer interface.

7.1.3 Electrode Design

In Chapter 3, we addressed the beneficial properties of planar structures, such as the IDEs for sensing applications. Yet, planar structures also bring along technical problems. For capacitive measurement techniques, for which detection occurs within an electric field, it is of essence to prevent *parasitic electric-field bending*. This can be achieved via the application of guarding electrodes. However, as explained in Chapter 3 and 5, for planar electrode structures as the IDEs, the electric sensing field lies primarily out-of-plane, which makes it geometrically difficult to guard. We demonstrated that water-enhanced guarding is a simple and effective mechanism to achieve response immunity to parasitic coupling events. In addition, we showed that thick polymer layers support the reduction of electric-field bending towards external ‘third’ electrodes but on cost of longer response times. A more advanced structure to achieve full guarding of the electric sensing field is the deposition of a guarding electrode directly on top of polymer layer. Such a guarding electrode would have to meet certain requirements, such as being 1) porous to enable analytes to enter the polymer affinity layer, 2) flexible and mechanically strong to withstand mechanical stresses, such as induced by polymer swelling, and 3) chemically resistant to corrosion. Also, the possible occurrence of undesired redox reactions on the water exposed electrode may lead to the necessity of introducing a reference electrode, a problem that is not encountered when in-plane and thus polymer-coated guarding electrodes are used. Evidently, the synthesis and fabrication of such advanced structures is more difficult and costly. This porous

electrode could either function as guarding electrode (Figure 7.6a) or be the counter electrode to a large planar main electrode, forming a simple parallel-plate capacitor as sensing element (Figure 7.6b²⁸). If the porous counter electrode is put directly at ground, the sensor element is placed within a grounded housing and active guarding based on either negative feedback or feed-forward technique is applied, then the system is protected against parasitic electric-field bending. Already during the last decade, universal transducer interfaces capable of performing capacitive measurements with one capacitor electrode at ground as just described have been developed.^{28, 29} In such interfaces the applied frequencies of the excitation signals are high enough (>25 kHz), so that the effects of electric double layers do not play a significant role.²⁹ Metal- or carbon-based porous electrodes that allow the passage of the target molecule have been studied, for example, in capacitive-type humidity sensors for the detection of humidity.^{30, 31} They measure the change in capacitance between the porous electrode and a single planar electrode upon absorption of water vapor in the intermediate, *e.g.*, oxide- or polymer-based dielectric layer (Figure 7.6b²⁸). The design of such electrodes and their suitability for aqueous applications for detection of larger organic molecules remains to be investigated.

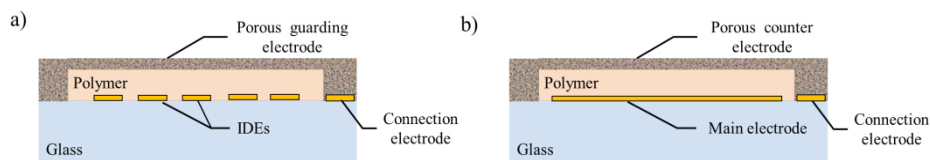


Figure 7.6. Schematic representation (not to scale) of the side view of a) polymer-coated IDEs on a glass substrate with a porous guarding electrode deposited on the polymer layer, and b) a single polymer-coated main electrode on a glass substrate with a porous counter electrode deposited onto the polymer layer (adapted²⁸).

It has to be noted that the electrical coupling effect between the IDEs, the main and the counter electrodes, and the guarding electrodes are also dependent on the dielectric constant of the polymer layer and its changes upon pollutant absorption. This includes also swelling effects, *i.e.*, changes in polymer layer thickness. Hence, the application of guarding electrodes leads to a more complex response interpretation. The

optimization of the system geometry, including the design of possible alternative three-dimensional electrode structures, such as based on the electrode arrangement of a coaxial stub resonator,³²⁻³⁴ and the optimization of the system dimensions as well as of the polymer layer thickness requires intense future modelling and response simulation work.

7.1.4 Lead Design

Another challenge encountered in the design phase of the sensing element was the arrangement of the leads. The leads represent the electrical connects between the IDE plane and the contact pads to the measuring device. In the application at hand, the IDE plane is situated within a measuring chamber containing the aqueous solutions and the contact pads are lying outside the flow cell chamber in the dry environment. Therefore, at some point the polymer-coated leads must ‘cross out’ of the flow cell chamber as shown in Figure 7.7.

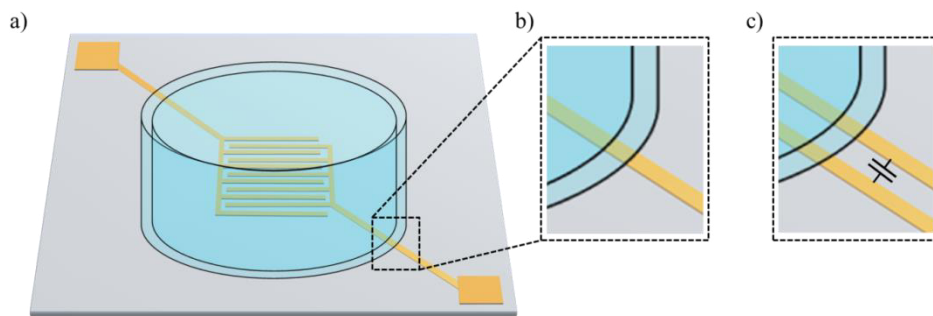


Figure 7.7. Schematic representation of a side/front view (not to scale) of a) a polymer-coated IDE platform with diagonally arranged leads, onto which a flow cell chamber is placed, b) a magnified view of the border of the chamber where one of the diagonal arranged lead exits, and c) a magnified view of the chamber border where parallel arranged leads exit. Also shown is the capacitance formed between the parallel arranged leads.

The presence of leads may be viewed as a weak spot of the designed detection system as it also brings along two problems. Firstly, the flow cell chamber may damage the underlying thin polymeric sensing layer, thereby increasing the chance of water/lead contact. Secondly, small changes in water uptake at the flow cell border can lead to

undesired response drifts if the capacitance between the leads is large. Preferably, only changes in the capacitance of the IDE plane determine the response change of the system. A state-of-the-art solution is to make electrical connections on the backside of the substrate by metallic through-hole technique.³⁵ In that case, the leads do not lie planar on the substrate but run vertically through the substrate as shown in Figure 7.8. As the dielectric constant of the substrate may be assumed to be constant under operation conditions, the capacitance formed between the leads will be constant, too, and the leads could be arranged parallel to each other at close distance to also minimize the chance of inductive loops. Then larger leads, *i.e.*, metallic through holes, can be chosen in order to decrease the resistance of the leads of the current design as explained in Chapter 4.

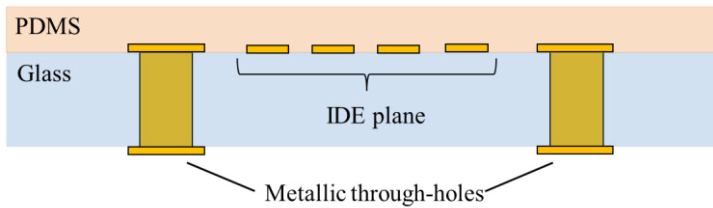


Figure 7.8. Schematic representation (not to scale) of a side view of PDMS-coated IDEs on a glass substrate and the metallic through-holes for making electrical connects at the backside of the glass substrate.

7.1.5 Setup Design

For environmental monitoring systems, it is of interest to measure the aqueous pollutant concentration directly onsite. When taking a water sample and transferring it into a measurement cell, the aqueous concentration of the pollutant may change. This is, for example, due to evaporation, wetting, and phase separation (Figure 7.9), which is in particular a problem for volatile organic compounds that do not mix well with the water phase and quickly evaporate upon exposure to air. This latter property can very well be exploited for detection systems that measure the aqueous volatile pollutants *indirectly* in a headspace and if possibly by inserting the sensing probe directly into the polluted water phase.^{36, 37}



Figure 7.9. Schematic representation of a side/front view of a pipe section containing an aqueous solution of a chemical compound that a) is well mixed in the water phase, b) wets the pipe surface, and c) phase separates from the water phase.

Hence, when developing a detection and measuring system to perform accurate qualitative and quantitative analysis, it is of essence to preserve the exact environmental aqueous composition. For the designed flow detection system, that serves for research purposes, the following can be summarized and concluded regarding its optimization:

Preferably, the solutions are prepared within the measuring system just before transporting them to the measuring cell. By creating turbulent flow within the measuring chamber, a concentration gradient within the chamber can be prevented and a well-mixed composition is created just above the sensing element. A control measurement of the aqueous concentration should be performed right at the outlet of the flow system by means of laboratory instrumentation, such as gas chromatography (GC) combined with mass spectrometry (MS) or flame ionization detection (FID). In addition, a bubble trap must be provided to quickly remove introduced or formed air and vapor bubbles. Bubble formation can occur when, *e.g.*, flushing a flow system with hydrophobic surfaces, such as that of the PDMS layer, which is due to the reason that a thin air film can be initially trapped at the polymer/water interface, that dissolves slowly into the aqueous phase.

In a fully matured detection and measuring system, all other significant parameters including pressure and temperature are conditioned or calibrated for. Since the water solubility of chemical compounds is temperature-dependent, the temperature of the entire flow system including the liquid reservoirs, pipe system, and measuring chamber has to be stabilized. This is especially of importance for hydrophobic organic compounds. As demonstrated in our experiments, the response reproducibility of the designed measuring system decreases for increasing hydrophobicity of the tested chemicals. Finally, continuous monitoring of and accountancy for other environmental

parameters including pH, oxygen content, and solution conductivity is of great importance to obtain accurate and reliable system responses.

7.2 Concluding Remarks

We addressed the fundamental issues encountered during the study, research, and development stage of the project “Polydimethylsiloxane-Coated Interdigitated Electrode Platforms for the Capacitive Detection of Organic Pollutants in Water”. Resulting future research tasks lie in the improvement of the individual system levels; the polymer layer, the polymer/transducer interface, the transducer platform including the IDE structure, the leads, and finally the flow cell and measuring system. Innovative polymers have to be designed to achieve chemical diversity within a multi-array. The polymers must be sufficient hydrophobic to keep water vapor uptake low, and they must provide good mechanical strength and anti-fouling properties. Good contact between the polymer and the transducer platform is a requirement for good adhesion and can be promoted with surface modification techniques. Another challenge lies in the proper guarding technique of the out-of-plane electric sensing field of the IDEs. The applications of further guarding electrodes, either situated as porous layer on top of the polymer layer or as planar guarding electrodes between the sensing IDEs, seem promising techniques to get rid of parasitic effects or to reduce response times. Further system optimization can be achieved by applying metallic through-hole techniques to make electrical connects at the backside of the sensing platform. Finally, a detection and measuring system that allows reliable quantitative pollution detection should be fully condition controlled (*i.e.*, temperature, pressure, flow rate, etc.) to have certainty about the concentration profile of the pollutant within the flow system.

7.3 References

- 1 J. W. Gardener, Barlett, B. N., Techniques and mechanism in gas sensing (Bristol, England: IOP-Publishing, 1991).
- 2 A. Hierlemann, M. Schweizer-Berberich, U. Weimar, G. Kraus, A. Pfau, and W. Göpel, Pattern recognition and multicomponent analysis, *Sensors Update*, 2 (1996), 119-180.
- 3 G. C. Osbourn, J. W. Bartholomew, A. J. Ricco, and G. C. Frye, Visual-empirical region-of-influence pattern recognition applied to chemical microsensor array selection and chemical analysis, *Accounts of Chemical Research*, 31 (1998), 297-305.
- 4 W. Olthuis, A. J. Sprenkels, J. G. Bomer, and P. Bergveld, Planar interdigitated electrolyte-conductivity sensors on an insulating substrate covered with Ta₂O₅, *Sensors and Actuators B-Chemical*, 43 (1997), 211-216.
- 5 J. W. Grate, D. A. Nelson, and S. N. Kaganove, Polymers for chemical sensors using hydrosilylation chemistry, (Richland, U.S.A.: Pacific Northwest National Laboratory, 2001).
- 6 J. Burke, Solubility parameters: Theory and application, *The Book and Paper Group Annual*, 3 (1984), 13-58.
- 7 A. Mata, A. J. Fleischman, and S. Roy, Characterization of polydimethylsiloxane (PDMS) properties for biomedical micro/nanosystems, *Biomedical Microdevices*, 7 (2005), 281-293.
- 8 F. Abbasi, H. Mirzadeh, and A.-A. Katbab, Modification of polysiloxane polymers for biomedical applications: A review, *Polymer International*, 50 (2001), 1279-1287.
- 9 B. K. M. M. Shivashankar, A review on interpenetrating polymer network, *International Journal of Pharmacy and Pharmaceutical Sciences*, 4 (2012), 1-7.
- 10 H. Yan, and K. Row, Characteristic and synthetic approach of molecularly imprinted polymer, *International Journal of Molecular Sciences*, 7 (2006), 155.
- 11 G. Vasapollo, R. D. Sole, L. Mergola, M. R. Lazzoi, A. Scardino, S. Scorrano, and G. Mele, Molecularly imprinted polymers: present and future prospective, *International Journal of Molecular Sciences*, 12 (2011), 5908.
- 12 D.-L. Huang, R.-Z. Wang, Y.-G. Liu, G.-M. Zeng, C. Lai, P. Xu, B.-A. Lu, J.-J. Xu, C. Wang, and C. Huang, Application of molecularly imprinted polymers in wastewater treatment: A review, *Environmental Science and Pollution Research*, 22 (2015), 963-977.
- 13 R. Cuypers, Hydrogen bonding in the recovery of phenols and methyl-*t*-butyl ether (Ph.D. Thesis, Wageningen University, 2010).
- 14 B. Burghoff, E. L. V. Goetheer, and A. B. de Haan, Solvent impregnated resins for the removal of low concentration phenol from water, *Reactive and Functional Polymers*, 68 (2008), 1314-1324.
- 15 B. Burghoff, J. Sousa Marques, B. M. van Lankvelt, and A. B. de Haan, Solvent impregnated resins for MTBE removal from aqueous environments, *Reactive and Functional Polymers*, 70 (2010), 41-47.
- 16 A. Camenzind, W. R. Caseri, and S. E. Pratsinis, Flame-made nanoparticles for nanocomposites, *Nano Today*, 5 (2010), 48-65.

- 17 I. A. M. Ibrahim, A. A. F. Zikry, M. A. Sharaf, M. J. E. Mark, K. Jacob, I. M. Jasiuk, and R. Tannenbaum, Dielectric behavior of Silica/Poly(dimethylsiloxane) nanocomposites. Nano size effects, *IOP Conference Series: Materials Science and Engineering*, 40 (2012), 2001-2011.
- 18 M. Charnley, M. Textor, and C. Acikgoz, Designed polymer structures with antifouling-antimicrobial properties, *Reactive and Functional Polymers*, 71 (2011), 329-334.
- 19 E. W. Merrill, Distinctions and correspondences among surfaces contacting blood, *Annals of the New York Academy of Sciences*, 516 (1987), 196-203.
- 20 E. Ostuni, R. G. Chapman, R. E. Holmlin, S. Takayama, and G. M. Whitesides, A survey of structure-property relationships of surfaces that resist the adsorption of protein, *Langmuir*, 17 (2001), 5605-5620.
- 21 J. L. Dalsin, and P. B. Messersmith, Bioinspired antifouling polymers, *Materials Today*, 8 (2005), 38-46.
- 22 E. P. O'Brien, C. C. White, and B. D. Vogt, Correlating interfacial moisture content and adhesive fracture energy of polymer coatings on different surfaces, *Advanced Engineering Materials*, 8 (2006), 114-118.
- 23 W.-C. Heerens, Application of capacitance techniques in sensor design, *Journal of Physics E: Scientific Instruments*, 19 (1986), 897.
- 24 I. Byun, A. W. Coleman, and B. Kim, Transfer of thin Au films to polydimethylsiloxane (PDMS) with reliable bonding using (3-mercaptopropyl)trimethoxysilane (MPTMS) as a molecular adhesive, *Journal of Micromechanics and Microengineering*, 23 (2013), 085016.
- 25 J. C. Love, L. A. Estroff, J. K. Kriebel, R. G. Nuzzo, and G. M. Whitesides, Self-assembled monolayers of thiolates on metals as a form of nanotechnology, *Chemical Reviews*, 105 (2005), 1103-1170.
- 26 S. P. Pujari, L. Scheres, A. T. M. Marcelis, and H. Zuilhof, Covalent surface modification of oxide surfaces, *Angewandte Chemie International Edition*, 53 (2014), 6322-6356.
- 27 Y. Shao, M. V. Mirkin, G. Fish, S. Kokotov, D. Palanker, and A. Lewis, Nanometer-sized electrochemical sensors, *Analytical Chemistry*, 69 (1997), 1627-1634.
- 28 X. Li, and G. C. M. Meijer, Capacitive sensors, in *Smart Sensor Systems*, ed. by G. C. M. Meijer (Chichester, U.K.: John Wiley & Sons, Ltd., 2008), pp.
- 29 A. Heidary, A low-cost universal integrated interface for capacitive sensors (Ph.D. Thesis, Delft University of Technology, 2010).
- 30 L. Jiawei, L. Ying, T. Min, L. Jie, and L. Xinhua, Capacitive humidity sensor with a coplanar electrode structure based on anodised porous alumina film, *Micro & Nano Letters, IET*, 7 (2012), 1097-1100.
- 31 H. Hyun Pyo, J. Kyung Hoon, M. Nam Ki, R. Yong Hoon, and P. Chan Won, A highly fast capacitive-type humidity sensor using percolating carbon nanotube films as a porous electrode material, in *Sensors, 2012 IEEE*, (2012), pp. 1-4.
- 32 N. A. Hoog, M. J. J. Mayer, H. Miedema, R. M. Wagterveld, M. Saakes, J. Tuinstra, W. Olthuis, and A. van den Berg, Stub resonators for online monitoring early stages of corrosion, *Sensors and Actuators B: Chemical*, 202 (2014), 1117-1136.

- 33 N. A. Hoog-Antonyuk, W. Olthuis, M. J. J. Mayer, H. Miedema, F. B. J. Leferink, and A. van den Berg, Extensive modeling of a coaxial stub resonator for online fingerprinting of fluids, *Procedia Engineering*, 47 (2012), 310-313.
- 34 N. A. Hoog, M. J. J. Mayer, H. Miedema, W. Olthuis, A. A. Tomaszewska, A. H. Paulitsch-Fuchs, and A. van den Berg, Online monitoring of biofouling using coaxial stub resonator technique, *Sensing and Bio-Sensing Research*, 3 (2015), 79-91.
- 35 T. Abe, X. Li, and M. Esashi, Endpoint detectable plating through femtosecond laser drilled glass wafers for electrical interconnections, *Sensors and Actuators A: Physical*, 108 (2003), 234-238.
- 36 C. K. Ho, and R. C. Hughes, In-situ chemiresistor sensor package for real-time detection of volatile organic compounds in soil and groundwater, *Sensors*, 2 (2002), 23-34.
- 37 R. Pozzi, F. Pinelli, P. Bocchini, and G. C. Galletti, Rapid determination of methyl tert-butyl ether using dynamic headspace/ion mobility spectrometry, *Analytica Chimica Acta*, 504 (2004), 313-317.

SUPPLEMENTARY INFORMATION
CHAPTER 4

A.1 Phase Shift versus Frequency

The phase shift of an IDE platform was measured within a frequency range of 100 Hz and 100 MHz with the 4294A impedance analyzer by Agilent. The oscillation level was set at 750 mV. The sweep type was log frequency with a total number of points of 201. The resulting measurement plot is depicted in Figure A.1.

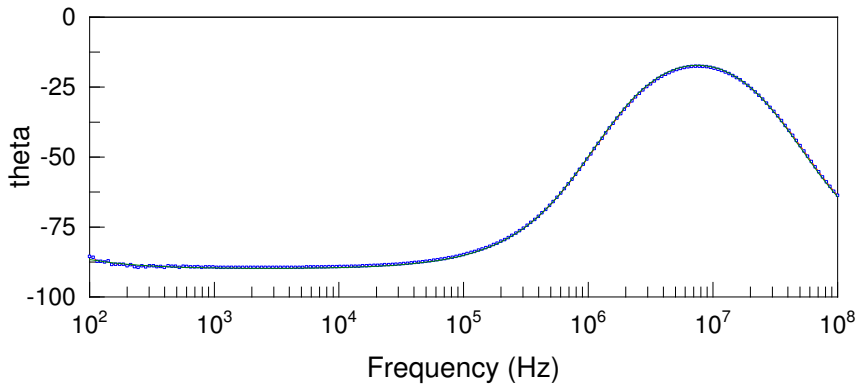


Figure A.1. Phase shift (theta) versus frequency within a range of 100 Hz – 100 MHz for a bare IDE platform.

As can be seen, the phase shift on the lower frequency range is ca. -90° , indicating the capacitive response of the system. For this platform at 1 kHz, the phase shift measures -89.4° and at 30 kHz, which is the measurement frequency of the UTI, the phase shift measures -88° . For increasing frequency, the phase shift approaches quickly a minimum value of -17.5° at 7.5 MHz and then drops again.

It was found that the leads have a high resistance (R_{Leads}) of ~ 3.5 kOhm and that a secondary capacitance (C_p) exists that measures about 0.5 pF. The impedance response was fitted with the equivalent circuit model presented in Figure A.2 as obtained from the modeling and analysis software ZView®:

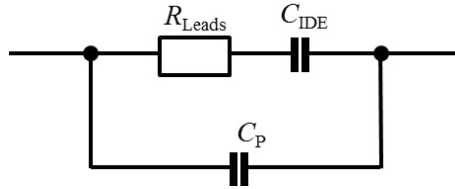


Figure A.2. Equivalent circuit model of the impedance response of the designed IDE platform.

SUPPLEMENTARY INFORMATION
CHAPTER 5

B.1 Dimensions and Material Properties

Detailed information on the dimensions and dielectric constants of the materials of the IDE chip, the PCB, and on the arrangement of the flat-tipped third electrode is provided in Figure B.1.

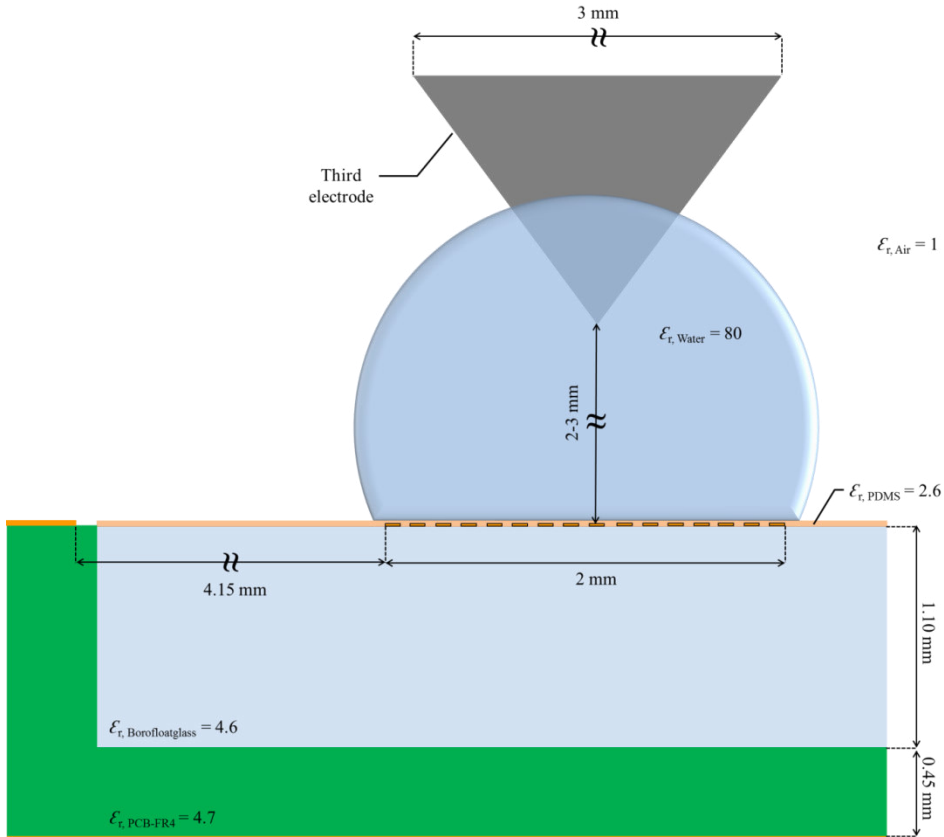


Figure B.1. Schematic representation of the PDMS-coated IDE chip placed into the PCB with the grounded top and bottom shields and the approximate system part dimensions and the relative dielectric constants of the materials. Also shown is a water drop deposited on the center of the IDE plane and the introduced third electrode. All labelled dimensions, except for the distance of the IDE plane to the PCB top shield and its perpendicular distance to third electrode as well as the maximal width of the third electrode, are to scale.

B.2 Solution Conductivity

The conductivity of the sodium chloride (NaCl) solutions as function of the salt concentration is given in Figure B.2. Within the range of 1 mM and 20 mM, the conductivity of the solution increases linearly. For zero concentration of salt, the Milli-Q water measures a conductivity of $\sim 0.35\text{--}0.75\ \mu\text{S}/\text{cm}$, which is about a factor of 200 lower than that of the solution with the lowest salt concentration that we have used (1 mM) and about a factor of 4000 lower than that of the solution with the highest salt concentration that we have used (20 mM).

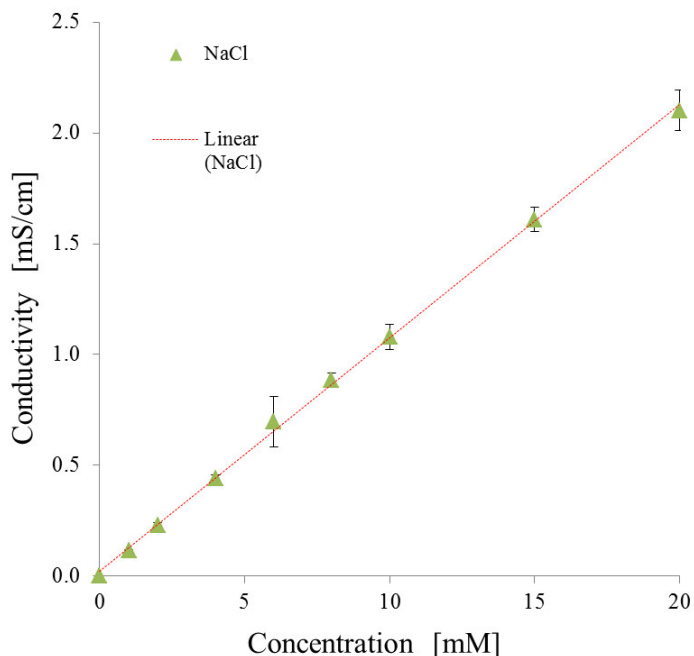


Figure B.2. Average of conductivity as function of NaCl concentration in Milli-Q water as measured for 4 individually prepared solutions given with error bars based on their standard deviation.

B.3 Detection Performance of Guarded and Unguarded IDE Chips

In order to compare the detection performance and sensitivity of the unguarded and guarded IDE chip for a test pollutant, that is methyl-tert butyl ether (MtBE), both chip versions with a $\sim 25\ \mu\text{m}$ thick PDMS coating were tested under continuous flow conditions as described in Chapter 6. The measurements done with the unguarded and guarded IDE-chip were both performed with the identical MtBE solution and in sequence in order to avoid solution effects and to limit the chance for changes in the ambient conditions. The results are depicted in Figure B.3.

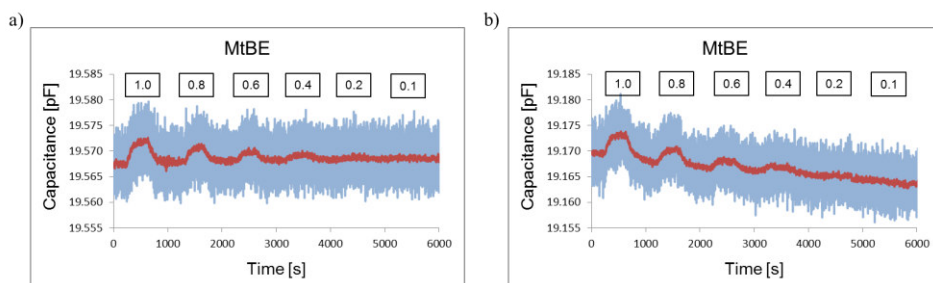


Figure B.3. Real-time (blue) and averaged over 100 points (red) capacitive response upon alternating exposure to Milli-Q water and different concentrations in mM of MtBE for a) the unguarded and b) the guarded IDE platform, both with a $\sim 25\ \mu\text{m}$ thick PDMS coating.

The measurement series demonstrate clearly similar sensitivities of the unguarded and the guarded IDE chip to the same MtBE concentration. The lower baseline of the guarded IDE chip under water conditions is attributed to enhanced electrical coupling between the IDEs and the guarding electrodes. The observed negative slope may be attributed to slowly advancing water uptake between the leads and the guarding electrodes at the site of the O-ring at the flow cell boundary, which enhances gradually the guarding effect. Also, temperature variations are possible causes for such drift characteristics and can be observed for both platform types. As discussed in Chapter 7 in Section 7.1.4, metallic through-holes that allow electrical connections at the backside of the IDE chip at the site of the IDE plane is an optimistic remedy technique for avoiding the drift characteristic that is due to water migration at the flow cell boundary.

SUPPLEMENTARY INFORMATION
CHAPTER 6

C.1 Contact Angle Measurements

Sylgard®184 is a hydrophobic silicone. Its water contact angle was measured to be $\sim 112^\circ$ for a $4\ \mu\text{l}$ drop of Milli-Q water as depicted in Figure C.1. Therefore, as in contrast to drop depositions of hydrophobic organic solvents, water is not readily absorbed by the polymeric sensing layer (Figure C.2). Though water has a much higher dielectric constant ($\epsilon_r = 80$) than any of the deposited organic liquids, the change in the IDE capacitance of the performed drop experiments was significantly less. This also indicates that the sensitivity to events on and above the polymer surface have become negligible due to the layer thickness of $\sim 50\ \mu\text{m}$, which measures about 2.8 times the spatial electrode wavelength of the utilized IDE design. Slow water or water vapor absorption into the polymer structure can be assumed because of the gradual increase in capacitance with time after deposition.

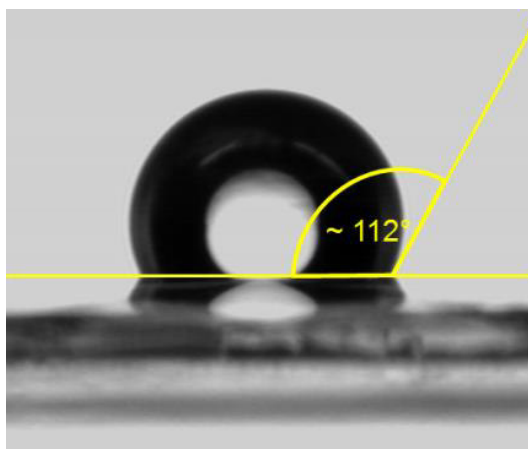


Figure C.1. Picture of a $4\ \mu\text{l}$ drop of Milli-Q water on a Sylgard®184 surface and the schematic representation of the water contact angle.

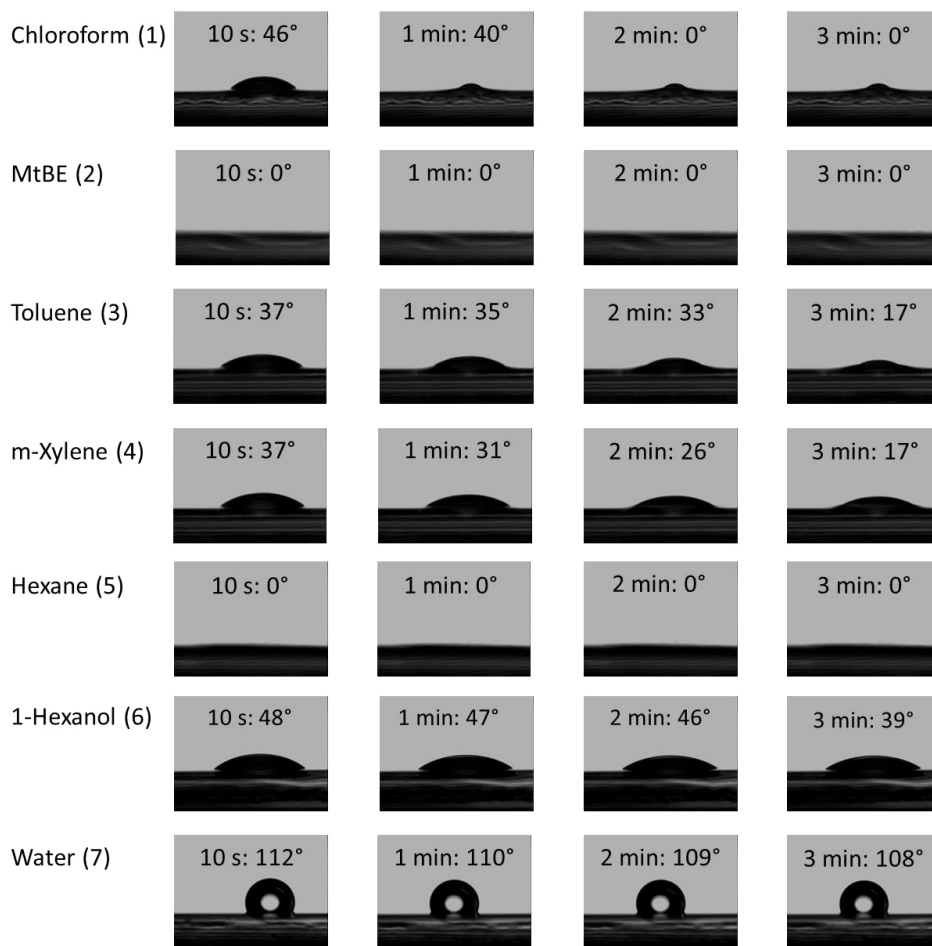


Figure C.2. Pictures showing the evolution of the contact angle of a 4 μ l drop of Milli-Q water and the organic compounds on Sylgard®184 surfaces after 10 s, 1 min, 2 min, and 3 min.

SUMMARY

There is a high motivation to develop smart sensor systems based on surface-engineered sensor elements for environmental and biomedical monitoring purposes. Key characteristics are that the sensors perform reliable, accurate, sensitive, and ideally selective measurements while being low-cost, portable, robust for online and on-field applications, and allowing wireless communication. Polymer-coated interdigitated electrodes (IDEs), which are able to convert a change in the properties of a dielectric material into an electrical signal, have shown promising detection performances in the gaseous phase. Within this concept, the collection of the target compounds, mostly by absorption, results in dielectric changes that can be measured capacitively. In this thesis, we pursue to study this type of sensors when brought in direct contact with an aqueous phase for the capacitive detection of organic pollutants.

For this goal, planar IDE structures centred on 1 cm² large borosilicate glass chips were fabricated with the following electrode dimensions: 221 golden interdigitated fingers of 2 mm in length, 6 μm in width, with a 3 μm gap between them, and diagonally arranged leads of 6 μm in width to the contact pads. IDE chips with and without in-plane guarding electrodes were designed. The IDE chips were wire-bonded to a printed circuit board, from where further connections to the electronic readout device were made. Measurements were performed using the LabVIEW supported universal transducer interface (UTI) by the Smartec Company in the Netherlands. The polymeric sensing layers were prepared using Sylgard®184, a commercially available polydimethylsiloxane (PDMS) product by the Dow Corning Company. The polymer layers were deposited with controlled thicknesses via a spin-coating technique. For polymer layer thicknesses larger than the spatial electrode wavelength, *i.e.*, 18 μm, the capacitances for IDE chips with and without in-plane guarding electrodes were in the order of ~19 pF and ~20 pF, respectively. The measurement resolution—and hence detection limit—was measured to be ~500 aF. PDMS has beneficial properties for both sensing and water-contact applications as the visco-elastic and hydrophobic silicone network allows quick and reversible diffusion of small molecules, and simultaneously it serves as a water sealant, protecting the electrode structure. The polymer-coated IDE chip also forms the bottom part of a flow cell chamber, which is completed by mounting

a Teflon flow cell with a sealing Viton O-ring centred on top of the IDE chip. The flow cell system allows measurements under continuous flow conditions, using a syringe pump with two individual syringe drives.

The polymer layer thickness with respect to the spatial electrode wavelength is an important design parameter. The electric sensing field established between the planar IDEs lies primarily out-of-plane. If the polymer layer is sufficiently thick and the electric field is restrained within the layer, only the absorption of pollutants into the layer will be detected. For thin polymer layers, for which the electric field extends beyond the polymer surface, also adsorption and swelling as induced by pollutant uptake will contribute to changes in the capacitive response. We show that the polymer layer thickness also plays a significant insulation role. The out-of-plane electric field of the planar IDEs is geometrically difficult to guard, especially when the chip is being exposed to an electrically challenging environment, such as water. This is —because in contrast to air— water is relatively conductive, especially when it contains dissolved solids, and it has a relatively high dielectric constant. For this reason, the electrical complexity for aqueous systems is enhanced and the chance for parasitic electrical coupling effects to other system parts and the surrounding increases. If the electric sensing field is parasitically coupled through the water phase, then device sensitivity to electrical changes of the aqueous solution is induced. By means of the two-port technique, the UTI is not affected by parasitic capacitances of parallel capacitors to ground, such as introduced, *e.g.*, by the coax cables. Yet, electrical coupling events that lead to a reduction in the IDE capacitance cannot be distinguished. It was found that for the designed system and for an unguarded IDE chip with $\sim 50\ \mu\text{m}$ thick PDMS coating an increase in the aqueous salt (NaCl) molarity from 0 up to 20 mM results in a capacitance decrease down to $\sim 175\ \text{fF}$. This is attributed to enhanced parasitic coupling to the system environment for increasing solution salinity. The parasitic coupling effect further increased for lower layer thicknesses, showing its role of insulation. We demonstrated how water-enhanced electrical coupling to in-plane guarding electrodes or ideally a third electrode, which connects the water phase with the ground terminal, is a key mechanism in achieving response immunity to further parasitic coupling. This way the device sensitivity to solution conditions can be significantly decreased for reasonable layer thicknesses and without impairing the detection performance.

Eventually, we investigated the capacitive response of interdigitated electrodes covered with ~50 μm thick PDMS films from the moment of deposition until full evaporation of drops of pure volatile organic compounds (VOCs), including chloroform, methyl tert-butyl ether, 1-hexanol, toluene, m-xylene, and n-hexane. Then the direct exposure to aqueous solutions of these VOCs (up to 1 mM) under continuous flow conditions was studied. It is shown that the capacitive response changes upon absorption of the VOCs into the PDMS are in line with their relative dielectric constants as compared to the one of the thin PDMS layer and that the response changes were fully reversible. The response changes were in the low fF range with a detection limit of ~0.1 mM for the more water-soluble VOCs, which include chloroform, methyl tert-butyl ether, and 1-hexanol. However, the response reproducibility decreased for the more hydrophobic organics toluene, m-xylene, and n-hexane, pointing at distribution processes such as evaporation, wetting, and phase separation within the system.

Research challenges are the design of innovative polymeric sensing layers that provide both tuned chemical selectivity within an IDE multi-array and sufficient sealing properties when being directly exposed to water. This may require also the design of new surface modification techniques to achieve good adhesion with the transducer substrate. Further research on the detection and partitioning processes will demand the design of fully conditioned and calibrated measuring systems. Finally, the development of more sensitive transducer interfaces and fully integrated smart sensor systems are further requirements to achieve the goal of target detection at governmental water standards.

Er bestaat een grote behoefte aan het ontwikkelen van smart sensor systemen die gebaseerd zijn op oppervlakte-gemodificeerde sensorelementen ten behoeve van milieu- en biomedische toepassingen. Belangrijke kenmerken van dergelijke sensoren zijn een grote betrouwbaarheid, een hoge nauwkeurigheid en gevoeligheid en –in het ideale geval– het vermogen om uiterst selectieve metingen te kunnen uitvoeren. Bovendien moeten dergelijke sensoren goedkoop, draagbaar en robuust zijn om *online* applicaties in het veld mogelijk te maken al dan niet in combinatie met draadloze communicatie. Met polymeer-gemodificeerde vinger- of ook wel genoemd kam-elektroden (*interdigitated electrodes*, IDEs) kunnen veranderingen in diëlektrische eigenschappen van het polymeer omgezet worden in een elektrisch signaal. Dergelijke sensoren hebben inmiddels veelbelovende resultaten getoond voor detectie in de gasfase. Selectieve opname van de te detecteren component door het polymeer verandert de diëlektrische constante ervan, welke via een elektrische capaciteitsmeting kan worden waargenomen. In dit proefschrift worden deze sensoren onderzocht voor sensing van organische verontreinigingen aanwezig in de vloeistof water. Het nieuwe is dus dat deze sensoren nu niet in de gasfase worden gebruikt maar in de vloeistoffase. Dat brengt de nodige complicaties met zich mee en wordt in dit proefschrift nader beschreven.

IDE structuren werden daartoe op *chipjes* van boriumsilaat glas (1 cm^2) gefabriceerd met de volgende dimensies: 221 IDE vingers gemaakt van goud (2 mm lang, $6 \mu\text{m}$ breed, elk gelegen op een onderlinge afstand van $3 \mu\text{m}$) en voorzien van diagonaal gerangschikte verbindingen ($6 \mu\text{m}$ breed) naar de externe contactpunten. Er zijn zowel IDE chips met als zonder zogenaamde *in-plane guarding* elektroden ontworpen en gefabriceerd. De IDE *chips* werden gemonteerd op een printplaat en vandaar uit aangesloten op het meettoestel. De metingen werden alle uitgevoerd met door LabVIEW-ondersteunde *universal transducer interface* (UTI), gemaakt door Smartec B.V. in Nederland. De polymeer selectorlagen werden bereid met Sylgard®184, een commercieel verkrijgbaar polydimethylsiloxaan product (PDMS) van de Dow Corning Company. De polymeerlagen werden opgebracht via een *spin-coating* techniek, waardoor de laagdikte gecontroleerd kon worden. Voor polymeerlagen met

diktes groter dan de zogenaamde electrodenlengte (hier 18 μm) waren de gemeten capaciteiten van de IDE *chips* zonder en voorzien van *in-plane guarding* elektroden in de orde van ~ 20 pF en ~ 19 pF respectievelijk. De meetresolutie en daarmee dus ook de detectielimiet is ~ 500 aF.

PDMS heeft bijzonder gunstige eigenschappen voor sensortoepassingen in waterig milieu, zoals de visco-elastische en het gevormde hydrofobe siliconen netwerk dat snelle en reversibele diffusie van kleine hydrofobe moleculen toelaat. Tegelijkertijd verzorgt het PDMS een goede afdichting waardoor de elektrodenstructuur zorgvuldig beschermd wordt tegen water. Deze polymeer-gebaseerde IDE *chip* vormt vervolgens de bodem van een vloeistofstromingscel (*flow cel*) die gemaakt is uit Teflon en via een afdichtende Viton O-ring contact met elkaar maken. Een continue vloeistofstroom wordt gerealiseerd door een pomp aan te sluiten via injectiespuiten. Een belangrijke ontwerpparameter is de verhouding van polymeerlaagdikte en electrodenlengte. Het elektrische veld dat tussen de planaire IDEs wordt opgebouwd, ligt voornamelijk buiten het vlak van de IDEs. Bij voldoende dikke polymeerlaagjes blijft het elektrische veld binnen deze polymeerlaag. Hierdoor worden alleen de door het polymeer opgenomen verontreinigingen gedetecteerd. Voor dünnere polymeerlagen, waarbij het elektrische veld ook buiten de polymeerlaag significant aanwezig is, gaan ook adsorptie aan het polymeer-water grensvlak en zwellen van het polymeer bijdragen aan de gemeten verandering van de elektrische capaciteit. Ons werk laat zien dat de polymeerlaagdikte een grote rol speelt bij de elektrische isolatie van de elektroden. Het elektrische veld van deze planaire vingerelektroden is geometrisch namelijk heel moeilijk af te schermen, in het bijzonder als de *chip* aan een 'elektrisch uitdagend milieu' zoals water wordt blootgesteld. Dit komt omdat, in vergelijking tot de gasfase lucht, de vloeistoffase water een relatief hoge elektrische geleidbaarheid en een relatief hoge diëlektrische constante heeft. Hierdoor neemt de elektrische complexiteit toe en kunnen parasitaire elektrische koppelingen naar andere systeemonderdelen in de nabije omgeving een belangrijke rol spelen. Indien het elektrische veld parasitair door de waterfase heen is gekoppeld, wordt tevens de gevoeligheid voor elektrische veranderingen van de waterige oplossing als geheel opgemerkt. Parasitaire capaciteiten zijn in essentie condensatoren die parallel aan de 'aarde' (*ground*) liggen. Een UTI kan deze capaciteiten elimineren door gebruik te maken van de zogenaamde twee-poorten techniek. Echter, elektrische koppelingseffecten, die tot een reductie van de IDE capaciteit leiden, kunnen hiermee

niet worden onderscheiden. Een verhoging van de zoutconcentratie (een toename voor NaCl van 0 naar slechts 20 mM) resulteerde voor het door ons ontworpen systeem voor een sensor tot een capaciteitsafname van ~175 fF (IDE chip zonder *in-plane guarding* elektroden met een ~50 μm dikke PDMS laag). Dit wijst op een versterkte, parasitaire koppeling naar de directe omgeving van het systeem bij hogere zoutconcentraties. We demonstreerden dat water-versterkte elektrische koppeling naar *in-plane guarding* elektroden of –in het ideaal geval– een derde electrode, welke het water direct met een aard potentiaal verbindt, een sleutel mechanisme is om responsiviteit voor verdere parasitaire koppeling te bereiken. Het parasitaire koppelingseffect neemt toe voor dunnere polymeerlagen, waarmee het belang van een isolerende functie van deze laag wordt geïllustreerd.

Vervolgens hebben we de capacitieve *response* van IDEs voorzien van een ~50 μm dikke PMDS laag nader onderzocht bij en na het in contact brengen met druppels van de zuivere en vluchtige organische componenten (VOC) chloroform, methyl tert-butyl ether, 1-hexanol, toluen, m-xyleen en n-hexaan. Ook zijn deze IDEs onderzocht door deze in contact te brengen met waterige oplossingen, die lage concentraties bevatten van deze VOC (tot een concentratie van maximaal 1 mM) onder condities van continue stroming. De gemeten verandering van elektrische capaciteit van deze sensoren is gecorreleerd met de diëlektrische constanten van deze VOCs in relatie tot de dielektrische constante van de dunne PDMS laag. Deze gemeten veranderingen zijn volkomen reversibel, zodra de sensor in contact gebracht wordt met water dat deze componenten niet bevat. De gemeten veranderingen waren in de orde van enkele femtoFarads met een lage detectielimiet van ~0.1 mM voor de meer water-oplosbare VOCs (chloroform, methyl tert-butyl ether en 1-hexanol). Echter, de reproduceerbaarheid nam af voor de meer hydrofobe VOCs (toluen, m-xyleen en hexaan). Dit komt vermoedelijk door fasescheiding binnen het systeem.

Onderzoekuitdagingen voor de toekomst zijn het ontwerpen en maken van innovatieve polymeer selectorlagen, die een instelbare hoge chemische selectiviteit en sensitiviteit combineren voor detectie in waterige media en die worden toegepast binnen een *array* van IDEs. Nieuwe oppervlaktomodificatietechnieken zullen nodig zijn, die zorgen voor een goede aanhechting tussen polymeer en transducer interface. Daarnaast zal nader onderzoek nodig zijn op de detectie- en partitieprocessen, waardoor volledig geconditioneerde en gekalibreerde meetssystemen kunnen worden ontwikkeld.

Ontwikkeling van nog hoger gevoelige transducer interfaces en volledig geïntegreerde *smart* sensor systemen zullen de detectielimieten mogelijk verder verlagen.

Publications

Staginus, J., Chang, Z.-Y., Meijer, G.C.M., Sudhölter, E.J.R., Smet, L.C.P.M de, - *Surface-engineered Transducer Platforms for Capacitive Pollutant Detection in Aqueous Environments - System Aspects and Design Consideration*, (article in preparation).

Staginus, J., Chang, Z.-Y., Sudhölter, E.J.R., Smet, L.C.P.M de, Meijer, G.C.M., - *Water-enhanced Guarding of Polymer-coated IDE Platforms as a Key Mechanism for Achieving Response Immunity towards Parasitic Coupling Events*, accepted for publication (2015) in *Sensors and Actuators A-Physical* (article).

Staginus, J., Aerts, I.M., Chang, Z.-Y., Meijer, G.C.M., Smet, L.C.P.M de, Sudhölter, E.J.R., - *Capacitive Response of PDMS-coated IDE Platforms Directly Exposed to Aqueous Solutions Containing Volatile Organic Compounds*, *Sensors and Actuators B-Chemical*, 184 (2013) 130-142 (article).

Staginus, J., Aerts, I.M., Chang, Z.-Y., Meijer, G.C.M., Smet, L.C.P.M de, Sudhölter, E.J.R., - *Surface-engineered Sensors: Polymer-based Sensors for the Capacitive Detection of Organic Water Pollutant*, IMCS 2012 – The 14th International Meeting on Chemical Sensors, Nürnberg, Germany, May 20-23, 2012 (proceeding).

Presentations

Smet, L.C.P.M. de, Staginus, J., Sudhölter, E.J.R., - *Capacitive Response of PDMS-coated IDE Platforms Directly Exposed to Aqueous Solutions Containing Volatile Organic Compounds*, *Interfaces against Pollution (IAP): Interfaces in Water and Environmental Science*, Leeuwarden, the Netherlands, May 27, 2014 (lecture).

Smet, L.C.P.M de, Staginus, J, Aerts, I.M, Chang, Z.-Y, Meijer, G.C.M, Sudhölter, E.J.R - *Capacitive Response of PDMS-coated IDE Platforms Directly Exposed to Aqueous Solutions Containing Volatile Organic Compounds*, 2nd European Congress of Applied Biotechnology, The Hague, The Netherlands, April 21-25, 2013 (lecture).

Smet, L.C.P.M. de, Staginus, J., Sudhölter, E.J.R., - *Capacitive Response of PDMS-coated IDE Platforms to Aqueous Solutions of HCl and NaOH*, 3rd International Conference on Materials and Applications for Sensors and Transducers, Prague, Czech Republic, September 16, 2013 (lecture).

Staginus, J., Aerts, I. M., Chang, Z.-Y., Meijer, G.C.M, Smet, L.C.P.M. de, Sudhölter, E.J.R., *Polymer-based Sensors for the Capacitive Detection of Organic Pollutants in Water*, Sense of Contact 15, Soesterberg, the Netherlands, April 10, 2013 (poster).

Staginus, J., Miedema, H., Smet, L.C.P.M. de, Sudhölter, E.J.R., *Towards Surface-engineered Sensors: The Capacitive Response of PDMS-coated IDEs in Aqueous Solutions Containing Volatile Organic Compounds*, MicroNanoConference '12, Ede, the Netherlands, December 8, 2012 (lecture).

Staginus, J., Aerts, I.M., Chang, Z.-Y., Meijer, G.C.M., Smet, L.C.P.M de, Sudhölter, E.J.R., - *Surface-engineered Sensors: Polymer-based Sensors for the Capacitive Detection of Organic Water Pollutant*, IMCS 2012 – The 14th International Meeting on Chemical Sensors, Nürnberg, Germany, May 21, 2012 (poster).

Collaborative and Earlier Work

Deshpande, K.S., Kuddannaya, S., Staginus, J., Thune, P.C., Smet, L.C.P.M. de, Horst, J.H. ter & Wielen, L.A.M. van der (2012). Biofunctionalization and Self-interaction Chromatography in PDMS Microchannels. *Biochemical Engineering Journal*, 67, 111-119 (article).

Block, C., Vandecasteele, C., Van Caneghem, J., Staginus, J., Van Hooste, H., Vlaanderen, *Achtergronddocument 2007 - Verspreiding van Vluchtige Organische Stoffen (VOS)*, MIRA - Milieu- en natuurrapport Vlaamse Milieumaatschappij (2007) (report).

ACKNOWLEDGEMENT

This work was literally built from scratch, needless to say that it could only be realized with the great support from great people that I had the honor to work and spend valuable time with throughout my stay at Delft and the Delft University of Technology.

Ernst Sudhölter, my promotor: Ernst, ik denk dat je het al vaker hebt gehoord, maar je bent een bron van ideeën en een schatkist vol kennis. Ik dank je van harte voor onze gesprekken, niet alleen die op wetenschappelijk gebied, maar ook die over het leven en wat ons allemaal nauw aan het hart ligt.

Louis de Smet, my mijn copromotor: Louis, je hebt een onmiskenbare bijdrage geleverd aan de kwaliteit mijn werk en proefschrift! Je doet je werk met hart en ziel en dat vind je ook in dit proefschrift terug! We hebben een spannende reis gemaakt, waar het soms bergaf en bergop ging, en die houd ik warm in herinnering!

Zu-yao Chang, my best collegae: Zu-yao, jij bent een kanjer! Jouw rust en doorzettingsvermogen hebben me heel veel vertrouwen en sterkte gegeven. Hartelijk bedankt voor de samenwerking, het samen kletsen en samen lachen. Ik hoop op vervolg ervan!

Gerard Meijer, my mentor at EWI: beste Gerard, het was echt een grote eer met een pionier op het gebied van capacitieve sensoren te mogen samen werken. Je hebt me als wetenschapper en als mens zoveel geleerd. Ik hoop dat je nog lang bij EWI aan het werk blijft; jij bent onvervangbaar!

Isabelle Aerts, my master student during the third year and now my good friend: Iesje, je bent een bron van positieve energie en blijdschap! Je was mijn engel tijdens de zware tijd die ik had met het overlijden van mijn grootmoeder. Heel erg bedankt! Ik hoop dat onze vriendschap voor altijd blijft bestaan!

Many thanks go out to my sponsor Wetsus – Centre of Excellence for Sustainable Water Technology. I would like to thank the participants of the research theme Sensoring for the fruitful discussions and their financial support. Special thanks go out to my supervisor Henk Miedema (Wetsus) and to Mateo Mayer (now EasyMeasure B.V.), both members of the doctoral committee, as well as to Gert-Jan Euverink (now Rijksuniversiteit Groningen).

I would further like to thank Prof. dr. Dam, Prof. dr. van Rijn, Prof. dr. Gardeniers, and Prof. dr. Picken for being part of the doctoral committee.

Jochen Rutz, my Erasmus student during the second year: Jochen, vielen, lieben Dank für deine grosse Unterstützung an diesem Projekt! Auf dich war immer Verlass! Mit deinem Witz und deiner Freundlichkeit ist man immer leicht und locker durch den Arbeitstag gekommen.

Thomas Lambricht, my Erasmusstudent during the first year: Thomas, you are truly an amazing, smart, kind and yet humble person. You always looked at the bright sight of everything and made the best out of it. Thank you so much for all your creative and indispensable input into this work!

To my former NOC-ies and now OMI-ies (in alphabetical order): Aldo, Anping, Christian, Daniela S., Daniela U., Lars, Sumit, Venkatesh and Wolter: I know I have strolled around quite much, but I truly appreciated all the time spent with you and the nice coffee breaks we had, guys. Thank you for all your support and talks on both science and life! I wish you all the best and success along your way!

Goulielmos alias Will: my ‘lovely’, did I really forget to mention you? Not possible! Miss you buddy! Hope you have a great time and much fun! Many hugs and best wishes for your future!

Duco Bosma, technical support and coffee & swimming partner: Duco, heel hartelijk bedankt voor alles! Ik hoop dat je je vindingrijke ideeën kunt uitwerken en de juiste herkenning ervoor krijgt.

Bart Boshuizen, the LabView specialist: heel hartelijk bedankt dat je onze ideeën over het LabVIEW programma altijd snel kon omzetten en dat je het steeds nog beter hebt gemaakt. Mijn beste wensen aan jou en dat je nog veel fijne vakanties in Duitsland zult hebben!

Many thanks go out to the following TU Delft members for their great technical and engineering support: Wil Straver, John Suijkerbuik, Ger de Graaf, Marcel Bus, Piet Droppert, Ben Norders, Gerard Vos, Alex Boot, Nico Alberts, and David Jager.

Erik Kelder, a specialist in electrochemistry, and Ger Koper, a specialist in thermodynamics: heel hartelijk bedankt voor onze fijne gesprekken en jullie input. Ik zie jullie als echte experts en jullie hebben me kritischer naar mijn eigen werk laten kijken en harder laten werken. Jammer dat we niet vaker hebben gepraat. Ik wens jullie het beste toe!

Arend Kolk, an inspiring professor of Molecular Science: beste Arend, hartelijk dank voor al de leuke en inspirerende gesprekken over onze vakgebieden en meer! Ik wens jou en jouw broer gezondheid, liefde en geluk toe!

Louw, technical support: beste Louw, heel erg hartelijk bedankt, niet alleen voor jouw technische en wetenschappelijke steun, maar ook het delen van ervaring en ideeën.

I send many thanks out to Ronald Dekker, Shreyas Kuddannaya, Kedar Deshpande, Marcel Otten and Erwin Schmidt for our collaborative work on PDMS, glass and gold surface modification techniques.

Special thanks to my best men from the gas and safety team at ChemE: Nico, Erwin, Alex, Ruud, Tom, Samir, and Nayyar. Ik mis de grappige koffiepauzes met jullie! Hartelijk dank!

I want to thank our organizational talents at the secretaries of ChemE en EWI: Astrid, Marian en Joyce: hartelijk bedankt voor alles! Mijn beste wensen voor jullie!

Kevin, Wesley, Stefan, Derck, my LO1 students, and Sherwin, Richard, Wim and Joan, my LO2 students, that I supervised during my first and second year: hoi jongens! Bedankt voor al de grappige momenten die we samen hadden naast het ‘zware werk’ in het lab en de gezellige pauzes met de lekkere toasties en oliebollen. Ik wens jullie het beste voor jullie toekomst toe!

Marta, my former office mate: thanks for all your support and fun in the office! I hope you have a great future and that your dreams may come true!

Florian, Katrin, and Tim, my German colleagues: schön war die Zeit! Ich wünsche euch alles Liebe und Gute für eure Zukunft!

Aernout, Christopher, and Krishna, colleagues who left some time ago: it has been a while, but thanks so much for all the inspiring talks on both research and life!

Lukasz, officemate of Zu-yao Chang: thanks for all the fun and for letting me occupy your office occasionally ;)

Riccardo, Emanuela and Venkatesh, my flat mates in Delft: Thank you, guys! It is so great to come home and have always someone nice to talk to!

Finally, I want to thank my people at home for their support, encouragement, love, and patience: my family headed by Papa, my brother Julius, and my sister Laura with her husband Wolfgang and little Aaron, Helen, and Muriel, and my uncle Helmut and my cousin Carina with their families, thank you all for being there all along the way; my ‘aunty’ Chris and my childhood friends Ariane and Iara for their open ears, their cheering ups, and our laughs; Janusz and his craftsmen team for fixing my grandparents’ house, and Virginie and her family for filling it back with life; wise and amazing Ria and her lovely husband Joop for having given me such a nice and warm home; Susi and all the people from my brother’s workplace for all their good advices and funny jokes; Iris and Harald with Tapsi for being my source of inspiration and peace; and Lothar for sharing some of the freedom of life; finally, of course, I thank my trusty dog Columbo for filling every moment of my day with joy and happiness.

ABOUT THE AUTHOR

Judith Stagnus was born in Düsseldorf, Germany, on Rose Monday, February 26 in 1979. After her Abitur in 1998, she finished a 3-year apprenticeship as a car electrician at the Daimler Sprinter Werk in Düsseldorf (Germany) in 2001. She received the academic degree of Master in Industrial Science: Chemical Engineering at the Group T Engineering College in Leuven (Belgium) in 2007. Her master thesis was carried out at the local institute IMEC, formerly also



called the Interuniversity Microelectronic Centre. In 2008, she completed the Master-after-Master programme in Environmental Science and Technology at the Catholic University of Leuven (Belgium). In 2009, Judith joined the Nano-Organic-Chemistry group (Organic Materials & Interfaces as of 2014) headed by Prof. Ernst Sudhölter at the Department of Chemical Engineering of the Delft University of Technology (the Netherlands). Her Ph.D. project on polymer-based chemical capacitive sensors for the detection of organic water pollutants was performed under the daily supervision of Dr. Louis de Smet. The project was carried out in collaboration with Wetsus, the European Centre of Excellence for Sustainable Water Technology in Leeuwarden (the Netherlands). During the four year Ph.D. period, Judith was involved in several teaching activities and collaborative projects.

ISBN: 978-94-6186-565-6